UNDERSTANDING THE KINETICS OF ASPHALTENE PRECIPITATION FROM CRUDE OILS

by

Tabish Maqbool

A dissertation submitted in partial fulfillment
of the requirements for the degree of
Doctor of Philosophy
(Chemical Engineering)
in The University of Michigan
2011

Doctoral Committee:

Professor H. Scott Fogler, Chair
Professor Massoud Kaviany
Professor Phillip E. Savage
Professor Michael J. Solomon

ACKNOWLEDGEMENTS

All Praise is for Allah, the Cherisher and Sustainer of the worlds. I thank Him for all His blessings, seek His help in affairs of my life and ask His forgiveness for my shortcomings.

This work has been made possible due to the contribution of many individuals whose support and encouragement have made a huge impact on my life – both personal and professional. I am certain that an attempt to sum up everyone's contributions in a few paragraphs would be far from perfect. Therefore, I hope that my friends, family and colleagues will excuse any oversight on my part as I list their contributions.

First of all, I would like to thank Professor Fogler for giving me this wonderful opportunity to join his research group and pursue my doctoral degree under his guidance. He was always very supportive of new ideas and encouraged creative thinking and problem solving. He has a unique way of encouraging his students to become more independent and is always there to support them when they need his guidance. He always motivated the graduate students in his group to understand about each other's research projects and have healthy discussions about them so that we could contribute to everyone's success.

I would also like to thank Professors Michael Solomon, Phillip Savage and Massoud Kaviany for serving on my doctoral committee and providing helpful inputs that

have enhanced the impact of this work. They also asked lots of insightful questions which helped me in developing a good balance of depth and breadth of the knowledge related to this research area. Their flexibility in scheduling the data meeting and oral defense is greatly appreciated. I am also thankful to Professor Savage for being a very helpful mentor during the course of my stay at Michigan. I also had the privilege to having a great mentoring relationship with Dr. Susan Montgomery and Dr. Tershia Pinder-Grover and thank them for their help and advice during various stages of my doctoral degree. Prof. Hamid Ali and Seemi Rafique from my undergraduate institution, Aligarh Muslim University in India, need special mention for preparing me for grad school. The thorough teaching methods and clear explanations of Prof. Hamid Ali made me interested in pursuing Chemical Engineering as a career. Seemi Rafique deserves complete credit for sowing the idea of grad school in my heart and guiding me through the application steps. Had it not been for her, I would likely have never started grad school. She has also been a trusted personal mentor to me for over ten years now.

The current and previous members of the Fogler group need special mention. Everyday spent with them has been an exciting and enjoyable learning experience for me. Ryan Hartman, Prashant Singh, Kris Paso and Hyun Lee were excellent senior members who helped me establish myself during my initial years in the program. Ponchai Saelim and I started in the group together and I am thankful for his company and friendship as I was just figuring my way around in the domain of academic research. Kriangkrai Kraiwattanawong helped me in familiarizing myself with the theory and experiments related to asphaltenes and also taught me play tennis. Elizabeth Gorrepati and Michael Senra were amazing group members and we overlapped with each other for most of our

stay in the Fogler group. Their help, support and humor are greatly appreciated. Dr. Sasanka Raha helped me in laying the foundations of the population balance model and our late evening discussions on the intricacies of the model while taking a quick bite at Pierpont Commons makes me nostalgic. Dr. Probjot Singh has also been a great mentor and provided me with encouragement and helpful tips through all stages of my doctoral work, including job search. The younger members of the group brought in a lot of energy into the group and made it more fun to be in the office. Jason Huang has a unique way of livening things up and was always eager to take additional responsibility in running the group. Michael Hoepfner was a dependable group member and helped in streamlining the functioning of group activities. Nasim Haji Akbari Balou should not be mistaken due to her quiet demeanor… her questions and comments about asphaltenes were very thought provoking. The discussions that I had with Michael and Nasim were very helpful for my work and I hope that they benefitted from these discussions as well. I also had the privilege of working with several Masters and undergraduate students and without their help this work would be far from complete. I would like to thank Arjames (Jim) Balgoa, Perapat (Oat) Srikiratiwong, Claudio Vilas Boas Favero, Kelly Martin, Elisabeth Molina and Emily Moceri for their help in conducting experiments and for asking thought-provoking questions which helped me in shaping this research project. I would also like to thank the sponsors of the University of Michigan Industrial Affiliates Program for their financial support and intellectual contribution for this project.

The staff in the Department of Chemical Engineering have been very supportive through all these years and I would like to thank all of them for their help. Pablo LaValle helped me in brainstorming new experimental approaches and in reviewing the safety

aspects of these experimental protocols. Susan Hamlin was always on top of the paperwork and guided me through various administrative requirements of the doctoral program. Laura Bracken has been a helpful resource in organizing meetings and group travel and handling all the paperwork related to the research group. She was also very sensitive about the needs of the students and was a helpful interface between Prof. Fogler and the research group. Shelley Fellers was always willing to help with ordering supplies and arranging rooms for meetings. She maintained a patient and welcoming demeanor while addressing administrative needs of the graduate student community. Michael Africa was very helpful in maintaining the IT infrastructure for the research group and educating us about best practices in computing. He was also a good friend and our discussions frequently extended outside the world of computing but I was never able to convince him to love the PCs as much as the Macs.

My friends in Ann Arbor made life more fun and provided me the support that kept me going. I thank Yaseen Elkasabi, Javed Mannan, Shihan Khan, Bilal Mansoor, Deshpremy Mukhija, Abhishek Shetty, Zohair Ahmed, Khamir Mehta, Indranil Saha Dalal, Raghunandan Kainkaryam and Mohammed Sobhy for their camaraderie and will remember the time spent with them. The Quraishi brothers – Abdur Rahman, Umar, Usama, and Ali – taught me a lot about life in the United States… barbecuing, driving, swimming and are definitely among the most hospitable and friendly folks that I have come across. Abu Mokhtarul Hassan has been a true and trusted friend. His simplicity and willingness to listen are hard to find in the current times. My two other friends from undergrad – Mohd. Yusuf Ansari and Zaid Bin Khalid – showed immense confidence in my abilities and encouraged me to set the bar high for myself.

Being a family oriented person, I could be pretty homesick had it not been for the several families in Ann Arbor who treated me as one of their own. My stay in Ann Arbor was dotted with family get-togethers, tea times, home cooked meals and memorable playtimes with the kids in these families. I am indebted to the families of Mozaffarul Islam, Abdul Wakeel Quraishi, Mehboob Chishty, Hamid Chishty, Ahmed Chishty, Br. Haroon, Ajmal Malik, Asim Ashraf, Aarif Ahsan and Amjad Khan for filling what could have been a big void during my stay in Ann Arbor.

My family deserves special thanks for their love and support without which I would not have reached to this point in life. My parents – Mr. Ibrar Hassan and Mrs. Talat Siddiqui – have showered unconditional love upon me and I cannot thank them enough for being there for me whenever I needed them. The trust that they demonstrated in my decisions related to both personal life and career choices made me learn the balance between choice and responsibility. My sister, Naushin Ibrar, has been very affectionate, caring and supportive and I cherish the times that we have spent together. She has a unique way of bringing out the best in people without making them feel the least bit uncomfortable. My wife, Sameera Ahmed, was very supportive through the last stages of my doctoral work. Her love, care and motivation kept me going. She was very understanding when I had to spend a large portion of my time in finishing my dissertation. I thank my in-laws, Mr. Ahmed Ali Khan and Mrs. Sayeeda Ahmed and their family, for their support and prayers. Their love and hospitability are greatly appreciated. Finally, I am thankful to members of my extended family who have always rejoiced in my success and supported me in times of need.

I feel that I have been fortunate to come across so many wonderful people who have contributed to my success in many different ways and I thank Allah for this blessing.

TABLE OF CONTENTS

LIST OF TABLES

TABLE

LIST OF FIGURES

FIGURE

LIST OF APPENDICES

APPENDIX

ABSTRACT

The precipitation of asphaltenes from crude oils can lead to serious challenges during oil production and processing. This study investigates the kinetics of asphaltene precipitation from crude oils using n-alkane precipitants. For several decades, it has been understood that the precipitation of asphaltenes is a solubility driven phenomenon and the previous studies on the effect of time are usually limited to short time scales. By using optical microscopy and centrifugation based separation, we have demonstrated that the time required to precipitate asphaltenes can actually vary from a few minutes to several months, depending on the precipitant concentration used. Our results demonstrate that no single concentration can be identified as the critical precipitant concentration for asphaltene precipitation. Based on long term experiments, we have also been able to establish the solubility of asphaltenes as a function of the precipitant concentration and it is shown that the short-term experiments over-predict the solubility.

The effect of temperature on the precipitation kinetics of asphaltenes is also investigated and different competing effects have been identified. We demonstrate that at higher temperatures the precipitation onset time for asphaltenes is shorter and their solubility is higher. We also present a hypothesis to explain these results and demonstrate that the viscosity difference resulting from a change in temperature in the key parameter in the aggregation of asphaltenes and controls the onset time for precipitation. We also consider the effect of expansion of hydrocarbons, oxidation of crude oil and the loss of

light hydrocarbons due to evaporation, all of which are possible when temperature is increased.

In order to simulate the growth of asphaltene aggregates from the nanometer scale to micron-size particles a generalized geometric population balance model has been successfully developed. The Smoluchowski kernel has been incorporated to describe the aggregation of the asphaltene nanoaggregates that is induced by the addition of a precipitant e.g. heptane. The model has been validated with experimental data for various heptane concentrations and a good fit has been observed in each case. The particle size distribution (PSD) of the asphaltene aggregates as a function of time was also determined and it was observed that the shift of the PSD to larger diameters is faster in the case of higher heptane concentrations because of higher driving force for asphaltene aggregation.

Finally, it is shown that the asphaltenes that precipitate earliest in the precipitation process are the most unstable fraction. They have a higher dielectric constant and contain greater quantities of metals like Ni and V than other asphaltenes. Additionally, they also contain relatively larger quantities of the high polarity fractions as compared to the asphaltenes that precipitate later.

CHAPTER 1

INTRODUCTION

Background

The steady increase in the global energy demand has led to a renewed interest in research pertaining to the exploration, production and processing of crude oils which are complex mixtures of hydrocarbons containing a variety of components with different physical and chemical properties. Many of the difficulties encountered in oil production, transportation, and processing are related to the precipitation of asphaltenes in crude oils (Wattana 2004, Hammami 2007). Some of the adverse consequences of asphaltene precipitation include reservoir damage, reduction of well productivity, and plugging of the tubing and production facilities. The processing of asphaltenic oil in refinery operations causes storage capacity loss, equipment fouling, and catalyst deactivation, along with various process and control problems (Wattana 2004).

Asphaltene precipitation can occur at any point during production where the stabilizing equilibrium has been altered. Changes in temperature, pressure, and chemical composition of oil induced by production and enhanced oil recovery processes such as CO_2 flooding, acid stimulation and mixing a crude oil with diluents and other oils, can cause destabilization of asphaltenes (Islam 1994; Kleinitz and Andersen 1998).

Motivation for this research

The economic impact of the asphaltene problem is tremendous. In the early 1980s, it was estimated that asphaltene deposition could cause a loss of oil production rate of up to 3000 barrels per day and that blockage over a few days could cost approximately over half a million dollars (Adialalis 1982). As time has progressed, reservoirs of conventional light crude oil have been depleted, driving exploration towards heavier crude oil reservoirs which generally contain higher amounts of asphaltene. The oil industry is facing more difficult operations and the importance of the asphaltene deposition problem has significantly increased over the years. The serious economic nature of the problems associated with asphaltenes has motivated numerous investigations on asphaltenes. (Wattana 2004).

One of the major focus areas for asphaltene research is to identify the conditions which may lead to the precipitation of asphaltenes from crude oils. For the past several decades researchers have focused on developing a generalized understanding of asphaltene stability in crude oils by using a variety of experimental tools. By focusing on key factors like temperature, pressure and composition they have also attempted to develop several thermodynamic models to describe/identify the conditions leading to asphaltene precipitation. It has largely been assumed in the literature that asphaltene precipitation is relatively fast and there are no associated kinetic effects.

It should be noted that although the asphaltenes in a given crude oil may seem stable under certain conditions, there is no certainty that this system will not destabilize and precipitate asphaltenes at longer time scales. Without a good understanding of the

associated kinetic effects during the precipitation of asphaltenes, the thermodynamic models can provide misleading predictions for asphaltene stability. There is a lack of both experimental data and theoretical understanding to account for the kinetics of asphaltene precipitation.

This research aims to identify the key factors involved in the kinetics of asphaltene precipitation. The major focus is on variations in composition and temperature. Additionally, the development of a mathematical model for the aggregation of asphaltenes from the nanometer scale to the micron scale is also presented.

Literature Review

Crude oils are complex mixtures of hydrocarbons containing a variety of components with different physical and chemical properties. Often these components are divided into four major fractions: saturates, aromatics, resins, and asphaltenes (SARA) (Speight 1999).

Asphaltenes are considered to be one of the most problematic and the least understood organic deposits because of their complex chemical structure and composition (Wattana, 2004). Operationally defined on the basis of solubility, asphaltenes are the components of crude oils that are soluble in aromatics such as benzene and toluene, but are insoluble in light aliphatics such as pentane, hexane and heptane (Bestougeff and Byramjee 1994; Speight 1999). They are the most polar and heaviest component of crude oils.

Asphaltenes are precipitated from crude oils by adding n-alkane solvents, such as n-pentane or n-heptane, in an oil:precipitant volume ratio of at least l:40 (oil:precipitant). They are dark brown to black friable solids with no definite melting point. In addition to the classical definition, asphaltenes tend to be classified by the particular alkanes used to precipitate them. Thus, there are pentane asphaltenes, hexane asphaltenes and heptane asphaltenes.

Asphaltene Precipitation Studies:

In order to understand the stability of asphaltenes in crude oils and the factors governing it, several studies have focused on asphaltene precipitation from crude oil. Two of the common techniques are presented here:

(i) Refractive Index Measurement: Wattana *et al.* (2003) developed a technique based on the refractive index measurement to monitor the precipitation process and the stability of asphaltenes in crude oil. For a mixture in which there is no significant change of volume after mixing, the refractive index function of the mixture, *f (n)*, is equal to the sum of the refractive index functions of each individual component times its volume fraction (φ_i):

$$f(n) = \sum_i \varphi_i f_i(n)$$

$$\left(\frac{n^2-1}{n^2+2}\right) = \sum_i \varphi_i \left(\frac{n^2-1}{n^2+2}\right)_i$$

where, *n* is the refractive index of the substance.

Thus, for a binary mixture, a linear relationship exists between the refractive index function and the volumetric fraction of the components. When crude oil is titrated

with a precipitant, a point is reached when asphaltenes start to precipitate out from the solution of crude and precipitant. Asphaltenes are highly refractory components of the crude oil. When they precipitate out, they no longer contribute to the refractive index of the solution and a decrease in the refractive index of the solution is observed (Figure 1.1). Therefore, the onset of asphaltene precipitation is detected from the deviation of refractive index behavior from linearity (Wattana, 2003).

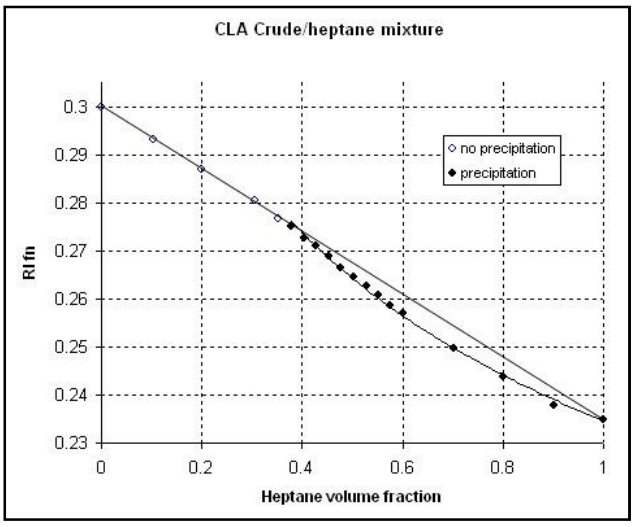

Figure 1.1 Determination of asphaltene precipitation onset point by refractive index technique (Wattana, 2003).

However, it needs to be pointed out that in these experiments samples of varying compositions were made and their refractive index was measured after a few minutes of mixing. Thus these results are valid only if asphaltene precipitation is instantaneous. The later chapters of this document show that asphaltene precipitation is a kinetic phenomenon and can take several hours, days, weeks or months in some cases. Additionally, this technique can only detect asphaltene precipitation if the asphaltene content of the crude oil is high, because it is based on bulk flocculation. If the crude oil

has very low asphaltene content, the change in refractive index upon the onset of precipitation will be minimal and will not be captured by the refractive index technique. In such circumstances, optical microscopy gives more precise results.

(ii) UV-visible Spectrophotometer Studies: Another method used to identify asphaltene precipitation is to titrate crude oil with an alkane and monitor its flocculation point using a spectrophotometer (Kraiwattanawong 2006). This is a simple and easy method to detect asphaltene precipitation onset under ambient or near ambient conditions because the sample preparation is less time-consuming and acquires data automatically.

The precipitation onset of asphaltene during titration with normal alkanes (asphaltene precipitants) is usually identified by the point of minimum light absorbance (Browarzik *et al.* 1999; ASTM D 6703 – 01). Kraiwattanawong et al. (2006) found that using the point of minimum light absorbance overpredicts the onset point as shown in Figure 1.2. The decrease in absorbance is due to the dilution of crude oil by the alkane, which makes the mixture lighter in color. When asphaltenes start to precipitate out, they provide hindrance to passage of light and hence increase the absorbance. However, at the exact onset of precipitation there is a very small amount of particles and hence the dilution effect dominates. Upon further dilution, more asphaltenes are precipitated, creating more obstruction to light, causing the absorbance to increase. Kraiwattanawong et al. (2006) suggested that a better technique to accurately identify the onset point was to plot a change in the slope of the absorbance as a function of the volume fraction of the normal alkane added. As shown in Figure 1.3, the absorbance slope remains relatively constant initially and then starts to increase at an alkane volume fraction of 0.58, which is the actual onset of precipitation. The ASTM method which defines the onset point as the

minimum of the absorbance curve (i.e. an alkane volume fraction of 0.62 in Figure 1.2), overpredicts the onset point.

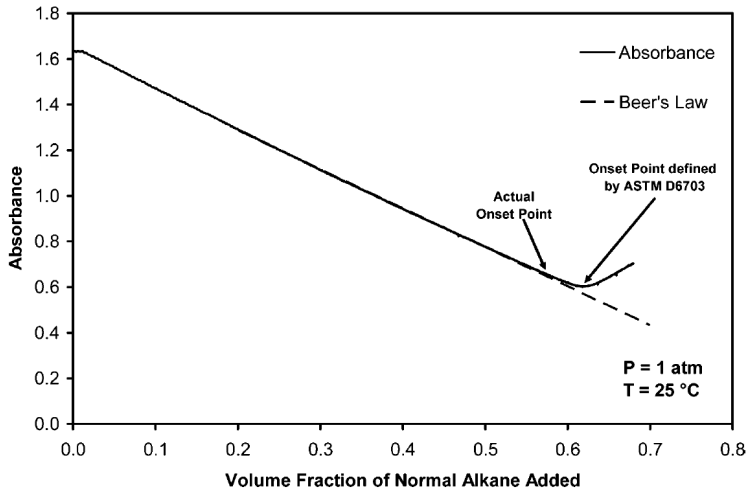

Figure 1.2 Absorbance of crude oil and precipitant mixture as a function of volume fraction of normal alkane added. Kraiwattanawong et al. (2006)

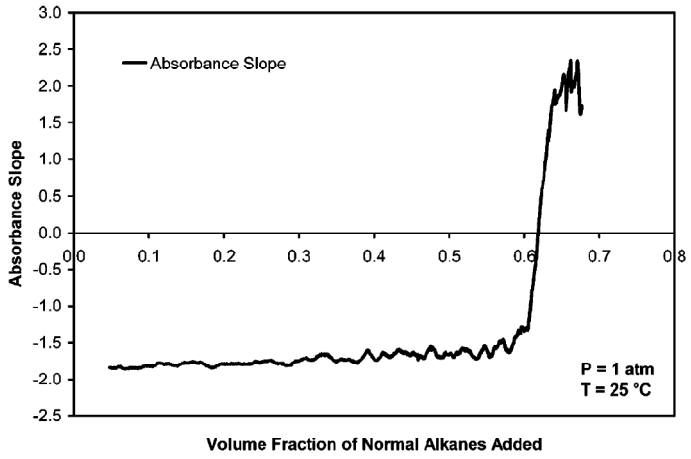

Figure 1.3 Absorbance slope as a function of volume fraction of normal alkane added. Kraiwattanawong et al. (2006)

In this technique, the crude oil is continuously titrated with the precipitant until the onset point is reached. Therefore, this technique also assumes that asphaltene precipitation is an instantaneous phenomenon. This approach is based on the subtle

assumption that if a crude oil – precipitant mixture is stable for the first hour or so after mixing, then it would be stable for an infinitely long time (i.e. the thermodynamic limit of solubility is reached within the first hour of the experiment). This assumption is largely unsubstantiated and the work of Angle *et al.* (2006) contradicts this assumption. This assumption also leads to an over prediction of the onset point and incorrect solubility values for asphaltenes in crude oils-precipitant mixtures.

Kinetics of Asphaltene Precipitation Using Optical Microscopy:

Angle *et al.* (2006) used optical microscopy to show the onset of asphaltene precipitation as a function of time and precipitant concentration. Most of the previous work in asphaltene precipitation does not consider the effect of time on precipitation of asphaltenes because the time-scale used for most of the previous experiments is less than one hour. Angle *et al.* (2006) showed that the onset of asphaltenes precipitation is a slow phenomenon and could take a few hours as shown in Figure 1.4.

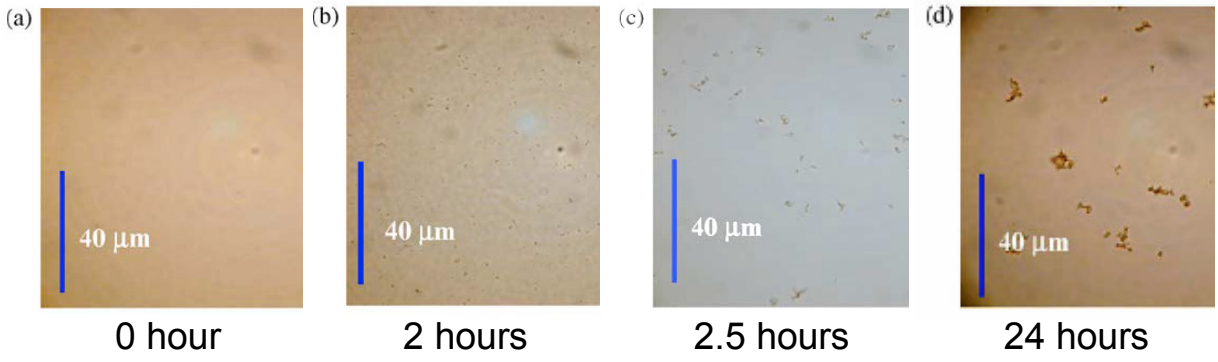

Figure 1.4 Micrographs of asphaltenes particles precipitated at different times for 10 wt% heavy oil in 90% toluene. (heptane/toluene mass ratio = 1.37). The asphaltene starts precipitating after 2 hours and then grows into larger clusters at later times. Angle et al. (2006)

In these experiments, the crude oil was diluted with 90% toluene before adding heptane. However, toluene is a very good solvent for asphaltenes. Therefore, it is difficult

to conclude if the observed kinetic effects were due to the delaying of the precipitation due to toluene addition or if there are kinetic effects inherently associated with the asphaltenes, irrespective of the presence of toluene.

Research objectives

For several of the studies discussed above, the measurements were taken either immediately after the preparation of the sample, or after a waiting period ranging from a few hours to 1-2 days. The choice of waiting time was not standardized and it was assumed that precipitation of asphaltenes reaches its thermodynamic limit within this experimental duration. Literature from the past several decades indicates that there is a critical concentration of the precipitant required for the asphaltenes to precipitate. Below this critical concentration (also known as the precipitation onset point), the asphaltenes were believed to be stable in the crude oil and would not precipitate (Escobedo 1995; Buckley 1999; Wang 2003; 2003; Mousavi-Dehghania 2004). ASTM International has also developed standard procedures for determining the precipitation onset point based on this approach (ASTM D 6703-01). Unfortunately, neglecting the effect of time leads to a major misconception about asphaltene stability, which will be discussed in the latter chapters.

The research presented here re-examines the conventional understanding of asphaltene precipitation from crude oil systems. The purpose of this study was to establish that the precipitant content of the crude oil – precipitant mixture determines the time required for the onset of asphaltene precipitation, the rate of growth of asphaltene aggregates, and the amount of asphaltenes precipitated at equilibrium. Therefore, by

varying the precipitant content, both kinetic and thermodynamic information pertaining to asphaltene precipitation from crude oils can be obtained.

The role of temperature on the kinetics of asphaltene precipitation is also not well understood because there can be various competing effects arising from temperature variations. Therefore, it is difficult to predict the overall impact of temperature. This research investigates the individual contributions of these competing effects in order to develop an overall understanding of how the variations in temperature can affect asphaltene precipitation kinetics.

Once a sound understanding of the role of precipitant concentration and temperature has been developed, the next step is to apply this knowledge to predict the precipitation kinetics for cases where conducting laboratory experiments may be challenging or even unrealistic. In order to achieve this goal, there is a need for a mathematical model capable of predicting the precipitation kinetics based on information about the crude oil, precipitant concentration and temperature. The development of the model and its validation with experimental data is discussed.

Brief Overview of Chapters

The chapters of this dissertation have been written in such a way that they can be read independently with a general knowledge of the relevant background. Each chapter represents a document prepared for either publication or information transfer. Because of this format, there may be some redundancy in the introductory material and references for the different chapters. An overview of the different chapters is provided here.

Chapter II provides a critical overview of the literature on the experiments and thermodynamic models related to asphaltene precipitation. The assumption that asphaltene precipitation is an instantaneous process is examined and experimental evidence is provided to demonstrate that this assumption is merely an experimental artifact. Novel experimental approaches for detecting the onset time for asphaltene precipitation and quantifying the amount of asphaltenes precipitated as a function of time are presented.

Chapter III extends the knowledge gained from Chapter II about the kinetics of asphaltene precipitation to incorporate the effect of temperature. The contributions of various competing arising due to temperature variations have been studied and compared to each other. Some of the key factors considered are changes is the viscosity, expansion of hydrocarbons, variation in the solubility of asphaltenes and oxidation of the crude oil resulting from temperature variations.

Chapter IV describes the development of a geometric population balance to model the aggregation of asphaltenes in the crude oil. The asphaltenes start as nanometer sized particles in the crude oil which get destabilized upon the addition of a precipitant and subsequently grown to micron size particles which can be detected by microscopy. The model is validated with experimental data from earlier chapters. A sensitivity analysis of the key parameters is also presented.

Chapter V describes the characterization of asphaltenes precipitated as a function of time. Asphaltenes are a polydisperse collection of molecules with varying properties.

Identifying the asphaltenes which precipitate at the earliest time will help in designing more effective treatment chemicals for asphaltene problems in the field.

Chapter VI provides an overall summary of the major conclusions of this research study and Chapter VII lists suggestions for future research directions relevant to understanding the kinetics of asphaltene precipitation from crude oils.

References

1. Adialalis, S. (1982) Investigation of physical and chemical criteria as related to the prevention of asphalt deposition in oil well tubings. M.Sc. Thesis, Imperial College, London.

2. Angle, C.W., Long, Y., Hamza, H., Lue, L. (2006) Precipitation of asphaltenes from solvent-diluted heavy oil and thermodynamic properties of solvent-diluted heavy oil solutions. Fuel 85, 492–506

3. ASTM D 6703 – 01 (2001) Standard test method for automated heithaus titrimetry. ASTM International

4. Bestougeff, M.A. and Byramjee, R.J. (1994) Chemical Constitution of Asphaltenes. Asphaltenes and Asphalts 1. T. F. Yen and G.V. Chilingarian. Amsterdam, The Netherlands: Elsevier, 40A: 67.

5. Browarzik, D., Laux, H. and Rahimian, I. (1999). Asphaltene flocculation in crude oil systems. Fluid Phase Equilibria, 154, 285–300.

6. Buckley J.S. Predicting the Onset of Asphaltene Precipitation from Refractive Index Measurements. Energy & Fuels 1999,13, 328-332.

7. Escobedo, J.; Mansoori, G.A. Viscosimetric Determination of the onset of asphaltene flocculation: a novel method. SPE Production and Facilities 1995, 10, 115-118.

8. Hammami, A.; Ratulowski, J. in Asphaltenes, Heavy Oils, and Petroleomics, O.C. Mullins; E.Y. Sheu; A. Hammami; A.G. Marshall, Eds.; Springer: New York, 2007; pp 617-660.

9. Islam, M.R. (1994) Role of asphaltenes on oil recovery and mathematical modeling of asphaltene properties. Asphaltenes and Asphalts 1. T. F. Yen and G.V. Chilingarian. Amsterdam, The Netherlands: Elsevier, 40A: 249-298.

10. Kleinitz, W. and S.I. Andersen (1998) Asphaltene properties in oil production wells. Oil Gas-European Magazine, 24(1), 30-33.

11. Kraiwattanawong, K., Fogler, H.S., Gharfeh, S.G., Singh, P., Thomason, W.H., and Chavadej, S. (2006) Thermodynamic solubility models to predict asphaltene instability in live crude oils. Energy & Fuels 2007, 21, 1248-1255

12. Mousavi-Dehghania, S. A.; Riazi, M. R.; Vafaie-Seftic, M. and Mansoori, G. A. An analysis of methods for determination of onsets of asphaltene phase separations. Journal of Petroleum Science and Engineering 2004, 42, 145-156.

13. Speight, J.G. (1999) The Chemistry and Technology of Petroleum. New York: Marcel Dekker, Inc.

14. Wang, J.X.; Buckley, J.S. Asphaltene Stability in Crude Oil and Aromatic Solvents - The influence of oil composition. Energy & Fuels 2003, 17, 1445-1451.

15. Wattana, P., Wojciechowski, D.J., Bolaños, G. and Fogler, H.S. (2003) Study of asphaltene precipitation using refractive index measurement. Petroleum Science and Technology, 21 (3-4), 591 – 613.

16. Wattana, P. (2004) Precipitation and characterization of asphaltenes. Ph.D. Thesis in Chemical Engineering, College of Engineering, University of Michigan – Ann Arbor.

CHAPTER 2

REVISITING ASPHALTENE PRECIPITATION FROM CRUDE OILS: A CASE OF NEGLECTED KINETIC EFFECTS

Introduction

The steady increase in the global energy demand has led to a renewed interest in research pertaining to the exploration, production and processing of crude oils which are complex mixtures of hydrocarbons containing a variety of components with different physical and chemical properties. Often these components of the oil are divided into four major fractions: saturates, aromatics, resins, and asphaltenes (SARA).[1] Asphaltenes are defined as the components of crude oils that are soluble in aromatics such as benzene or toluene, but are insoluble in light aliphatics such as n-pentane, n-hexane or n-heptane. They comprise of polycyclic aromatic hydrocarbons with a random distribution of heteroatoms (e.g. N, S, O) and trace metals (e.g. V, Ni, Fe).[1] In the laboratory, asphaltenes are typically precipitated from crude oils by adding n-alkanes, in an oil to precipitant volume ratio of 1:40. During oil production, changes in temperature, pressure, and oil composition induced by the production and enhanced oil recovery processes can cause destabilization of asphaltenes. The destabilized asphaltenes tend to aggregate into clusters and damage petroleum reservoirs (by blocking pore spaces), plug tubing and transportation facilities and foul downstream equipment causing a reduction in capacity

and productivity. These problems lead to severe economic consequences for the petroleum industry.

Previous work on asphaltene precipitation

In order to investigate the stability of asphaltenes in crude oils, numerous studies have been conducted on the thermodynamics of asphaltene precipitation. For example, optical microscopy has been used to study the precipitation of asphaltenes from crude oil-precipitant mixtures as a function of the precipitant concentration.[2] Researchers have also studied the refractive index of crude oil–heptane mixtures and used this approach to identify the conditions required for asphaltene precipitation.[3,4] Near-infrared light transmittance technique has also been utilized to detect the onset of asphaltene precipitation from crude oils upon titration with a precipitant.[5] This method was later improved by developing a more accurate approach for identifying the onset of precipitation using a UV–vis spectrophotometer.[6,7] The authors identified the onset of precipitation as the n–alkane concentration where the deviation from Beer's law starts. A viscosity–based method for the determination of the onset of precipitation has also been reported in literature.[8] At the onset of precipitation, precipitated asphaltenes increased the viscosity of the crude oil–precipitant mixture. Researchers have also used interfacial tension (IFT) of an oil/water system to define the onset of precipitation as the minimum amount of precipitant at which a sudden increase in IFT was observed and have noted that this phenomenon occurs due to the migration of precipitated asphaltenes to the oil/water interface.[9] Experiments have also been carried out using filtration to quantify

the amount of asphaltenes that precipitate from crude oils at a given precipitant concentration.[10,11]

In most of these experiments, the precipitation of asphaltenes is induced by adding precipitants directly into the crude oil or into solvent-diluted crude oils. An important parameter used to assess the chances of asphaltene precipitation is the "precipitation onset point" defined as the minimum volume of precipitant required to precipitate asphaltenes from the crude oil.[12] The terms onset of precipitation, onset of flocculation, onset of aggregation, and onset of asphaltene destabilization have been used interchangeably in asphaltene literature to refer to the formation of asphaltene particles from the crude oils. In this paper, the term "onset of precipitation" will be used for this purpose. Both, the precipitant concentration at the onset of precipitation and the amount of asphaltenes that precipitate from crude oils at a given precipitant concentration, are important parameters needed in developing a model for asphaltene precipitation. Several researchers have developed models [2,6,13-22] for predicting asphaltene stability in crude oils using the data from the different types of experiments listed earlier.

Goals of this study. For several of the studies discussed above, the measurements were taken either immediately after the preparation of the sample, or after a waiting period ranging from a few hours to 1-2 days. The choice of waiting time was not standardized and it was assumed that precipitation of asphaltenes reaches its thermodynamic limit within this experimental duration. Literature from the past several decades indicates that there is a critical concentration of the precipitant required for the asphaltenes to precipitate. Below this critical concentration (also known as the precipitation onset point), the asphaltenes were believed to be stable in the crude oil and

would not precipitate.[2-9,13-22] ASTM International has also developed standard procedures for determining the precipitation onset point based on this approach.[23] Unfortunately, neglecting the effect of time leads to a major misconception about asphaltene stability, which will be discussed in this paper.

The research presented here re-examines the conventional understanding of asphaltene precipitation from crude oil systems. The purpose of this study was to establish that the precipitant content of the crude oil – precipitant mixture determines the time required for the onset of asphaltene precipitation, the rate of growth of asphaltene aggregates, and the amount of asphaltenes precipitated at equilibrium. Therefore, by varying the precipitant content, both kinetic and thermodynamic information pertaining to asphaltene precipitation from crude oils can be obtained.

Materials and Methods

Materials. Two different chemical-free Alaskan crude oils were used in this study: K-1 oil and N-2 oil. HPLC grade heptane from Fisher Scientific was used as the asphaltene precipitant for both oils. Table 2.1 shows the SARA (Saturate, Aromatics, Resins, and Asphaltenes) analysis and the densities of the two oils used in this study. In order to remove water, sand and other particulates commonly present in field samples, both the oils used in this study were centrifuged at 2500 rpm for 10 hours before using them in the experiments.

Table 2.1 Properties of the crude oils used in this study

	K-1 Oil	N-2 Oil
SARA		
Saturates (wt%)	41.0	55.1
Aromatics (wt%)	28.5	23.6
Resins (wt%)	18.4	17.3
nC-7 Asphaltenes (wt%)	10.9	2.4
Loss (wt%)	1.2	1.6
Density @ 20°C (g/mL)	0.9218	0.8737

Detecting the Onset of Precipitation. Optical microscopy was used for studying asphaltene precipitation as a function of heptane concentration. An optical microscope from Nikon (Model: Eclipse E600) with a 50x objective lens was used to observe the asphaltene aggregates. A CCD camera from Sony (Model: AVC-D7) was connected to the microscope to capture the images. The first step was to make a crude oil – heptane mixture of desired heptane concentration. A known volume of crude oil was taken in a 25 mL flask. A specified volume of heptane was then added to the crude oil, based on the final vol. % of heptane desired in the mixture. The crude oil was kept well-stirred using a magnetic stirrer and heptane was added at a rate of 1 mL/min using a syringe pump until the desired heptane concentration was attained. The heptane flow was then stopped and the flask was sealed with a stopcock to prevent heptane evaporation and to limit the exposure to air. Care was taken to ensure that the heptane concentration was precise because the onset time varies exponentially with heptane concentration, as shown in our results later. To ensure the experimental accuracy, heptane and crude oil amounts were measured on a mass basis and these values were subsequently converted to vol. %. The heptane concentration for these experiments was accurate to ±0.05 vol. %. When heptane is added to the crude oil, it is important that there is a good degree of mixing, otherwise

regions of localized high heptane concentration may be formed leading to instantaneous precipitation of asphaltene. In the next step, 10 μL samples were withdrawn at different times using a micro-pipette and were placed on a microscope slide and covered with a cover slip. Images of all samples were recorded and compared with each other to determine the time required to for the first appearance of asphaltene particles, which is referred to as the precipitation onset time.

Quantification of Asphaltene Precipitation. A centrifugation based separation technique was developed to quantify the amount of asphaltenes precipitated as a function of time. A centrifuge from Eppendorf (Model: 5415 C) was used for these experiments. The centrifuge is rated to 14,000 revolutions per minute (RPM) corresponding to a relative centrifugal force (RCF) of 16,000g. In these experiments, 130 mL of the crude oil – heptane mixture of desired heptane concentration was prepared using a similar method as described above. The mixture was stirred using a magnetic stirrer to ensure homogeneity. 1.5 mL samples were withdrawn from the well-stirred mixture at different times and weighed. Each sample was centrifuged at 14,000 RPM for 10 minutes causing the asphaltene particles to settle at the bottom of the centrifuge tube. The liquid is decanted to separate it from the asphaltene particles which form a compact cake in the bottom of the tube. The inside walls of the centrifuge tube were then wiped with a cleaning tissue to remove the traces of oil sticking to the walls. The asphaltenes were then washed several times with heptane to remove the minor quantity of crude oil adhering to the asphaltene particles, dried in an oven and weighed.

All the microscopy and centrifugation experiments were conducted at room temperature and the samples were kept well stirred for the entire duration of the experiments.

Results and Discussion

Investigating Kinetics of Precipitation Using Microscopy. Figure 2.1 shows the micrographs for an experimental run with 50 vol. % heptane at various times. At t = 0 and 0.5 hours, it is observed that the sample is uniform, with no particles present (Figure 2.1 A, B). Around t = 0.9 hours, some haze (equivalent to particles that are 0.2-0.3 μm in diameter) is observed. Then, at t = 1.4 hours, distinct particles are seen (equivalent to a size of about 0.5-0.6 μm). From 1.4 hours to 2.5 hours, the number of detectable particles increases with a slight increase in the particle size as well. Finally, at 20 hours, the particles have grown to larger sizes – about 2-3 μm in diameter. When using optical microscopy, previous researchers have defined the appearance of 0.5 μm particles as the onset of asphaltene precipitation (which is close to the resolution limit of most optical microscopes).24 For the sake of comparison, we selected the same criterion and identified t = 1.4 hours as the "precipitation onset time" based on the first appearance of 0.5 μm particles for 50 vol. % heptane in K-1 crude oil. It is worth mentioning that "precipitation onset time" is a functional definition and it does not necessarily indicate a phase change of asphaltenes in crude oil to produce asphaltene particles of 0.5 μm initial size. The transition from haze to well-defined particles (Figure 2.1) shows that asphaltene particles smaller than 0.5 μm are already present at t = 0.9 hours but cannot be observed distinctly because of the limitations of the microscope. A more realistic mechanism for

the generation of these micron-size asphaltene particles is presented in the discussion section. Similar runs were performed with different heptane concentrations for K-1 and N-2 oils. The precipitation onset time varies between few minutes and several months, depending on the heptane concentration (Figure 2.2).

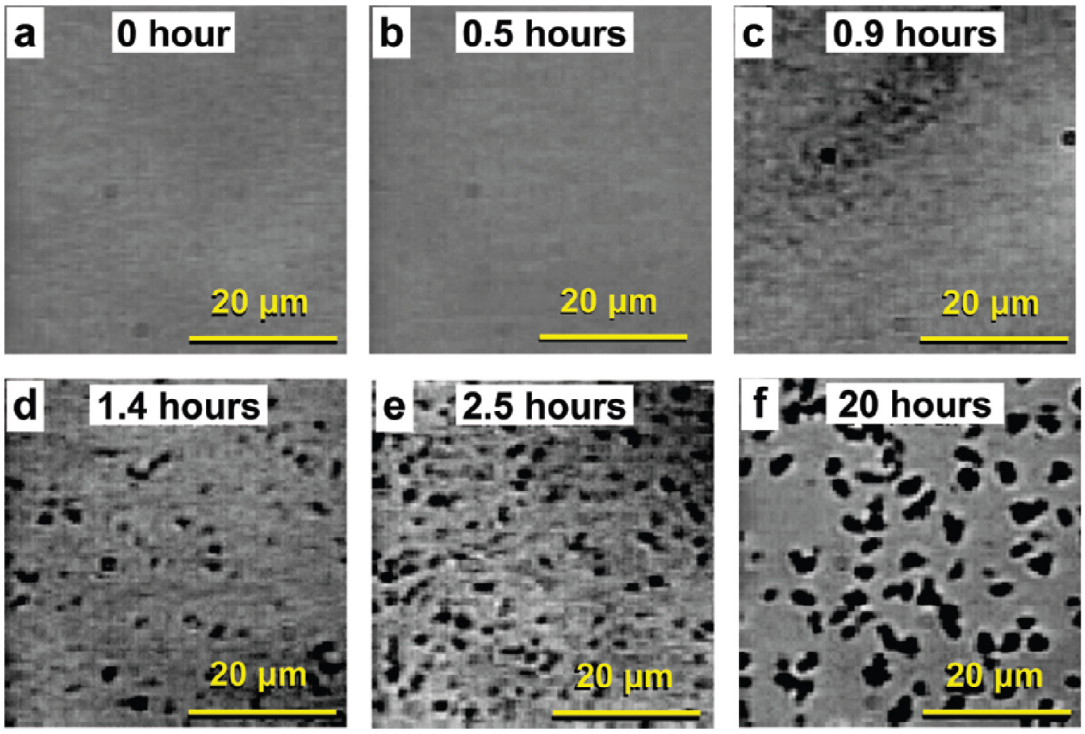

Figure 2.1 Micrographs showing the time dependence of asphaltene precipitation for a crude-heptane mixture containing 50 vol. % heptane and 50 vol. % K-1 crude oil.

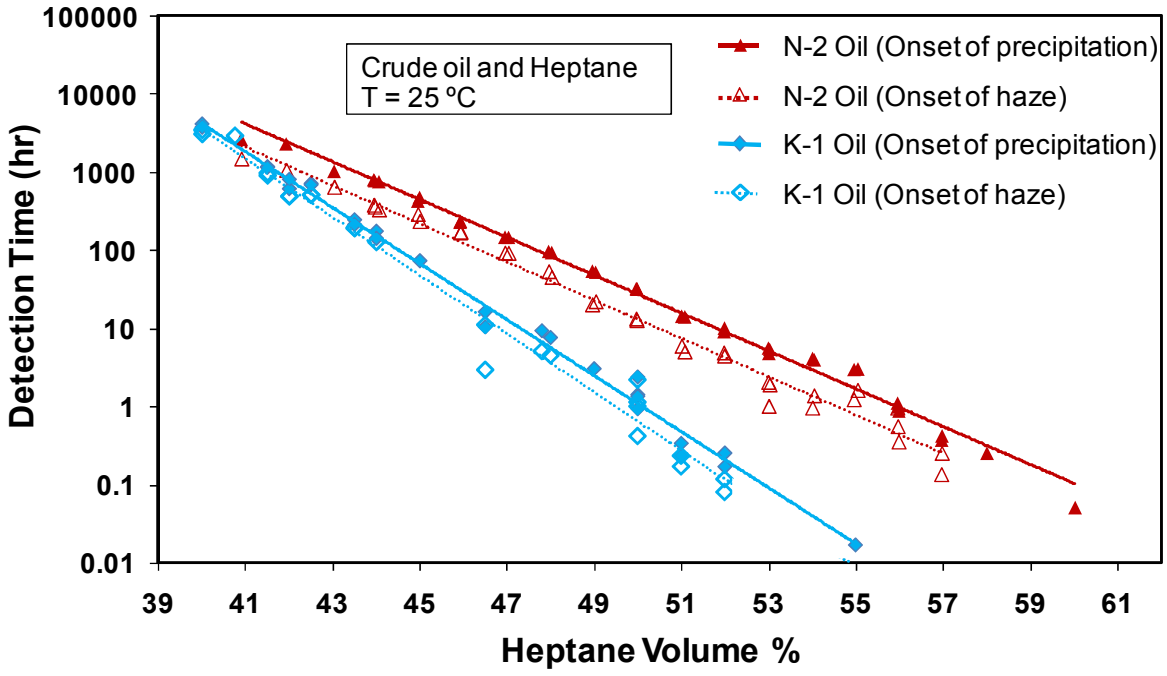

Figure 2.2: Detection times for onset of precipitation and onset of haze for varying heptane concentrations using K-1 and N-2 crude oils.

The data clearly demonstrates that the formation of asphaltene particles in crude oils is a kinetic phenomenon with similar trends for two different types of crude oils. The dotted lines in Figure 2.2 show the onset times for haze when the particles are 0.2-0.3 µm. These findings show that the previous experimental work [2,3,6,8,13,22-26] and modeling approaches [2,6,13,15,17-22] based on short time-span experiments, focus only at precipitation with relatively high precipitant concentration. For example, 46.5 vol. % heptane is the lowest precipitant concentration that will precipitate the asphaltenes in K-1 oil for an experiment lasting 24 hours (Figure 2.2). Based on the 24-hour experimental criteria commonly used in studying asphaltene precipitation, all concentrations lower than 46.5 vol. % heptane will be incorrectly identified as thermodynamically stable. We note from Figure 2.2 that the precipitation onset time increases exponentially with decreasing

heptane concentration. Therefore, no *critical precipitant concentration* exists for asphaltene precipitation.

Quantifying asphaltene precipitation. Centrifugation experiments provide further insight into the kinetics of asphaltene precipitation. Figure 2.3 shows the weight percentage of asphaltenes precipitated as a function of the time elapsed after the crude-oil heptane mixtures were prepared. For 46.5 vol.% heptane, the amount of precipitated asphaltenes gradually increases over a few hundred hours and reaches a plateau value of 3.5 wt% at around 400 hours (Figure 2.3A). This plateau value of precipitated asphaltenes represents the actual amount of asphaltenes precipitated for 46.5 vol. % heptane at equilibrium. As the heptane concentration is increased, the trend remains the same, but the plateau height increases and the time required to reach the plateau decreases sharply, to the extent that at 70.0 vol. % heptane the plateau is reached virtually instantaneously (Figure 2.3). The 55 vol. % heptane mixture has a precipitation onset time of one minute (Figure 2.2) and can be referred to as the concentration of heptane needed for "instantaneous" asphaltene precipitation. For precipitant concentrations well above the instantaneous precipitation (e.g. at 70.0 vol. % heptane when using K-1 crude oil), the precipitation kinetics are very fast and the data from short time-scale experiments will be reasonably close to the plateau value shown in Figure 2.3D. At precipitant concentrations below the instantaneous precipitation, the precipitation process is slow and can take days, weeks, months or even years to reach the plateau. It can be concluded from Figure 2.3 that at lower heptane concentrations, a smaller amount of asphaltenes is precipitated at equilibrium, and a longer time is required for reaching equilibrium

solubility. The slower kinetics with lower heptane concentrations are also supported by the results of the microscopy experiments discussed earlier.

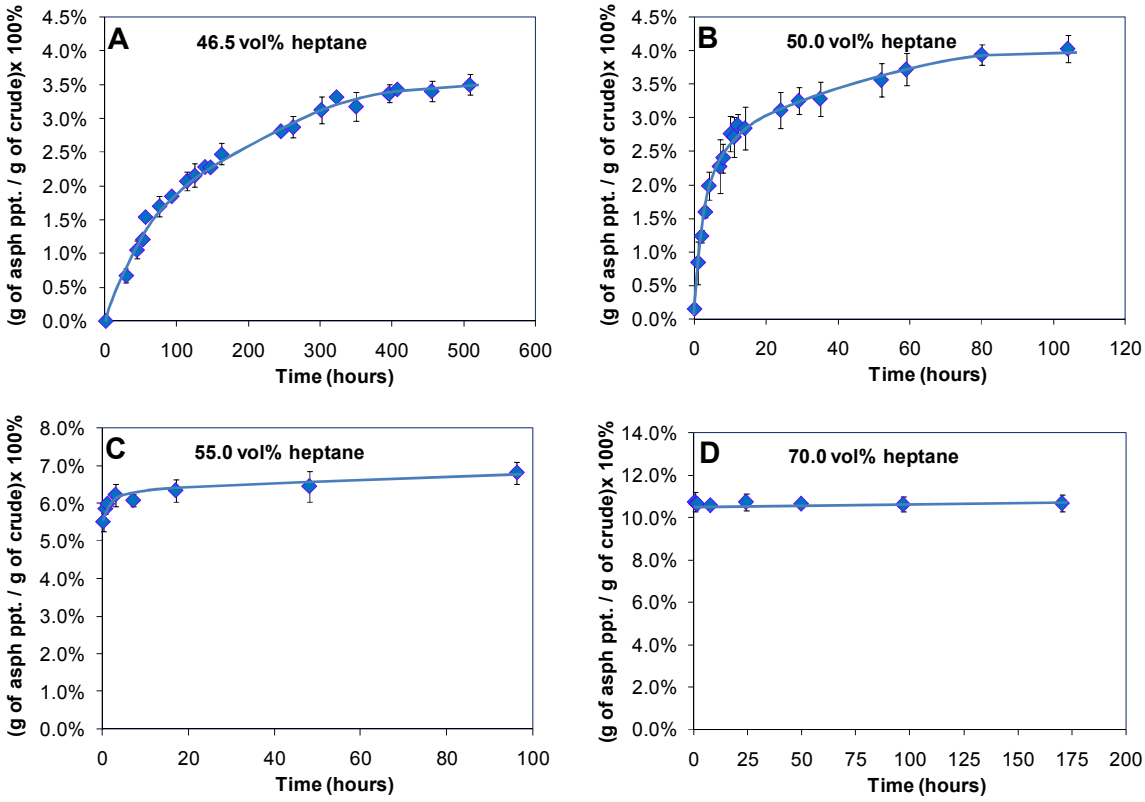

Figure 2.3 Amount of asphaltenes precipitated as a function of time for K-1 crude oil for varying heptane content (a) 46.5 vol. % heptane (b) 50.0 vol. % heptane (c) 55.0 vol. % heptane (d) 70.0 vol. % heptane (Note: Different time scales have been used for the x-axis for different concentrations).

In order to calculate the correct thermodynamic solubility of asphaltenes in crude oil as a function of precipitant concentration, the plateau values from Figure 2.3 (which correspond to the amount of asphaltenes precipitated at equilibrium) are subtracted from the total asphaltene content of the crude oil. Based on the SARA analysis, the total asphaltene content of the crude oil is 10.9 wt%. (Table 2.1). As seen in Figure 2.4A, the solubility of asphaltenes decreases with increasing heptane content and reaches essentially zero at 70 vol.% heptane. i.e. the amount of asphaltenes precipitated with 70

vol.% heptane is in good agreement with the total asphaltene content in the crude oil, based on 40:1 ratio of precipitant to oil. This graph is representative of the equilibrium amount of asphaltenes precipitated at different heptane concentrations which is an important parameter in understanding and modeling the stability of asphaltenes in crude oils.

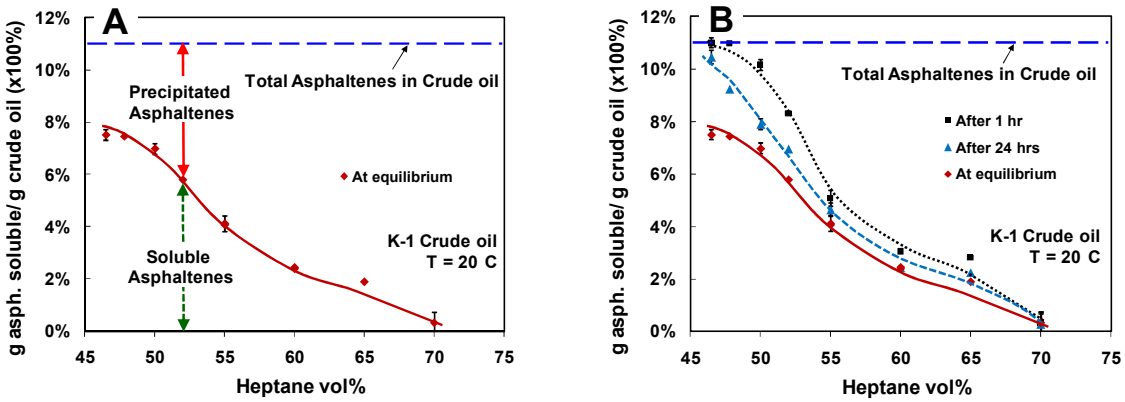

Figure 2.4: Solubility of asphaltenes in crude oil as a function of heptane concentrations with K-1 crude oil: (a) Calculation of the solubility at equilibrium (b) Comparison of asphaltene solubility at varying times after oil-precipitant mixture has been made.

Additionally, it should be noted that when the weight % of precipitated asphaltenes were measured at only 1 hour and 24 hours instead of at equilibrium, significant differences in asphaltene solubility were observed. Figure 2.4 clearly demonstrates that the solubility of asphaltenes will be overestimated if the data from shorter experiments is used. These errors are more significant at lower precipitant concentrations. From Figure 2.4 it is clear that different amounts of asphaltenes precipitate at different precipitant concentrations. Asphaltenes in crude oil are a polydisperse system having a distribution of molecular weight, heteroatom content and stability. The most unstable asphaltenes would tend to precipitate at low precipitant concentrations. As the precipitant concentration is increased, the relatively stable

asphaltenes also start to precipitate out. At very high precipitant concentrations, asphaltenes of all levels of stability are precipitated out. An analysis of different stability fractions of asphaltenes as a function of precipitant concentration will help in elucidating this point and will form the basis for potential future work.

In an earlier work by Beck *et al.* on asphaltene precipitation, it has been discussed that asphaltene yields can be affected by oxidation.[26] Due to several differences in our work and that of Beck *et al.* we conclude that the effect of oxidation is minimal, if it exists at all, for our experiments. Beck *et al.* demonstrated that with higher heptane concentration, the *change in asphaltene yield* over time is greater than that at lower heptane concentrations and have attributed it to oxidation effects. In our experiments, this *change in yield* with time decreases as heptane concentration is increased, which is contrary to the observations of Beck *et al.* Additionally, they reported that the yield of asphaltenes continued to increase "for as long as these samples were observed; that is, several months."

From Figure 2.3, it is clear that once the plateau is reached for our experiments, the yield remains constant (within experimental error), which also does not match with the observations of Beck *et al.* To further establish that the yield does not change with time after the plateau has been reached, the results for N-2 crude oil (where the experiments were conducted for several months) are included in Figure 2.5. It is evident that at 60 vol.% heptane, the asphaltene yield reaches a plateau in about 850 hours (~ 35 days) and then remains constant for the rest of the experiment up to the last data point at about 1800 hours (~75 days).

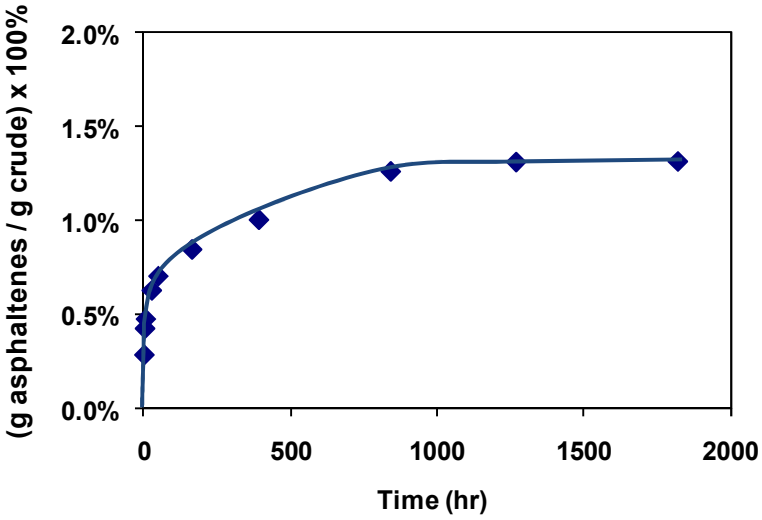

Figure 2.5 Amount of asphaltenes precipitated as a function of time for N-2 crude oil for 60 vol% heptane. (Note: The precipitation onset time for this oil is reported in Figure 2.2)

One reason for the differences in results reported in literature and our work may be the nature of asphaltene sources used for the experiments. The K-1 and N-2 oils used in our study are chemical-free crude oils from the field. Beck *et al.* used coker feed bitumen. Depending on the chemical nature and processing history of the bitumen sample used by Beck *et al.*, the nature of asphaltenes may be significantly different than that for the crude oils used in our study, which may cause the differences in the results mentioned earlier. Another possible effect could be the degree of the samples' exposure to air during the experiments. In our work, the exposure to air was not entirely eliminated but was significantly reduced by using sealed Erlenmeyer flasks which were opened for 30 seconds only at the sampling times. We also tried to minimize the air in the flask by keeping the headspace to a minimum. The precautions seem to have helped in minimizing the effect of oxidation during our experiments.

In order to explain the microscopy and centrifugation results presented here, the physical state of asphaltenes, as they exist naturally in crude oil, must be examined. Recent work has shown that asphaltenes exist in crude oils, not as dissolved molecules, but as nanoparticles that can further aggregate.[27-29] The mechanism we propose is that when heptane is added to the crude oil, it disturbs the stability of the asphaltene nanoparticles in the oil by altering the solvent properties of the oil. When these destabilized asphaltene nanoparticles collide with each other, they can aggregate to form larger particles. These aggregates continue growing from the nano-scale until they reach the micron-scale and can subsequently be seen under the optical microscope. The appearance of the haze before the appearance of definitive 0.5 μm asphaltene particles Figure 2.1 supports this hypothesis. It has been shown in our work that kinetics of aggregation can be very slow. The most likely reason for this observation is that the process of the destabilized asphaltene nanoaggregates finding each other and aggregating together may be slow. Additionally, some of the interactions between the nanoaggregates may not be strong enough and some deaggregation may also take place during the course of the experiments. At higher heptane concentrations, the aggregation is faster because more asphaltene nanoparticles are destabilized. Additionally, the reduction in the oil viscosity by heptane addition also increases the collision frequency of asphaltene nanoparticles, thus promoting faster aggregation. The appearance of 0.5 μm asphaltene particles is not a solid-liquid phase change phenomenon at the molecular scale, but is a colloidal destabilization and aggregation of asphaltene nanoparticles to reach the micron size. For the short-duration *asphaltene precipitation* experiments reported in literature, the systems have been overdriven due to addition of a high amount of precipitant.

Therefore, aggregation happens very quickly in these systems, leading to an incorrect perception that asphaltene molecules are precipitating out from the solution as 0.5 μm particles. Additionally, in the previous studies on *asphaltene aggregation*, the systems were similarly overdriven to high precipitant concentrations, which results in rapid formation of asphaltene particles of about 0.5 μm (or greater) in size and the relatively slow growth of these particles to larger sizes was subsequently monitored.[30-34] We note that in our proposed mechanism the first particles to aggregate are at the nano-scale; three orders of magnitude smaller than micron-size initial particles reported in these earlier studies on asphaltene aggregation. It should also be mentioned that in a previous work on kinetics of asphaltene precipitation, the crude oil was diluted with toluene before adding heptane in order to reduce the opacity of crude oil.[31] However, toluene is a very good solvent for asphaltenes. Therefore, it is difficult to conclude if the observed kinetic effects were due to a delay in precipitation caused by toluene addition or if there are kinetic effects inherently associated with the precipitation of asphaltenes, irrespective of the presence of toluene.

The implications of the current work can be extended to other research areas where the system requires extended time to reach equilibrium. In a recent work on protein precipitation, researchers showed that extended experimental time was required to determine the correct equilibrium solubility of lysozyme in solutions.[35] They have demonstrated that the effect of time, which has been previously neglected in their field, is indeed important in understanding the complete process of lysozyme precipitation.

Conclusions

Most studies on thermodynamics of asphaltene stability have neglected the kinetic effects associated with the precipitation and aggregation of asphaltenes. The experimental duration of these studies generally varies between near-instantaneous to one day, implicitly assuming that the system will reach equilibrium in this short time-span. These short time span experiments can provide misleading results because systems that appear to be stable are actually unstable at longer times, as shown in this study using two different crude oils. Our study shows that in order to understand the destabilization of asphaltenes from crude oils, the associated kinetic effects must be considered. Data from microscopy and centrifugation experiments demonstrates that depending upon the precipitant concentration, the onset time for asphaltene precipitation can vary from a few minutes to several months. We have also shown that the commonly referred criteria of a critical precipitant concentration required for asphaltene precipitation is not a fundamental parameter, but an experimental artifact originating from the relatively short waiting times used in the earlier studies. Therefore, the application of thermodynamic models using short term experimental data may need to be reexamined. In order to get the correct thermodynamic values, the experiments need to be conducted over long periods and by using this approach we have been able to obtain the solubility of asphaltenes as a function of the precipitant concentration. The research presented here opens up a new paradigm for the understanding of asphaltene stability in crude oils and for the related thermodynamic approaches.

References

1. Hammami, A.; Ratulowski, J. in Asphaltenes, Heavy Oils, and Petroleomics, O.C. Mullins; E.Y. Sheu; A. Hammami; A.G. Marshall, Eds.; Springer: New York, 2007; pp 617-660.

2. Wang, J.X.; Buckley, J.S. Asphaltene Stability in Crude Oil and Aromatic Solvents - The influence of oil composition. Energy & Fuels 2003, 17, 1445-1451.

3. Wattana, P.; Wojciechowski, D. J.; Bolaños, G.; Fogler, H. S. Study of Asphaltene Precipitation using Refractive Index Measurement. Petroleum Science and Technology 2003, 21, 591 – 613.

4. Buckley J.S. Predicting the Onset of Asphaltene Precipitation from Refractive Index Measurements. Energy & Fuels 1999,13, 328-332.

5. Gharfeh S.; Yen A.; Asomaning S.; Blumer D. Asphaltene Flocculation Onset determinations from Heavy crude oil and its implications. Petroleum Science & Technology 2004, 22, 1055-1072.

6. Kraiwattanawong K., et al. Thermodynamic solubility models to predict asphaltene instability in live crude oils. Energy & Fuels 2007, 21, 1248-1255.

7. Kraiwattanawong, K., et al., Effect of Asphaltene Dispersants on Asphaltene Size Distribution and Aggregation. Energy & Fuels. in press (available at http://pubs.acs.org/doi/abs/10.1021/ef800706c).

8. Escobedo, J.; Mansoori, G.A. Viscosimetric Determination of the onset of asphaltene flocculation: a novel method. SPE Production and Facilities 1995, 10, 115-118.

9. Mousavi-Dehghania, S. A.; Riazi, M. R.; Vafaie-Seftic, M. and Mansoori, G. A. An analysis of methods for determination of onsets of asphaltene phase separations. Journal of Petroleum Science and Engineering 2004, 42, 145-156.

10. Hong, E.; Watkinson, P. A study of asphaltene solubility and precipitation. Fuel 2004, 83, 1881-1887.

11. Galeana, C.L.; Buenrostro, E.; Gil-Villegas, A.; Wu, J. Asphaltene Precipitation in Crude Oils: Theory and Experiments. AIChE Journal 2004, 50, 2552-2570.

12. Pina, A.; Mougin, P.; Béhar E. Characterization of asphaltenes and modeling of flocculation-state of the art. Oil & Gas Science and Technology - Rev. IFP 2006, 61, 319-343.

13. Alboudwarej, H.; Akbarzadeh, K.; Beck, J.; Svrcek, W.Y.; Yarranton, H.W. Regular solution model for asphaltene precipitation from bitumens and solvents. AIChE Journal 2003, 49, 2948-2956.

14. Mohammadi, A.H.; Richon, D. A Monodisperse Thermodynamic Model for Estimating Asphaltene Precipitation. AIChE Journal 2007, 53, 2940 -2947.

15. Hirschberg, A.; deJong, L.N.J.; Schipper, B.A.; Meijer, J.G. Influence of Temperature and Pressure on Asphaltene Flocculation. Soc. Pet. Eng. J. 1984, 24, 283-293.

16. Ting, P.D.; Gonzales, D.L.; Hirasaki, G.J.; Chapman, W.G. in Asphaltenes, Heavy Oils, and Petroleomics, O.C. Mullins; E.Y. Sheu; A. Hammami; A.G. Marshall, Eds; Springer: New York, 2007; pp 301-325.

17. Garcia, D.M.; Correra, S. A Shortcut Application of a Flory-Like Model to Asphaltene Precipitation. Journal of Dispersion Science and Technology 2007, 28, 339-347.

18. Donaggio, F.; Correra, S.; Lockhart, T.P. Precipitation Onset and Physical Models of Asphaltene Solution Behavior. Petroleum Science and Technology 2001, 19(1&2), 129-142.

19. Cimino, R.; Correra, S.; Del Bianco, A.; Lockhart, T.P. in Asphaltenes Fundamentals and Applications, E.Y. Sheu; O.C. Mullins, Eds.; Plenum Press: New York, 1995; pp 97-130.

20. Mohammadi, A.H.; Richon, D. The Scott-Magat Polymer Theory for Determining Onset of Precipitation of Dissolved Asphaltene in the Solvent + Precipitant Solution. The Open Thermodynamics Journal 2008, 2, 13-16.

21. Wiehe, I.A. & Kennedy, R.J. The Oil Compatibility Model and Crude Oil Compatibility. Energy & Fuels 2000, 14, 56-59.

22. Wiehe, I.A.; Yarranton, H.W.; Akbarzadeh, K.; Rahimi, P.M.; Teclemariam, A. Paradox of Asphaltene Precipitation with Normal Paraffins. Energy & Fuels 2005, 19, 1261-1267.

23. ASTM International, Standard Test Method for Automated Heithaus Titrimetry (ASTM D6703-07, 2008; http://www.astm.org/Standards/D6703.htm)

24. Wang, J.X.; Buckley, J.S. In Proceedings of the 2001 SPE International Oilfield Chemistry Symposium, Houston, TX, 13 February 2001.

25. de Sousa, M.A.; Oliveira, G.E.; Lucas, E.F.; Gonzales, G. The onset of Precipitation of Asphaltenes in Solvents of Different Solubility Parameters. Prog. Colloid Polym Sci. 2004, 128, 283-287.

26. Beck, J.; Svrcek, W.Y.; Yarranton, H.W. Hysteresis in Asphaltene Precipitation and Redissolution. Energy & Fuels 2005, 19, 944-947

27. Betancourt, S.S. et al., Nanoaggregates of Asphaltenes in a Reservoir Crude Oil and Reservoir Connectivity. Energy & Fuels. in press (available at http://pubs.acs.org/doi/full/10.1021/ef800598a).

28. Mason, T.G.; Lin, M.Y. Time-resolved small angle neutron scattering measurements of asphaltene nanoparticle aggregation kinetics in incompatible crude oil mixtures. Journal of Chemical Physics 2003, 119, 565-571.

29. Mason, T.G.; Lin, M.Y. Asphaltene nanoaggregation in mixtures of incompatible crude oils. Physical Review E 2003, 67, 050401-1.

30. Angle, C.W.; Long, Y.; Hamza, H.; Lue, L. Precipitation of asphaltenes from solvent-diluted heavy oil and thermodynamic properties of solvent-diluted heavy oil solutions. Fuel 2006, 85, 492-506.

31. Rastegari, K.; Svrcek, W. Y.; Yarranton, H. W. Kinetics of asphaltene flocculation. Ind. Eng. Chem. Res. 2004, 43, 6861-6870.

32. Burya, Y.G.; Yudin, I.K.; Dechabo, V.A.; Kosov, V.I.; Anisimov, M. A. Light Scattering study of petroleum asphaltene aggregation. Applied Optics 2001, 40, 4028-4035.

33. Oh, K.; Deo, M in Asphaltenes, Heavy Oils, and Petroleomics, O.C. Mullins; E.Y. Sheu; A. Hammami; A.G. Marshall, Eds; Springer: New York, 2007; pp 469-487.

34. Hung, J.; Castillo, J.; Reyes, A. Kinetics of asphaltene aggregation in toluene-heptane mixtures studied by confocal microscopy. Energy & Fuels 2005, 19, 898-904.

35. Cheng, Y.; Lobo, R.F.; Sandler, S.I.; Lenhoff, A.M. Kinetics and equilibria of lysozyme precipitation and crystallization in concentrated ammonium sulfate solutions. Biotechnology and Bioengineering 2006, 94, 177-188.

CHAPTER 3

THE EFFECT OF TEMPERATURE ON THE PRECIPITATION KINETICS OF ASPHALTENES

Introduction

The petroleum crude is a complex mixture of hydrocarbons with varying physical and chemical properties. These components of the oil are divided into four major fractions: saturates, aromatics, resins, and asphaltenes (SARA).[1] Asphaltenes are defined as the components of crude oils that are soluble in aromatics such as benzene or toluene, but are insoluble in light alkanes such as n-pentane, n-hexane or n-heptane. Asphaltene molecules comprise of polycyclic aromatic hydrocarbons with a varying distribution of heteroatoms (e.g. N, S, O) and trace metals (e.g. V, Ni, Fe).[1] Asphaltenes can be destabilized during oil production due to variations in temperature, pressure, and oil composition. The destabilized asphaltenes tend to aggregate into clusters and damage petroleum reservoirs (by blocking pore spaces), plug tubing and transportation facilities and foul downstream equipment causing a reduction in capacity and productivity.

In this paper, we explore the effect of temperature on the kinetics of asphaltene precipitation from crude oils upon the addition of an n-alkane precipitant. Temperature is an important parameter for the stability of asphaltenes in crude oils. Both upstream and downstream processes involve temperature variations which can cause the precipitation

of asphaltenes leading to deposition and fouling problems during the production, transportation and processing of crude oils.[1-4]

The effect of temperature on asphaltene stability can be complex and various competing effects can be identified. The first factor is the solubility of asphaltenes which increases with increasing temperature.[1,2] Consequently, a smaller mass of asphaltenes will precipitate at higher temperatures. As discussed in our earlier work, the mechanism of asphaltene precipitation can be described as a process of destabilization of asphaltene nanoaggregates from the crude oil due to the addition of a precipitant. The destabilization is followed by their subsequent aggregation and particle growth. When the particles reach the micron size they become detectable by optical microscopy and other techniques.[7] Using this solubility argument, it can be proposed that the total mass of asphaltene nanoaggregates destabilized by the addition of n-alkanes at elevated temperatures is lesser than that at lower temperatures. Therefore, one hypothesis is that the lower initial mass (and concentration) of the destabilized asphaltene aggregates at higher temperatures could lead to a lesser number of particle collisions resulting in a slower rate of aggregation. Consequently, it could take the particles longer time to reach to the micron size and be detected by optical microscopy.

The second factor is the variation in liquid composition due to heating. As the oil-precipitant mixture is heated, its lighter fractions, predominantly alkanes, expand and effectively reduce the solubility parameter of this mixture, making the asphaltenes less soluble in it. This process is analogous to a reservoir situation where the asphaltenes become more unstable as the crude oil is depressurized from the reservoir pressure to the bubble point pressure.[1,8,9] Therefore, it can be argued that at higher temperatures the

lower solubility of asphaltenes will lead to faster aggregation and shorter onset time for the detection of precipitation. The precipitant used is also an important consideration in investigating role of temperature on the solubility of asphaltenes and different trends have also been reported in literature. For instance, it had been reported that in propane, asphaltenes become less soluble as temperature increases.[10] However, for titrations with heavier alkanes, e.g., C5+, asphaltene stability increases with increasing temperature.[11-13] *Vargas et al.*[14] have used PC-SAFT equation of state to model how asphaltene solubility can either increase or decrease with increasing temperature and validated their approach using the data from Jamaluddin et al.[15]

The next factor is the role of viscosity on the rate of aggregation.[16] The liquid medium in this case is the oil-precipitant mixture in which the asphaltene particles are aggregating. As the mixture viscosity decreases with temperature, the effective diffusivity of the particles increases and leads to faster aggregation. Therefore, it can be argued that at higher temperatures, the lower viscosity will lead to a shorter onset time for precipitation. All the above explanations seem plausible for the effect of temperature on precipitation kinetics but it is difficult to predict this relationship without a thorough analysis of the relevant factors. In this work we present data for the effect of temperature on the precipitation onset time and the rate of precipitation. After discussing the experimental procedure and results, we will describe a comprehensive and intriguing picture of the overall effect of temperature on asphaltene stability.

Materials and Methods

A chemical-free crude oil from Gulf of Mexico was used in this study and will be referred to as GM2 here. HPLC grade heptane from Fisher Scientific was used as the asphaltene precipitant. Table 3.1 shows the SARA (Saturate, Aromatics, Resins, and Asphaltenes) analysis and the density of the GM2 oil. In order to remove water, sand and other particulates commonly present in field samples, the crude oil was centrifuged at 10000 rpm for 3 hours before using it in the experiments. In order to minimize changes in the oil properties with time, oil samples were stored in amber glass bottles with nitrogen filled in the headspace. The bottles were fitted with PolySeal^{TM} caps and sealed with Teflon tape to minimize evaporation.

Table 3.1: Properties of crude oil used in this study

SARA Analysis	**GM2 Oil**
Saturates (wt%)	46.2
Aromatics (wt%)	41.7
Resins (wt%)	8.4
nC-7 Asphaltenes (wt%)	3.6
Loss (wt%)	0.1
Density @ 20°C (g/mL)	0.8678

Sample Preparation. The first step was to make a crude oil – heptane mixture of desired heptane concentration. A known volume of crude oil was taken in an Erlenmeyer flask and a specified volume of heptane was then added to the crude oil using a syringe pump. The crude oil was kept well-stirred using a magnetic stirrer during heptane addition and throughout the course of the experiment.

Detecting the Onset of Precipitation. Optical microscopy was used for studying asphaltene precipitation as a function of heptane concentration. 10 μL samples were

withdrawn at different times and were observed under the microscope. Images of all samples were recorded and compared with each other and with images of standard size particles in order to determine the time required for the first appearance of 0.5 μm asphaltene particles, which is referred to as the precipitation onset time.

Quantification of Asphaltene Precipitation. 1.5 mL samples were withdrawn from the well-stirred crude oil – heptane mixture at different times and centrifuged at 14,000 RPM for 10 minutes, forcing the asphaltene particles to form a compact cake at the bottom of the centrifuge tube. The liquid phase comprising of the crude oil and heptane was decanted and the asphaltene cake was then washed with heptane several times to remove any residual crude oil in the cake. The washed asphaltene samples were dried in an oven (usually for 24 hours) until the weight was constant and weighed to determine the mass of the precipitated asphaltenes.

Details of sample preparation, microscopy and centrifugation experiments can be found in our earlier work.[7]

High Temperature Experimental Apparatus. The experimental apparatus for high temperature (i.e. 50°C) investigations was developed in our laboratory. It consisted of a temperature controlled water-bath where the samples were kept stirred at all times using magnetic stirrers. The water-bath was heated using a heating tape wrapped around the bath. A thermocouple feed from the water-bath to the temperature controller was used to regulate the bath temperature. The water in the bath was well mixed to avoid temperature gradients within the water-bath. The bath was insulated to reduce heat loss and minimize

temperature fluctuations. The temperature was maintained at 50°C and the maximum variation was ±2°C.

Samples for the oil-precipitant mixtures were prepared as discussed earlier. In order to minimize the evaporation of lighter hydrocarbons from the oil-precipitant mixture, the Erlenmeyer flasks for the high temperature experiments were fitted with Mininert™ push-button valves which provided a leak-tight closure. Microscopy and centrifugation samples were drawn out with a needle that would pass through the septum of the sampling port. This procedure helped in minimizing evaporation losses in the high temperature experiments.

Results and Discussion

Microscopy Results. Figure 3.1 shows the microscopy pictures taken at various times for 34 vol% heptane samples at 20°C and 50°C respectively. It is clear that the 50°C sample precipitates much faster than the 20°C sample. The onset time for precipitation is 1.6 hours at 50°C and 3.6 hours at 20°C. It is also seen that the sizes of the particles at 50°C are much larger (5-10 μm) than at 20°C (1-2 μm). Even after 24 hours the particles in the 20°C samples did not grow beyond the sizes of 2-3 μm.

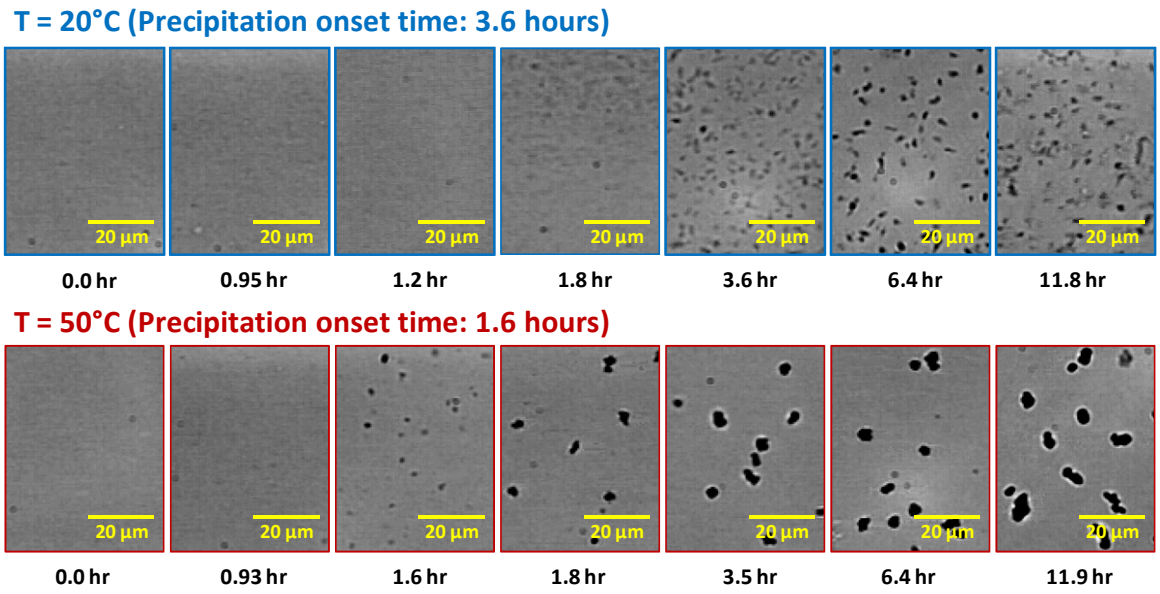

Figure 3.1: Micrographs for the detection of asphaltene precipitation as a function of time for 34 vol. % heptane at 20°C and 50°C. The precipitation onset time for the 20°C sample is 3.6 hours (and the onset of haze is at 1.8 hours). The precipitation onset time for the 50°C sample is 1.6 hours.

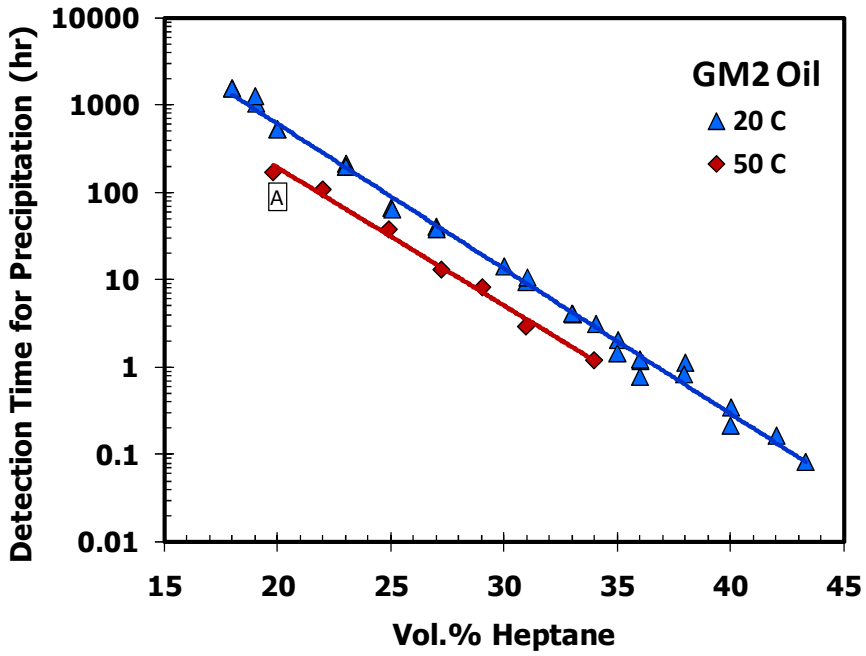

Figure 3.2: Detection time for onset of asphaltene precipitation for GM-2 crude oil for 20°C and 50°C. For details about Point A, refer to the latter section on the effect of hydrocarbon expansion.

The onset time for GM-2 crude oil for 20°C and 50°C at varying concentrations of heptane is shown in Figure 3.2. It is clear that the asphaltene precipitation happens more rapidly at 50°C for at all heptane concentrations shown. The onset time for 20°C experiments is almost 2.5 times longer than that for the 50°C experiments. Based on these results it may seem that of the three effects listed in the introduction section, the change in asphaltene solubility with temperature has no effect and the shorter onset time at higher temperatures may be attributed to the decrease in mixture viscosity, the expansion of the light ends or a combination of both. Although these conclusions may seem reasonable, it is important to substantiate them with definitive experiments. Therefore, in order to objectively determine the change in asphaltene solubility with temperature, centrifugation experiments were conducted to provide the mass % of asphaltenes precipitated per gram of the crude oil as a function of time, the details of which were discussed earlier.

Centrifugation Results.

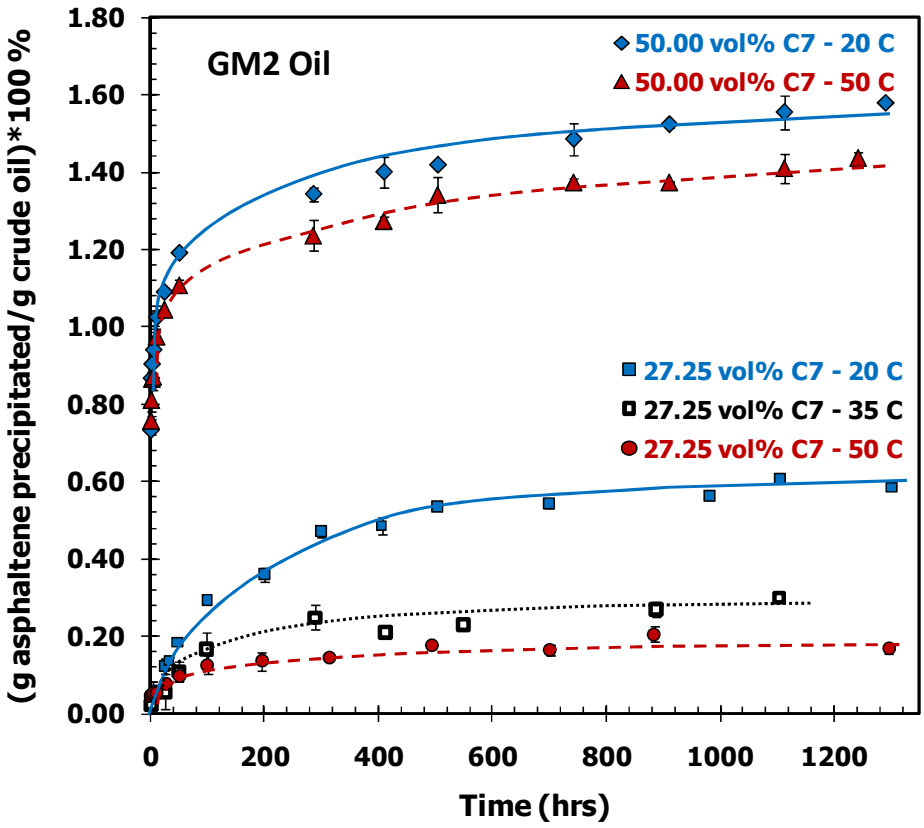

Figure 3.3: Comparison of the mass% of asphaltenes precipitated with time for two different heptane concentrations: - 50.0 vol% and 27.25 vol % - at different temperatures – 20°C and 50°C. Data for 35°C is also included for the 27.25 vol% sample.

The mass % of asphaltenes precipitated with time is shown in Figure 3.3 for two different heptane concentrations (50 vol. % and 27.25 vol. %) at different temperatures (20°C, 35°C and 50°C). The plateau values in this plot show the total amount of asphaltenes precipitated at equilibrium for different temperatures and precipitant concentrations. The greater the mass of asphaltenes precipitated at equilibrium, the lower is their solubility. The results from Figure 3.3 demonstrate that a greater amount of asphaltenes is precipitated at higher heptane concentrations at both temperatures

investigated here. Moreover, the amount of asphaltenes precipitated is smaller at 50°C than for 20°C at the same heptane concentration which indicates that asphaltenes are more soluble in oil-precipitant mixtures at higher temperatures. However, microscopy experiments show a shorter onset time for asphaltene precipitation at 50°C indicating that asphaltenes are less stable at higher temperatures (Figure 3.2). In the later part of this paper, we will propose a hypothesis to reconcile these two seemingly contradictory outcomes. Additionally, it is observed that at 27.25 vol. % heptane, the data for 35°C are not exactly in between that of 20°C and 50°C. The likely reason for this observation is that the solubility curve for these asphaltenes may be non-linear with temperature in this temperature range.

Another important conclusion that can be drawn from Figure 3.3 pertains to the difference between the amount of asphaltenes precipitated at 20°C and 50°C for the same heptane concentration i.e. the difference in the plateau values at the two temperatures. The difference in the plateau (i.e. equilibrium) values is larger at 27.25 vol. % heptane as compared to that at 50.0 vol. %. This observation means that the effect of temperature is more pronounced at lower precipitant concentrations. As the precipitant concentration is increased the difference in the amount of asphaltenes precipitated at different temperatures diminishes. This observation suggests that when the precipitant concentration is high, the dominant factor for asphaltene stability is the amount of precipitant and that temperature has a minor role. This finding can have major implication for the field operations when the driving force for asphaltene precipitation due to compositional changes is relatively small. In such cases, the temperature may have a very pronounced effect on asphaltene solubility.

The microscopy and centrifugation procedures were conducted at 20 °C for both 20 °C and 50 °C experiments reported here. Cooling of the 50 °C sample during the microscopy and centrifugation procedures may affect the accuracy of these measurements to some degree. However, it should be noted that if the entire procedure for the 50 °C sample could be conducted at that temperature, the differences between the results for the microscopy and centrifugation procedures could potentially be even more pronounced between 20 °C and 50 °C than that reported here.

In light of this information, the magnitude of differences in the precipitation kinetics and mass of asphaltenes precipitated for the two temperatures reported here shows a conservative limit, but does not reduce the impact of these results.

Temperature cycling. In order to understand why the precipitation of asphaltenes is faster at higher temperatures while their solubility is greater, temperature cycling experiments were developed. In this approach, the precipitation onset time experiments were initially conducted at 50°C and the samples were observed until large particles (of 5-10 µm size) were detected by microscopy. Next the temperature of the oil-precipitant mixture was lowered to 20°C and maintained at this value for several hours (as described below) after which it was increased back to 50°C. The results of this experiment are shown in Figure 3.4 for 34 vol.% heptane.

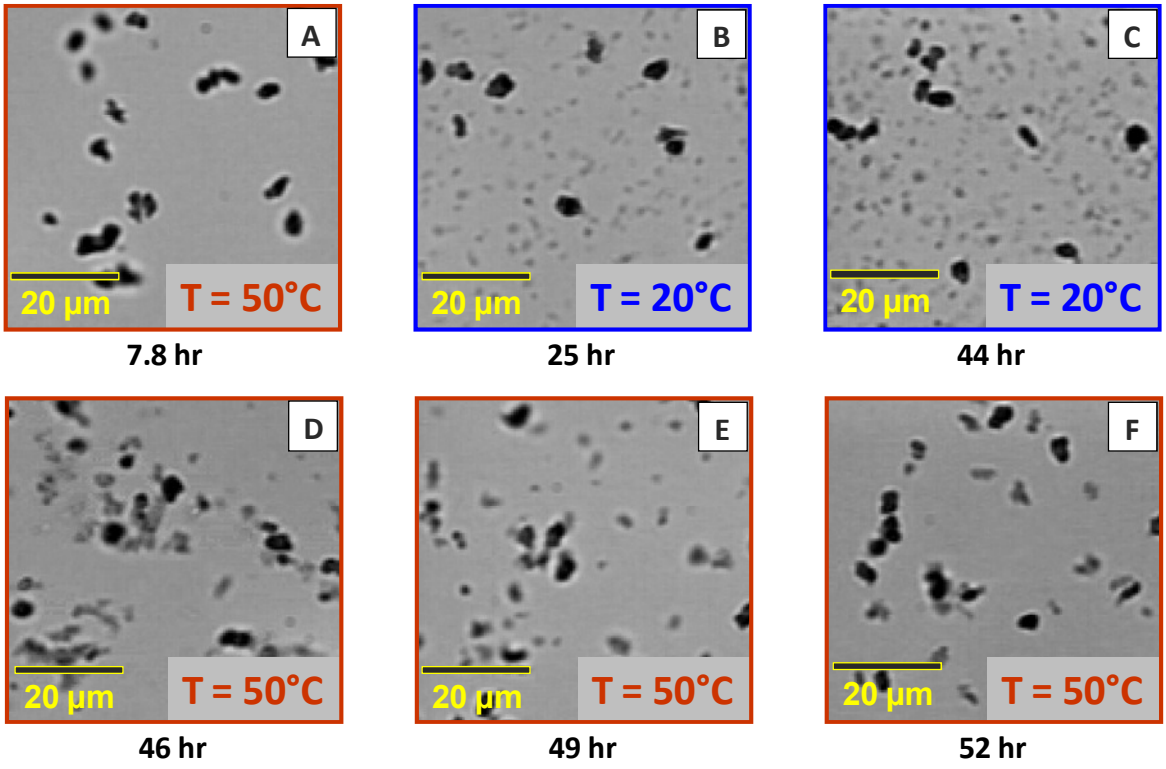

Figure 3.4: Micrographs showing the evolution of asphaltene particles during the temperature cycling experiments for 34 vol.% heptane. The precipitation onset time at 50°C was about 1.6 hours and the particles grew to 5-10 µm size by about 7.8 hours.

The precipitation onset time for the 34 vol.% heptane sample was 1.6 hours at 50°C. Here t= 0 hours represents the time when the precipitant has been added to the crude oil. Asphaltene particles of size 5-10 microns were formed after 7.8 hours (Figure 3.4-A). The system was cooled to 20°C after 7.8 hours and maintained at 20°C until 44 hours. It is observed that that at 25 hours a new generation of smaller particles (of about 1 μm size) was formed (Figure 3.4-B) that were very distinct from the larger particles precipitated at 50°C. The system was maintained at 20°C until 44 hours and the system did not exhibit much change after 25 hours (Figure 3.4-C). Two different particles sizes are still present and one observes that the concentration of the smaller particles has increased over time due to additional precipitation. At 44 hours the heating was restarted and the temperature of the mixture was brought to 50°C within about 10 minutes. It is observed that at 46 hours the number density of the smaller particles decreasing as a result of heating (Figure 3.4-D). By 52 hours the smaller particles were completely removed and only the larger size particles were visible (Figure 3.4-F) and the system essentially reached the same state as the initial condition shown in Figure 3.4-A. This observation is in agreement with the conclusions regarding the greater solubility of asphaltenes at higher temperatures (Figure 3.3). When the system is cooled from 50°C to 20°C, the solubility is decreased and additional asphaltenes precipitate out as the smaller size particles. Upon reheating to 50°C these smaller particles likely dissolve back into the solution because they were originally soluble at this temperature.

Hydrocarbon Expansion due to Heating. When considering the effect of temperature, expansion of hydrocarbons also needs to be investigated because it can affect asphaltene solubility as is common in cases of reservoir depressurization. In order to simplify our analysis, we make the following conservative assumption: the crude oil (i.e. asphaltene solvent) does not expand upon heating while heptane (i.e. asphaltene precipitant) does. Therefore, the effective precipitant vol. % in the oil-precipitant mixture will increase upon heating. In terms of the solubility parameter, this relative expansion of the n-alkane precipitant would reduce the overall solubility parameter of the system and would cause a greater driving force for asphaltene destabilization and aggregation.

To illustrate the magnitude of the expansion effects, the differences between 20 vol. % heptane samples at 20°C and 50°C were compared (Figure 3.2). Let us assume that the difference in the onset times for these samples can be entirely explained by the increase in heptane vol. % in the 50°C sample due to expansion. The coefficient of thermal expansion for heptane is 0.0012 $°C^{-1}$. Therefore, heating a 20 vol. % heptane sample from 20°C to 50°C, would increase the effective concentration to 20.4 vol. % heptane which would decrease the precipitation onset time from about 600 hours (for 20.0 vol.% at 20°C) to about 520 hours (for 20.4 vol.% at 20°C). However, the experimentally observed onset time for 20.0 vol% heptane sample at 50°C is about 170 hours (Figure 3.2-Point A).

These simple calculations illustrate that the thermal expansion of heptane cannot explain the faster precipitation onset time observed for 50°C samples. Therefore, we can conclude with certainty that, for the experimental conditions discussed in this paper, any thermal expansion effects for alkanes will have very limited effect on decreasing the

onset time of asphaltenes and we have to consider other factors in order to explain the greater than factor of two decrease in onset time for experiments at 50°C.

Chemical Change in Oil due to Heating: Another factor to consider is the possibility of a chemical change in the oil due to heating. Literature suggests that crude oils may change chemically due to oxidation or other reactions when heated at high temperatures.[4,17] A crude oil sample was stirred and heated at 50°C for 14 days in a sealed Erlenmeyer flask with a blanket of air on top to allow for oxidation (or other possible chemical reactions) that may change the properties of the crude oil upon heating. The heating was stopped after 14 days and the oil was cooled to 20°C. This arrangement allowed the oil to possibly change due to chemical reactions, while eliminating the change of oil due to evaporation of light ends. The heat-treated oil in the closed system (as discussed above) was used to conduct onset time experiments at 20°C. The results shown in Figure 3.5 demonstrate that there is no difference in the onset times of the original, untreated GM-2 oil and that of the heat-treated oil. These experiments illustrate that the faster onset times for 50°C experiments presented in Figure 3.2 are not due to oxidation or other chemical changes in the crude oil that may occur when conducting onset time experiments at 50°C.

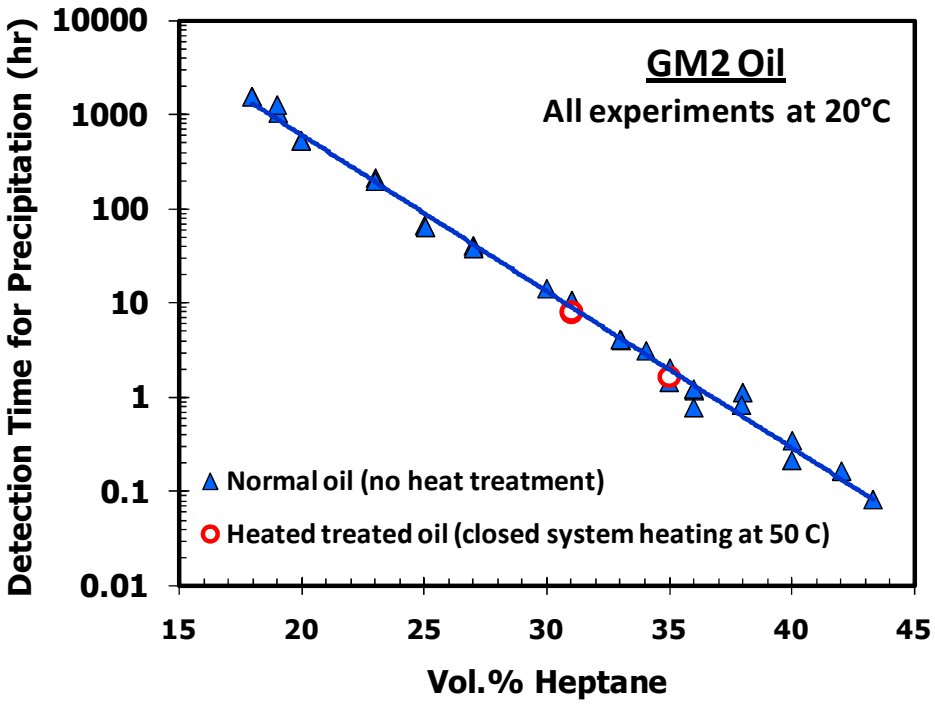

Figure 3.5: Comparison of the precipitation onset times for untreated GM-2 oil (blue triangles) and heat treated GM-2 oil (red circles). Heat treated samples were obtained by heating GM-2 oil at 50°C for 14 days in a sealed and well-stirred flask.

Change in Composition due to Evaporation. One possibility when conducting the high temperature experiments is that light ends may evaporate and cause a change in the overall composition of the system, thereby altering the solubility of asphaltenes. Heptane being more volatile than the crude oil is more likely of the two to evaporate during the experiment. However, a loss of heptane from the oil-precipitant mixture due to evaporation at 50°C would make the system a better solvent for asphaltenes and should increase the onset time, which is contrary to the results shown in Figure 3.2. Therefore, heptane loss cannot explain the faster precipitation kinetics observed at 50°C.

Additionally, in order to ensure that the heptane vol. % reported for 50°C experiments did not reduce significantly with time we conducted control experiments for

monitoring heptane loss by evaporation. In these experiments the system was heated to 50°C and the flask was opened for sampling from time to time but no samples were withdrawn. Therefore the change in sample mass could entirely be attributed to the heptane evaporation during the experiment. By performing calculations for heptane evaporation from this control sample, we found that the maximum possible loss of heptane would be in the order of 1.0-1.5 vol. % (See Appendix - B for details). This loss may slightly reduce the effective heptane concentration for the 50°C experiments in Figure 3.2 and marginally increase the difference between the observed precipitation onset times for 20°C and 50°C experiments.

Resolving the Apparent Inconsistency between the Precipitation Onset Time and the Solubility of Asphaltenes.

One may think that in the case where a greater mass of asphaltenes is precipitated, the driving force for asphaltene instability is greater which will lead to a shorter onset time for asphaltene precipitation. Therefore, based on the plateau values for the two temperatures in Figure 3.3, it may be expected that the onset time for 20°C samples should be shorter. However, data from Figure 3.2 shows that this the onset time for 20°C samples is greater than that of the 50°C samples by more than a factor of two. These results can be explained by using two concepts in conjunction: the polydispersity of asphaltene molecules and the aggregation process for asphaltenes.

We will first discuss the effect of polydispersity. Asphaltenes are defined as a solubility class of molecules which are insoluble in n-alkanes and soluble in toluene. This family of molecules has a distribution of properties e.g. molecular weight, elemental

composition, functional groups and heteroatom content and a combination of these properties will make some asphaltenes more unstable than the others.[18,19] It has been reported earlier that the asphaltenes precipitated at elevated temperature are more aromatic (lower H/C), have higher apparent molecular weight and their alkyl chains are apparently diminished.[20,21]

An increase in the temperature increases the overall solubility of the family of asphaltene molecules as is evident from the lower plateau values at 50°C in Figure 3.3. However, we postulate that the solubility of the most unstable fraction of asphaltene molecules is possibly not increased to the extent that will prevent their destabilization and precipitation. Therefore, the most unstable asphaltenes will destabilize upon the addition of heptane, regardless of the experimental temperature: 20°C or 50°C, for the heptane concentrations shown in Figure 3.2 and Figure 3.3.

The second key concept is the aggregation of asphaltenes. We have proposed the mechanism of asphaltene precipitation based on Brownian aggregation where the asphaltenes grow from the nano-level to the micron-level.[7] Asphaltenes exist in the crude oil as nanoaggregates[22] and the addition of heptane to the crude oil leads to their destabilization. This approach is also consistent with the work of Khoshandam *et al.* (2010)[23] who investigated the kinetics of asphaltene precipitation in a heptane-toluene mixture at one temperature. Their experiments show that asphaltenes particles start at the 8 nm range and grow with time to about 2000 nm which is consistent with this work and our earlier research (Maqbool et al. 2009). When the destabilized asphaltene nanoaggregates collide with each other they aggregate to form larger particles which grow from the nano-scale to the micron-scale. Once the particles cross the 0.5 μm

detection limit of optical microscopy, they are identified as precipitated asphaltene particles. A key factor controlling the time for aggregation to the micron level is the fluid viscosity. The oil-precipitant mixture viscosity controls the collision frequency of asphaltene nanoaggregates and will affect their rate of aggregation.

Therefore, in order to understand the shorter onset time for precipitation experiments at 50°C (Figure 3.2) the two concepts discussed above need to be taken into consideration in tandem. Upon the addition of heptane the most unstable asphaltenes will destabilize at both 20°C and 50°C and will start aggregating from the nano-scale to form larger particles. The process of aggregation will be faster for the 50°C sample because of the lower viscosity at higher temperature. Hence, the time required for the aggregating particles to cross the 0.5 micron detection limit of optical microscopy will be shorter for the 50°C experiments. Consequently, the precipitation onset time (defined as the time when the first particles of about 0.5 micron size are detected) will be shorter at 50°C. It needs to be clarified that the appearance of 0.5 μm asphaltene particles is not a solid-liquid phase change phenomenon at the molecular scale, but is a colloidal destabilization and aggregation of asphaltene nanoparticles to reach to the micron sizes that can then be detected by optical microscopy or other techniques. Therefore, by using the concept of varying degrees of stability in the polydisperse asphaltene molecules together with the proposed aggregation mechanism, we can explain why the 50°C experiments have a higher solubility for asphaltenes and at the same time have a shorter onset time for precipitation.

In order to validate that viscosity will govern the aggregation kinetics the following analysis is provided. The rate of formation of a larger specie k from smaller

particles *i and j* can be described by a Smoluchowski type aggregation process which takes the following form[24]:

$$\frac{dC_k}{dt} = \frac{1}{2}\sum_{\substack{i+j\to k \\ i=1}}^{i=k-1} K_{i,j} C_i C_j - C_k \sum_{j=1}^{\infty} K_{k,j} C_j \tag{1}$$

$$\text{or, } \frac{dC_k}{dt} \propto K_{i,j} C_i C_j \tag{2}$$

where, C_i, C_j and C_k are the concentrations of particles of different sizes and $K_{i,j}$ is the collision kernel which describes the interaction between particles *i* and *j*.

Considering that the flocculation of asphaltenes starts from the nano-scale, the Brownian flocculation kernel is utilized in this study and is expressed as:[8]

$$K_{i,j} = \frac{2R_g T}{3\mu_m} \frac{(d_i + d_j)^2}{d_i d_j} \beta \tag{3}$$

where: d_i and d_j represents the diameter (m) of colliding aggregates *i* and *j*, μ_m is viscosity of the medium (kg $m^{-1}s^{-1}$), R_g is the universal gas constant (J K^{-1} $kmol^{-1}$) and T is the absolute temperature (K). The collision efficiency (β) is included to account for the collisions that do not result in aggregation.

The onset time for precipitation is actually the time for destabilized asphaltene nano-particles to aggregate and grow to micron-level. Integrating Eq. (2), we see the dependence of the onset on the collision kernel is:

$$t_{onset} \propto \frac{1}{K_{i,j}} \tag{4}$$

In Eq. (2), T and μ_m are the temperature dependent terms. Therefore, combining Eqs. (3) and (4), the ratio of onset times at 20°C and 50°C is given as:

$$\frac{t_{onset}(20°\text{C})}{t_{onset}(50°\text{C})} = \frac{K_{i,j}(50°\text{C})}{K_{i,j}(20°\text{C})} = \frac{T(50°\text{C})/T(20°\text{C})}{\mu_m(50°\text{C})/\mu_m(20°\text{C})} \tag{5}$$

We measured the viscosity of the oil-precipitant mixture at 50°C and 20°C and calculated the ratio of the viscosities at these temperatures, which was found to be about 1:2. Therefore, the theoretical ratio of the onset times is found to be:

$$\frac{t_{onset}(20°\text{C})}{t_{onset}(50°\text{C})} = \frac{323\,\text{K}/293\,\text{K}}{1/2} = 2.2$$

These results are in good agreement with the data shown in Figure 3.2 which shows that the experimental onset time for precipitation at 20°C is greater than that 50°C by slightly more than a factor of two. Consequently we conclude that even though a smaller the mass of asphaltenes is precipitated at higher temperatures, a shorter onset time for precipitation observed at higher temperatures can be explained by the effect of viscosity on the aggregation of asphaltenes from the nanometer scale to the micron size.

Conclusions

In this paper we have discussed an experimental and theoretical approach to identify the effect of temperature on the kinetics of asphaltene precipitation from crude oil – precipitant mixtures. We have demonstrated that at higher temperatures the precipitation onset time for asphaltenes is shorter and their solubility is higher. We have established that the change in temperature leads to a change in viscosity which in turn

affects the collision kernel for the Brownian flocculation of asphaltenes and controls the onset time for precipitation. We have also discussed the microscopy results from temperature cycling experiments which visually illustrate how the solubility of asphaltenes varies with changes in temperature.

Other possible factors affecting the onset time due to changes in temperature have also been discussed and analyzed for their individual contributions for asphaltene precipitation kinetics. It has been shown here other factors like the expansion of hydrocarbons, the possibility of oxidation (or other chemical changes) upon heating the crude oil to 50°C and loss of light hydrocarbons due to evaporation have little or no effect on asphaltene precipitation kinetics for the experimental conditions discussed here. This research provides a unified approach to understand the variety of factors that change as a result of temperature variation and evaluates their individual contributions to changes in asphaltene precipitation kinetics and their solubility.

References

1. Hammami, A.; Ratulowski, J. in *Asphaltenes, Heavy Oils, and Petroleomics,* O.C. Mullins; E.Y. Sheu; A. Hammami; A.G. Marshall, Eds.; Springer: New York, **2007**; pp 617-660.

2. Creek, J. L. Freedom of Action in the State of Asphaltenes: Escape from Conventional Wisdom *Energy Fuel.* **2005**, 19, 1212– 1224

3. Pina, A.; Mougin, P.; Béhar E. Characterization of asphaltenes and modeling of flocculation-state of the art. *Oil & Gas Science and Technology - Rev. IFP* **2006,** *61*, 319-343.

4. Asomansing, S.; Watkinson, A. P. Petroleum Stability and Heteroatom Species Effects in Fouling of Heat Exchangers by Asphaltenes. *Heat Transfer Eng.* **2000**, *21* (3), 10−16.

5. Hu, Y. F.; Guo, T. M. Effect of temperature and molecular weight of *n*-alkane precipitants on asphaltene precipitation. *Fluid Phase Equilibria,* **2001,** *192* , 13–25.

6. Andersen, S.I.; Stenby, E. Thermodynamics of Asphaltene Precipitation and Dissolution Investigation of Temperature and Solvent Effects *Fuel Science and Technology International.* 1996, *14* (1), 261 – 287.

7. Maqbool, T.; Balgoa A.T.; Fogler H. S. Revisiting Asphaltene Precipitation from Crude Oils: A Case of Neglected Kinetic Effects. **2009,** *Energy Fuels*, *23* (7), 3681–3686

8. Kraiwattanawong K., *et al.* Thermodynamic solubility models to predict asphaltene instability in live crude oils. *Energy Fuels* **2007**, *21*, 1248-1255.

9. Gonzalez, D. L.; Hirasaki, G. J.; Creek, J.; Chapman W. G. Modeling of Asphaltene Precipitation Due to Changes in Composition Using the Perturbed Chain Statistical Associating Fluid Theory Equation of State. *Energy Fuels* **2007**, *21* (3), 1231–1242

10. Wu, J. Ph.D. Thesis, University of California at Berkeley, Berkeley, CA, **1998**

11. Wu, J. Z.; Prausnitz, J. M.; Firoozabadi, A. *Molecular-thermodynamic framework for asphaltene-oil equilibria* AIChE J. **1998**, 44, 1188.

12. Fuhr, B. J., C. Cathrea, L. Coates, H. Kalya, and A. I. Majeed *Properties of Asphaltenes from a Waxy Crude*. Fuel, **1991**, 70, 1293.

13. Ali, L. H., and Al-Ghannam. K. A. *Investigations into Asphaltenes in Heavy Crude Oils: 1. Effect of Temperature on Precipitation by Alkane Solvents.* Fuel, **1981**, 60, 1045.

14. Vargas, FM; Gonzalez, DL; Hirasaki, GJ, et al. *Modeling Asphaltene Phase Behavior in Crude Oil Systems Using the Perturbed Chain Form of the Statistical Associating Fluid Theory (PC-SAFT) Equation of State.* Energy & Fuels **2009**, 23, 1140–1146

15. Jamaluddin, A. K. M.; Joshi, N.; Iwere, F.; Gurnipar, O. SPE 74393, 2001

16. Friedlander, S. K., Smoke, dust and haze: fundamentals of aerosol dynamics, Oxford University Press, New York, **2000**.

17. Beck, J.; Svrcek, W. Y.; Yarranton, H. W. Hysteresis in Asphaltene Precipitation and Redissolution. *Energy Fuels*, **2005**, 19 (3), 944–947

18. Wattana, P.; Fogler, H. S.; Yen, A.; Garcìa, M. D. C.; Carbognani, L. Characterization of Polarity-Based Asphaltene Subfractions. *Energy Fuels* **2005**, *19* (1), 101–110

19. Wattana, P. *Precipitation and characterization of asphaltenes*. Ph.D. Thesis 2004, University of Michigan – Ann Arbor

20. Andersen, S.I. *Effect Of Precipitation Temperature on the Composition of n-Heptane Asphaltenes* , Fuel Science & Technology International, **1994**, 12 (1), pp 51-74

21. Andersen , S.I. *Effect Of Precipitation Temperature on the Composition of n-Heptane Asphaltenes.2,* Fuel Science & Technology International, **1995**, 13 (5), pp 579-604

22. Betancourt, S. S. *et al.* Nanoaggregates of Asphaltenes in a Reservoir Crude Oil and Reservoir Connectivity. *Energy Fuels* **2009,** *23*, 1178-1188

23. Khoshandam, A. and Alamdari, A. Kinetics of Asphaltene Precipitation in a Heptane−Toluene Mixture, *Energy Fuels* 2010, 24 (3), pp 1917–1924

24. Elimelech, M.; Gregory, J.; Jia, X.; Williams, R. Particle deposition and aggregation: measurements modeling and simulation, Butterworth-Heinemann Ltd., Oxford, **1995**

CHAPTER 4

MODELING THE AGGREGATION OF ASPHALTENE NANO-AGGREGATES IN CRUDE OIL-PRECIPITANT SYSTEMS

Introduction and Background

Asphaltenes are one of the least understood and the most problematic organic deposits for the oil industry. The deposition process likely begins with asphaltene destabilization due to thermodynamic factors such as changes in temperature, pressure loss during production, or change in composition of fluid during enhanced recovery operations, such as CO_2 flooding, acid stimulation and mixing of crude oil with diluents and other oils. Once asphaltenes destabilize, they tend to aggregate. Research has been carried out on asphaltene precipitation and deposition but there is relatively less work on asphaltene flocculation.[1-4] The flocculation studies that have been undertaken are with model systems consisting of precipitated asphaltene aggregates that were separated, washed, dried and then redispersed in a solvent (e.g. heptane-toluene mixture). These separated aggregates have an initial aggregate size of the order of 1 micron and grow to the order of 100 microns after the flocculation is essentially complete.[2] Many researchers have chosen to study the flocculation of these separated aggregates because the measurements of aggregate growth in-situ in the oil-alkane mixture (specially with high oil content) during flocculation is difficult.

The flocculation process depends on the population size and the reactivity of the primary units that undergo aggregation and growth. Studies in the literature on the amount of asphaltene precipitation and the related thermodynamics have been reported.[5-9] Unfortunately, the thermodynamic data used in these studies presumes that asphaltene precipitation and growth is instantaneous, which is not always the case. Experimental studies using optical microscopy show that onset of asphaltene precipitation is a function of precipitant concentration in systems of heavy oil diluted with heptane and toluene.[10] It should be mentioned here that these experiments were conducted for only 24-48 hours. Additionally, large amounts of toluene (65-90 wt%) were added to the heavy oil and it is unclear if the observed kinetic effects were inherent to crude oil or were a result of toluene addition. Murzakov et al. have quantified the flocculated asphaltene aggregates under natural settling as a function of time, temperature and resin concentration in alkane-resin solutions.[11] In our earlier work we have investigated the onset of asphaltene precipitation as a function of the amount of heptane added to crude oil systems and have demonstrated that the time required to detect the asphaltene aggregates by microscopy can vary from a few minutes to several weeks or months depending upon the amount of n-alkane precipitant added.[12]. We also developed a centrifugation-based technique to quantify the total amount of asphaltenes precipitated for varying amounts of heptane added to a crude oil.

It is recognized that the onset of precipitation for asphaltenes, as observed by microscopy, is actually the onset of detection of asphaltene aggregates as they grow to larger sizes. The time required for aggregates to grow to an identifiable size depends on the degree of destabilization which is caused by addition of a precipitant (or other means

like temperature and pressure variations in the field). In conventional studies on asphaltene aggregation, the evolution of the aggregate size distribution is monitored and the typical initial size of the asphaltene particles is in the micron range. Recent literature shows that asphaltenes exist as nanoaggregates in crude oil. This study focuses on the destabilization of asphaltenes at the nanometer scale and models their subsequent growth to particle sizes of a few microns. Details of the physical mechanism for destabilization and aggregation are discussed later. Data from centrifugation and microscopy experiments are used to validate the model.

Experimental work

Sample Preparation A known volume of crude oil was taken in an Erlenmeyer flask and a specified volume of heptane was then added to the crude oil using a syringe pump. The crude oil was kept well-stirred using a magnetic stirrer during heptane addition and throughout the course of the experiment.

Identification of the state of aggregation

Detecting the Onset of Precipitation:

Samples were withdrawn from the oil-precipitant mixture at different times and were observed under the microscope. Images of all samples were recorded and compared with each other and with images of standard size particles in order to determine the time required for the first appearance of 0.5 μm asphaltene particles, which is referred to as the precipitation onset time.

Quantification of Asphaltene Precipitation:

Samples were withdrawn from the well-stirred crude oil – heptane mixture at different times and centrifuged at 14,000 RPM for 10 minutes, forcing the asphaltene particles to form a compact cake at the bottom of the centrifuge tube. The liquid phase comprising of the crude oil and heptane was decanted and the asphaltene cake was then washed with heptane several times to remove any residual crude oil in the cake. The washed asphaltene samples were dried in an oven (usually for 24 hours) until the weight was constant and weighed to determine the mass of the precipitated asphaltenes.

Details of sample preparation, microscopy and centrifugation experiments can be found in our earlier work.[12]

Modeling of asphaltene flocculation

Development of a generalized geometric population balance equation (PBE)

The evolution of the aggregate size can be simulated using a population balance model. The Smoluchowski equation for the *k*-th aggregate having *k* number of primary units is given as (Elimelech et al., 1995),

$$\frac{dC_k}{dt} = \frac{1}{2}\sum_{\substack{i+j\to k \\ i=1}}^{i=k-1} K_{i,j} C_i C_j - C_k \sum_{j=1}^{\infty} K_{k,j} C_j \qquad (1)$$

Where k=1, 2, 3,., N and N represents the number of aggregate units in the domain,

C_k represents molar concentration of k-th aggregate (kmol m^{-3}),

$K_{i,j}$ represents the collision kernel between aggregate sizes i and j (m^3 $kmol^{-1}$ s^{-1}).

The first term on the right-hand side accounts for the rate of generation of k-th aggregates through binary collision of smaller aggregates. The second term represents the rate of depletion of k-th aggregate due to collision with other aggregates.

As seen in Equation (1), there are N number of coupled ordinary differential equations (ODE's) that need to be solved simultaneously. In many situations, the formulation and solution of the Smoluchowski flocculation equation turns out to be computationally intensive and in some cases does not even provide a practical option. For such situations, a geometric population balance has been used.[3,14,15]. In the geometric population balance, the k-th aggregate has R^{k-1} number of primary units in contrast to k number of primary units in discretized form of Smoluchowski equation, where R is the geometric spacing between two subsequent aggregates. For example, when R=2, the fourth aggregate in the geometric population balance (i.e. k=4) has 2^3 (i.e. 8) number of primary units. The number of primary units , n_a, in any aggregate is given by:[2,16],

$$n_a \approx \left(\frac{d_a}{d_p} \right)^{D_f} \tag{2}$$

Where D_f is the fractal dimension of the aggregate,

d_a is the aggregate diameter (m),

d_p is the primary unit diameter (m).

Equation (2) can be used to estimate n_a, provided D_f, d_a and d_p are known. Using Equation (2), n_a for different situations of D_f, d_a and d_p are estimated and shown in Table

4.1. In the Smoluchowski approach, the number of coupled ODE's required to be solved is n_a. The number of ODE's to be solved for geometric population balance is compared to Smoluchowski's approach in Table 4.1.

Table 4.1: Comparison of number of ODE's for Smoluchowski's equation and geometric population balance under different scenarios

Case	Diameter, m		D_f	n_a	Number of ODE's	
	Primary unit, d_p	Largest aggregate, d_a			Smoluchowski	Geometric (R=2)
1	$1x10^{-9}$	$1x10^{-5}$	3	$1.0x10^{12}$	$1.0x10^{12}$	41
2	$1x10^{-9}$	$1x10^{-6}$	2	$1.0x10^{6}$	$1.0x10^{6}$	28
3	$1x10^{-6}$	$1x10^{-4}$	1.6	$1.6x10^{3}$	$1.6x10^{3}$	12

Table 4.1 shows that Smoluchowski's approach becomes computationally intensive and impractical as the ratio of largest aggregate to primary unit size increases while the geometric population balance is a reasonable option from a computation standpoint. The Smoluchowski equation has been used in studies of asphaltene flocculation where the number of equations is not very large because the particle sizes only varied over a narrow range.[2] However, the stability of this computation along with the step size used are open to debate because of the large material balance error reported in the computation and the imposing of a 6 hour constraint on total computation time.[2] Because of the computational advantage of the geometric population balance, it is used here to model the aggregation of asphaltenes from the nanometer level to the micron size. A geometric population balance with volumetric discretization of $V_{i+1}/V_i = 2$ (V_i is the discretized volume of i-th segment) has been developed earlier where the aggregates were

discretized on the basis of aggregate volumes.[14,17] However, volumes of the aggregates may not be conserved as the aggregate sizes grow larger. In our work a generalized population balance equation is developed with a discretization based on the number of primary units of an aggregate and not in terms of the aggregate volume. While the volume of aggregates are not conserved as they grow larger[16,18,19] the number of primary units are conserved under all circumstances. The primary units are defined in a later section on the initial conditions for the population balance.

In this geometric discretization approach, the number of primary units in *i*-th aggregate is R^{i-1}. For example, the 1st, 2nd, 3rd, 4th and 5th and 6th aggregate has 1, R, R^2, R^3 and R^4 and R^5 number of primary units in a generalized geometric population balance scheme and for the special case of R=2 there are 1, 2, 4, 8, 16 and 32 number of primary units in these aggregates. The generation and depletion scheme of *i*-th aggregate by four mechanisms are shown in Table 4.2.

Table 4.2: Mechanism for generation and depletion of *i*-th aggregate in the geometric population balance model

Mechanism	Reaction	Example (i=4, R=2)
Generation 1	$RA_{i-1} \rightarrow A_i$	$2A_3 \rightarrow A_4$
Generation 2	$A_{i-1} + mA_j \rightarrow A_i$; j<i-1; $m = \frac{(R^{i-1} - R^{i-2})}{R^{j-1}}$	$A_3 + 2A_2 \rightarrow A_4$ (j=2, m=2) $A_3 + 4A_1 \rightarrow A_4$ (j=1, m=4)
Depletion 1	$A_i + mA_j \rightarrow A_{i+1}$; j<i; $m = \frac{(R^i - R^{i-1})}{R^{j-1}}$	$A_4 + 2A_3 \rightarrow A_5$ (j=3, m=2) $A_4 + 4A_2 \rightarrow A_5$ (j=2, m=4)
Depletion 2	$mA_i + A_j \rightarrow A_{j+1}$; j≥i; $m = \frac{(R^j - R^{j-1})}{R^{i-1}}$	$A_5 + 2A_4 \longrightarrow A_6$ (j=5, m=2) $A_6 + 4A_4 \longrightarrow A_7$ (j=6, m=4)

In order to understand the different mechanisms listed in Table 4.2, let us consider R=2. In Generation Mechanism 1, the formation of the 4th aggregate (8 primary units) occurs by the reaction of two immediately smaller A_3 aggregates each having 4 primary units. For the generalized case in mechanism 1, R number of (i-1) th aggregate form one i-th aggregate. In Generation Mechanism 2 (for R=2), the generation of 4th aggregate (8 primary units) occurs by reaction of one immediately smaller aggregate (i.e. A_3 having 4 primary units) with two A_2 aggregates (each having 2 primary units) or reaction of one A_3 aggregate with four A_1 aggregates. For the generalized case, the i-th aggregate is generated by reaction of the (i-1) th aggregate (larger aggregate) with smaller j-th aggregates (where $j < (i\text{-}1)$). It needs to be noted that as a general rule, m in Table 4.2 represents the number of smaller aggregates that react with one larger aggregate to generate the next larger aggregate (i.e. the i-th aggregate) which has R^{i-1} primary units. The larger aggregate of the reacting aggregates (i-1) has R^{i-2} primary units. Hence, number of primary units that come from smaller of the reacting aggregates (j-th aggregate) is (R^{i-1}- R^{i-2}). Each of the j-th aggregate has R^{j-1} number of primary units. Therefore, the number of j-th aggregates required to react with one (i-1)th aggregate to form the i-th aggregate is given by $m = \left(R^{i-1} - R^{i-2}\right) \big/ R^{j-1}$.

Depletion Mechanism 1 involves reaction of i-th aggregate with aggregates smaller than i-th aggregate. In this mechanism, one i-th aggregate (the larger aggregate) reacts with $(R^{i} - R^{i-1}) \big/ R^{j-1}$ number of j-th aggregates (where, $j < i$) to form (i+1)th aggregate. Depletion Mechanism 2 involves reaction of i-th aggregate with aggregates equal to or larger than i-th aggregate. In this mechanism, one of j-th aggregates (where, $j \geq i$) reacts with $(R^{j} - R^{j-1}) / R^{i-1}$ of i-th aggregates to form one (j+1) th aggregate.

In Generation Mechanism 1 of aggregate generation, R number of (i-1) aggregates form one i-th aggregate. This mechanism is written as $RA_{i-1} \rightarrow A_i$. Rate of disappearance of (i-1)-th aggregate is written as,

$$\left(\frac{dC_{i-1}}{dt}\right) = -K_{i-1,i-1}C_{i-1}^{\ 2} \tag{3}$$

Where $K_{i-1,i-1}$ represents the collision kernel between two i-1 aggregates.

From stoichiometric considerations, the rate of disappearance of (i-*1*) th aggregate is R times faster than the appearance of the i-th aggregate. Therefore,

$$\left(\frac{dC_i}{dt}\right)_{GM1} = -\frac{1}{R}\left(\frac{dC_{i-1}}{dt}\right) = \frac{K_{i-1,i-1}}{R}C_{i-1}^{\ 2} \tag{4}$$

Where $\left(\frac{dC_i}{dt}\right)_{GM1}$ represents the rate of generation of i-th aggregate from Mechanism 1.

The formation of i-th aggregate by mechanism 2 is presented as $mA_j + A_{i-1} \rightarrow A_i$ for $j=1,2,3,\ldots,i-2$. Following Table 4.2,

$$\text{m}=(R^{i-1} - R^{i-2})/R^{j-1} \tag{5}$$

The rate of depletion of j-th aggregate by interaction with (i-*1*) th aggregate is written as,

$$\left(\frac{dC_j}{dt}\right) = -K_{i-1,j}C_{i-1}C_j \tag{6}$$

From stoichiometric considerations, the rate of generation of *i*-th aggregate is m^{-1} times faster than the rate of depletion of each of the *j*-th aggregates (*j<(i-1)*). Therefore, the total rate of generation of the *i*-th aggregate by reaction of $(i-1)$ th aggregate with all smaller aggregates by birth mechanism 2 is

$$\left(\frac{dC_i}{dt}\right)_{GM2} = C_{i-1}\sum_{j=1}^{i-2} K_{i-1,j}\frac{C_j}{m} = C_{i-1}\sum_{j=1}^{i-2} K_{i-1,j}\frac{R^{j-1}}{R^{i-1}-R^{i-2}}C_j \tag{7}$$

Similarly, depletion of the *i*-th aggregate by depletion mechanism 1 is given as,

$$\left(\frac{dC_i}{dt}\right)_{DM1} = -C_i\sum_{j=1}^{i-1} K_{i,j}\frac{R^{j-1}}{R^{i}-R^{i-1}}C_j \tag{8}$$

Where $\left(\frac{dC_i}{dt}\right)_{DM1}$ represents the depletion of *i*-th aggregate from death mechanism 1.

Depletion of the *i*-th aggregate by depletion mechanism 2 is,

$$\left(\frac{dC_i}{dt}\right)_{DM2} = -C_i\sum_{j=i}^{N-1} K_{i,j}C_j \tag{9}$$

The net rate of generation of the *i*-th aggregate is represented by summation of terms for the different generation and depletion mechanisms presented above, i.e.,

$$\frac{dC_i}{dt} = \left(\frac{dC_i}{dt}\right)_{GM1} + \left(\frac{dC_i}{dt}\right)_{GM2} + \left(\frac{dC_i}{dt}\right)_{DM1} + \left(\frac{dC_i}{dt}\right)_{DM2} \tag{10}$$

Substituting Equations (4), (7), (8) and (9) in Equation (10) gives,

$$\frac{dC_i}{dt} = \frac{K_{i-1,i-1}}{R} C_{i-1}^{\ 2} + C_{i-1} \sum_{j=1}^{i-2} K_{i-1,j} \frac{R^{j-1}}{R^{i-1} - R^{i-2}} C_j - C_i \sum_{j=1}^{i-1} K_{i,j} \frac{R^{j-1}}{R^i - R^{i-1}} C_j - C_i \sum_{j=i}^{N-1} K_{i,j} C_j \quad (11)$$

The total number of primary units across all species at any instant must be equal to the total primary unit present initially, i.e.,

$$\sum_{i=1}^{N} R^{i-1} C_i(t) = \sum_{i=1}^{N} R^{i-1} C_i(t=0) \quad (12)$$

For the case where only the primary units are present at t=0, Equation (14) is rewritten as,

$$\sum_{i=1}^{N} R^{i-1} C_i(t) = C_1(0) \quad (13)$$

Initial conditions for the generalized geometric population balance equation

It is reported in recent literature that asphaltenes exist as nanoaggregates in the crude oil with each nanoaggregate being comprised of about 8 asphaltene molecules.[20-23] In the current model it is assumed that these nanoaggregates act like the primary units for asphaltene aggregation. When heptane is added to the crude oil, the nanoaggregates are destabilized and start aggregating to form larger particles. It is assumed that the destabilization of asphaltenes upon heptane addition is rapid and the flocculation process is relatively slow compared to destabilization kinetics. The quantity of destabilized asphaltenes is governed by the change in the solubility of asphaltenes upon the addition of a certain amount of heptane. The initial concentration of these primary units is determined by the total amount of asphaltenes precipitated for a given heptane concentration. The volume fraction of oil in the oil-heptane mixture is ϕ_o and the oil

density is ρ_o (kg/m^3). Therefore, the mass of oil per unit volume of mixture is given as $\phi_o\rho_o$. The mass fraction of destabilized asphaltene per unit mass of oil resulting from the addition of a specified quantity of heptane is m_A (kg/kg) and is given by the plateau value in a plot of the mass of asphaltene precipitated (for a given heptane concentration) versus time (Maqbool 2009). The amount of precipitated asphaltenes is determined by equilibrium thermodynamics i.e. composition of mixture, temperature and pressure.

The total mass of destabilized asphaltene per unit volume of mixture is $m_A\phi_o\rho_o$. At time t=0, the primary units (i.e. the asphaltene nanoaggregates for i = 1) are destabilized and begin to evolve into larger aggregates. The nanoaggregates have a molecular weight of $M_{w,A}N_{agg}$ (kg/kmol) where $M_{w,\ A}$ is the molecular weight of the asphaltene molecules and N_{agg} is the number of asphaltene molecules per nanoaggregate (Based on recent literature $N_{agg} \approx 8$. [20-23]). Consequently the initial molar concentration of primary units is:

$$C_1(0) = \frac{m_A\phi_o\rho_o}{M_{w,A}N_{agg}} \tag{14}$$

Where $C_1(0)$ is the molar concentration (kmol/m^3) of the asphaltene nanoaggregates (i=1) at t=0. At time t=0, only these primary units are present and initial concentration of larger aggregates is

$$C_i(0) = 0 \quad \text{for } i > 1 \tag{15}$$

Equation (11) along with the initial conditions (Equations (14) and (15)) form a set of N coupled ordinary differential equations (ODE). To solve this set of equations, the mass of destabilized asphaltene for a given heptane concentration is needed.

Collision kernel

In Equation (11), the kinetic parameter $K_{i,j}$ represents the product of collision frequency between species i and j (represented by $\alpha_{i,j}$) and the efficiency of collision, β (i.e. $K_{i,j} = \beta\alpha_{i,j}$). The collision efficiency needs to be included because not every collision results in aggregation. Considering the fact that flocculation of asphaltenes starts from its nanoaggregate state, the Brownian flocculation kernel is utilized in this study. For Brownian flocculation, the collision frequency between aggregates i and j can be expressed as:[24]

$$\alpha_{i,j} = \frac{2R_g T}{3\mu_m} \frac{(d_i + d_j)^2}{d_i d_j} \tag{16}$$

where d_i and d_j represents the diameter (m) of colliding aggregates i and j,

μ_m is viscosity of the medium (kg /m/s),

R_g is the universal gas constant (J/ K/kmol),

T is the absolute temperature (K).

It can be observed from Equation (16) that as the heptane content in the mixture increases, the medium viscosity decreases (because heptane has lower viscosity than oil) and hence the collision frequency of the mixture increases. This reduction in viscosity at

higher heptane concentrations helps to accelerate the flocculation kinetics. In case of reaction limited aggregation (RLA), repeated collisions are required for a successful aggregation event so that a collision efficiency, β must be included. For a given β, the set of ODE's discussed earlier can be solved numerically. The efficiency of collision depends on the interparticle interaction. The Smoluchowski collision kernel for the Brownian flocculation involving small aggregates is

$$K_{i,j} = \frac{2R_g T}{3\mu_m} \frac{(d_i + d_j)^2}{d_i d_j} \beta \tag{17}$$

Equation (17) can be rewritten as,

$$K_{i,j} = k \frac{(d_i + d_j)^2}{d_i d_j} \tag{18}$$

Where k for a given composition is,

$$k = \frac{2R_g T \beta}{3\mu_m} \tag{19}$$

The only unknown term on the right hand side of Equation (19) is the collision efficiency, β which needs to be estimated from experimental data involving the growth of the aggregates as estimated from theoretical considerations.

To solve the population balance equations, the aggregate diameter in the collision kernel (Equation (17)) needs to be expressed as a function of the primary unit diameter. The asphaltene aggregates are assumed to be spherical having a solid volume fraction, ε. A solid volume fraction for random close packing of spheres of 0.637 is used in this

study.[25] Considering the fact that R^{i-1} primary units form the *i*-th aggregate, the diameter of the *i*-th aggregate can be expressed as a function of the diameter of primary units and the void space. Hence,

$$d_i = \left(\frac{R^{i-1}}{\varepsilon} \right)^{1/3} d_1 \tag{20}$$

The diameter of an asphaltene nanoaggregate (the primary unit in the aggregation process) can be written as:[24]

$$d_1 = \left(\frac{6V_m}{\pi} \right)^{1/3} \tag{21}$$

Where $V_m \left(= M_{w,A} N_{agg} / (A_v \rho_A) \right)$ is the nanoaggregate volume (m^3),

N_a is Avogadro's number.

Using a molecular weight of 750 g/mol and density of 1.2 kg/l, the estimated diameter of an asphaltene nanoaggregate is 2.5 nm which is consistent with the value reported in recent literature.[21]

ODE solution procedure and model parameters

The system of differential equations was solved using the *ode45* function in Matlab, an explicit scheme utilizing 4th and 5th order Runge-Kutta formulas to provide an accurate, yet fast estimate. To determine the most accurate value for the fitting parameter, (β), the *fminsearch* function was used in Matlab. This task was accomplished by minimizing the sum squared error between experimental values of asphaltene mass separated vs. time and their predicted values based on the calculated particle

concentrations and centrifugation efficiency for each particle size. This scheme required repeated iterations of the differential equation solver to determine the optimum value for the collision efficiency. The solution to the differential equations provides the molar concentration of each particle size as a function of time. Combining the solution with the molecular weights for each particle size, a mass fraction based particle size distribution was calculated. The values and descriptions of the key parameters used in the model are listed in Table 4.3.

Table 4.3: Values of important parameters used in the model

Parameter	Value	Description
ρ_{asph}	1200 kg.m^{-3}	Density of asphaltenes (kg/m^3)
ρ_{hept}	679.6 kg.m^{-3}	Density of heptane at 20°C
ρ_o	923.8 kg.m^{-3}	Density of K-1 oil at 20°C
μ_{hept}	0.0004 Pa.s	Viscosity of heptane at 20°C
μ_o	0.16 Pa.s	Viscosity of K-1 oil at 20°C
D_f	3	Fractal dimension
$M_{w,A}$	750 kg/kmol	Molecular weight of asphaltenes
N_{agg}	8	Number of asphaltene molecules per nanoaggregate
R	2	Geometric scaling factor
ε	0.6366	Packing factor for random close packing of spheres
R_g	8.314 J/mol/K	Ideal gas constant
N_a	6.023x10^{23} mol^{-1}	Avogadro constant

Results and discussions

Modeling the mass of asphaltenes precipitated and centrifuged out as a function of time

The flocculation of asphaltenes was simulated by solving the generalized geometric population balance equations, appropriate kernel and initial conditions to estimate the concentration evolution of aggregates involving different numbers of primary units. The aggregate domain was discretized in 40 geometric sections with a geometric scaling of R that leads to the largest aggregate with R^{39} number of primary units (ca. 5.5×10^{11} units) and diameter of about 12 μm. This discretization for R=2 leads to 40 coupled nonlinear ordinary differential equations that were solved simultaneously by Matlab routine ODE45. The conservation of total number of primary units was checked at every time step to determine the correctness of the simulation code. It is important to note that in this analysis there is no loss in the total number of primary units in contrast to the earlier work on volume based discretization studies where significant volume loss has been reported.[2,15] The evolution of separated aggregate by centrifugation, $S_A(t)$ is estimated as,

$$S_A(t) = \frac{\sum_{i=1}^{N} R^{i-1} M_{w,A} s_i C_i(t)}{w_o} \tag{27}$$

Where $S_A(t)$ is mass of separated asphaltene per unit mass of oil (kg asphaltene/kg oil)

w_o is mass of oil per unit volume of mixture (kg/ m^3),

s_i is the separation efficiency of i-th aggregate in the centrifuge. (See Appendix-A for details).

$C_i(t)$ in Equation (27) is obtained from simulating the population balance equations.

We use the geometric population balance and Smoluchowski kernel to study the evolution of the centrifuged aggregates and to identify the collision efficiency. The experimental results for the mass of asphaltenes collected by centrifugation at different times for 50% heptane addition and the corresponding simulation results obtained by using the Smoluchowski kernel are shown in Figure 4.1. The plateau region of the plot represents the total quantity of asphaltenes that was destabilized and centrifuged out for this heptane concentration. Similarly, Figures 4.2 and 4.3 show the comparison between the experimental values of the amount of asphaltenes precipitated and the simulation results for 46.5% and 47.8% heptane respectively.

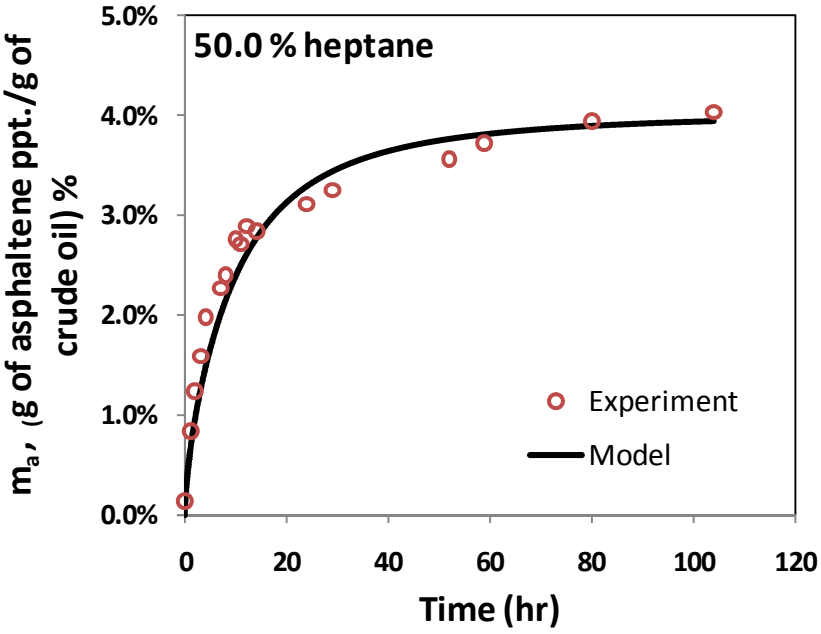

Figure 4.1: Experimental and simulated evolution of separated aggregates using the Smoluchowski kernel for 50% heptane

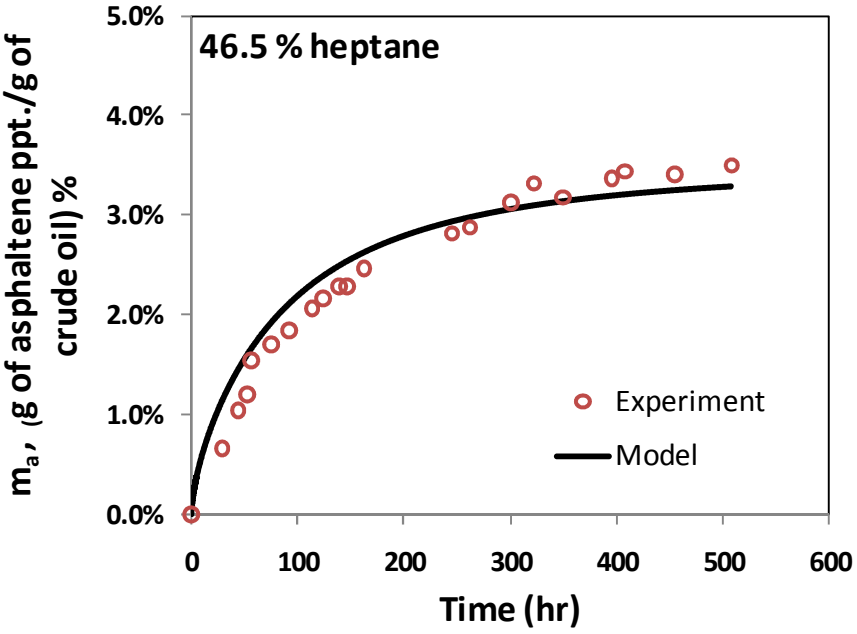

Figure 4.2: Experimental and simulated evolution of separated aggregates with 46.5 % heptane addition

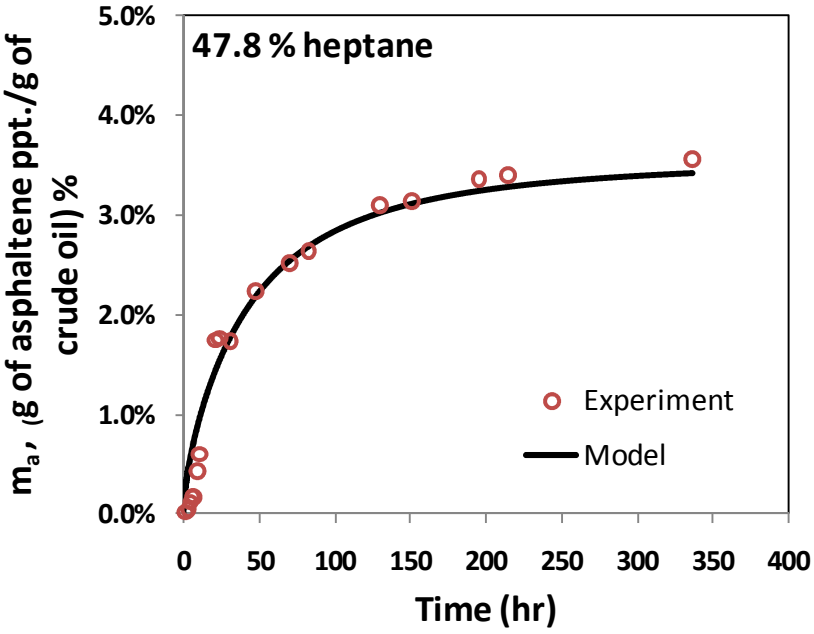

Figure 4.3: Experimental and simulated evolution of separated aggregates with 47.8 % heptane addition

One observes that the evolution of the experimentally measured mass of asphaltenes can be simulated very closely. It can be concluded that the geometric population balance along with the Smoluchowski kernel and collision efficiency parameter (β) is a good approach to capture the evolution of asphaltenes during their aggregation.

The collision efficiency (β) used to match the experimentally observed mass of asphaltenes precipitated as a function of time for various concentrations of heptane is plotted in Figure 4.4. It is seen that as heptane concentration increases the collisions become more successful. One explanation for the increase in the collision efficiency at higher heptane concentrations is that the liquid medium comprising of heptane and crude oil becomes a weaker solvent for asphaltenes. Therefore, when the destabilized asphaltene aggregated collide with each other at higher heptane concentrations, there is a

greater probability for them to stick with each other rather than staying as stable entities in the oil-heptane mixture.

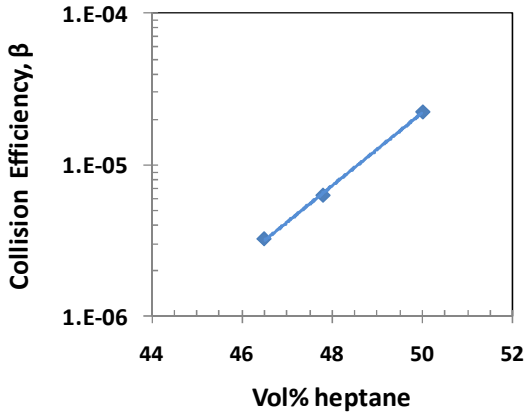

Figure 4.4: The optimized collision efficiency as a function of heptane concentration (R=2 and Df = 3)

Modeling the particle size distribution as a function of time

Figure 4.5 shows the calculated particle size distributions (PSDs) of asphaltene aggregates as a function of time for two different precipitant concentrations: 46.5 and 50.0 vol.% heptane with K-1 crude oil. The PSDs are plotted on a mass fraction basis. If plotted on number concentration basis, the data is difficult to visualize because the concentration on the smallest particles in the PSD is very high initially and overwhelms the concentration of the larger aggregates above 0.1μm size. As expected, the particle size distributions shift to larger sizes with time for both these cases. Comparing the modes of the PSD at different times for the two different concentrations, it is also observed that particles grow to larger sizes more rapidly for the 50.0 vol% heptane sample. At higher heptane concentrations the driving force for asphaltene destabilization is greater which leads to faster aggregation.

It should be noted that data markers in Figure 4.5 are the only particles sizes allowed by the geometric population balance and the connecting lines are only a visual guide – because of the geometric scaling, there are no intermediate particles sizes between any two consecutive data markers shown.

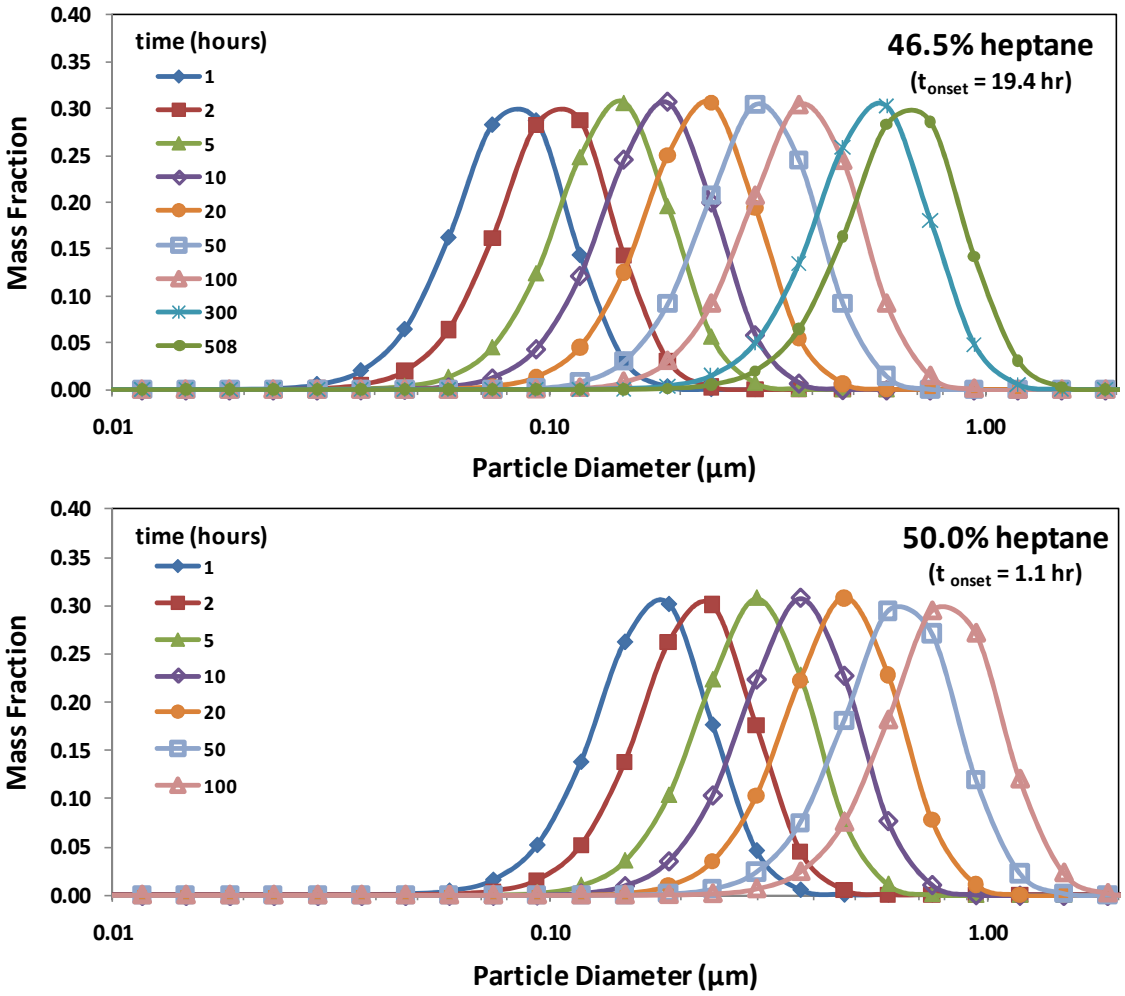

Figure 4.5: The particle size distribution (PSD) of asphaltenes particles as a function of time for 46.5 and 50.0 vol.% heptane with K-1 crude oil. The PSDs) are plotted on a mass fraction basis. As the larger particles are formed, the mass fraction of these particles outweighs that of the smaller particles which leads to a shift in the distribution to larger sizes on a mass fraction basis. On a number count or concentration basis, the model predicts that the distribution becomes wider with time.

Khoshandam *et al*. have also investigated the kinetics of asphaltene precipitation in a heptane-toluene mixture.[26] Their experiments show that asphaltenes particles start at the 8 nm range and grow with time to about 2000 nm which is consistent with our work. They used a spectrophotometer to detect the concentration of asphaltenes dissolved in the heptane-toluene mixture as a function of time and filtered their samples with a 0.2 micron filter to remove large asphaltene particles. However, the filtered samples can still contain particles smaller than 0.2 micron which can be erroneously identified by the spectrophotometer as dissolved asphaltenes molecules. Therefore, in order to avoid this error, Khoshandam *et al.* had to wait for about 20 minutes for the particle size distribution to grow larger than 0.2 microns and used t = 20 minutes as the initial time for their model. Consequently, even though the model proposed by Khoshandam *et al.* discusses about the growth of particles from the nanometer level to the micron level, the simulations are actually carried out only between sizes of 0.2 and 2.0 microns.

Predicting the onset time for asphaltene precipitation

In order to predict the onset time plots using the geometric population balance model, we need the concentrations of particles of different sizes as a function of time for the given heptane concentration. In the current work we utilized the geometric population balance model to predict the onset time for these lower heptane concentration experiments for which the experimental time can be prohibitively long. By using the plateau value of the centrifugation plots for different heptane concentrations, the solubility plot of asphaltenes as a function of heptane concentration can be generated Figure 4.6. Details about the development of the solubility plot are discussed elsewhere.[12]

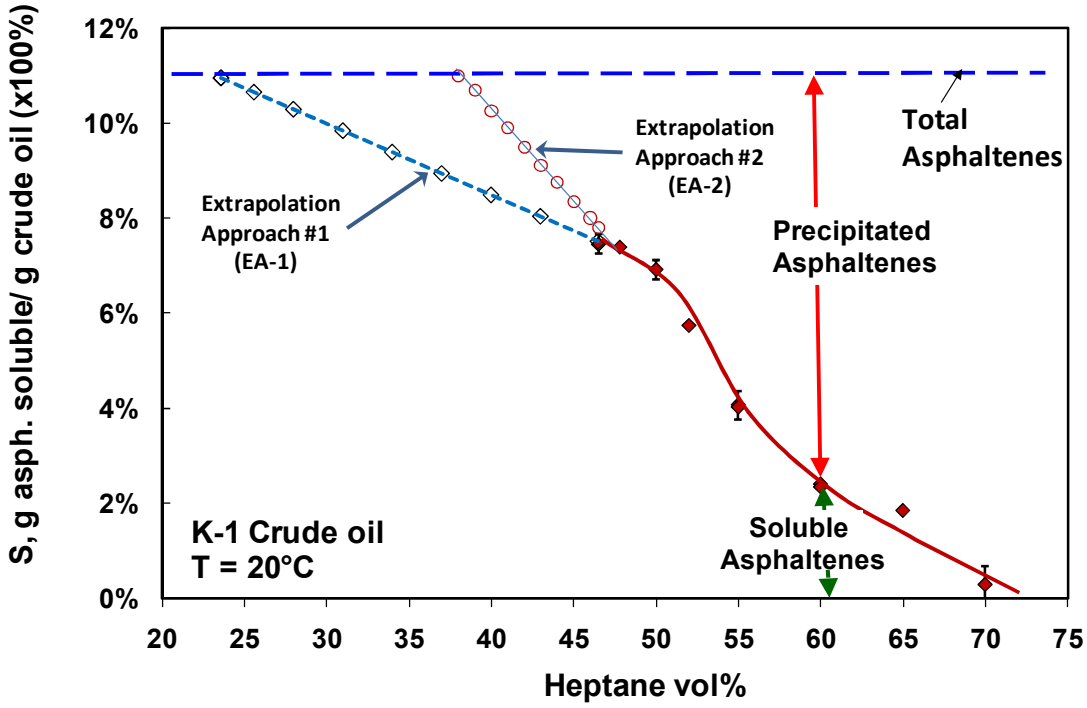

Figure 4.6: Extrapolating the solubility of asphaltenes to lower heptane concentrations.

The quantity shown on the y-axis (i.e. S) is the total wt. % of asphaltenes soluble in the crude oil for a given heptane concentration. In case of a pure crude oil, S represents the total asphaltene content of the oil. It needs to be noted that that no centrifugation experiments were performed below 46.5% heptane because the time for reaching a plateau would will span over several months to years, depending on the heptane concentration used. In order to get the mass of asphaltenes precipitated at equilibrium for the low heptane concentrations, two extrapolations of the solubility plot for K-1 oil to lower heptane concentrations were made (using the data points of from 46.5, 47.8, and 50.0 vol. % heptane experiments) as shown in Figure 4.6. One extrapolation shown in this figure is a linear extrapolation of the last three data points shown by dashed line (EA-1) in Figure 4.6. The other extrapolation (EA-2) is an extrapolation of the solubility curve

to 38 vol.% heptane where no precipitation has been observed for more than two years after the heptane addition. Subtracting the solubility from the total asphaltenes present in the K-1 oil, yields the total amount of asphaltenes precipitated as a function of heptane concentration. This value was used as an in input to the model. EA-1 is likely the lower limit of the solubility curve, which corresponds to the upper limit of the mass fraction of asphaltenes precipitated for a given heptane concentration. Similarly, EA-2 is the upper limit for solubility and the lower limit for mass fraction of asphaltenes precipitated.

Two parameters are required to run the geometric population balance simulations – the mass of asphaltenes precipitated upon the addition of a certain concentration of heptane to the crude oil and the collision efficiency, which governs how fast do the particles aggregate. The relationship between the collision efficiency and the heptane concentration was extrapolated to lower concentrations to obtain the collision efficiency below 46.5% heptane. With these two parameters as inputs, the simulations were carried out for heptane concentrations between 40% and 46.5% heptane and obtained the concentrations of each of the particles sizes as a function of time. The simulated particle size distribution for 40% experiment using extrapolation EA-1 is shown in Figure 4.7.

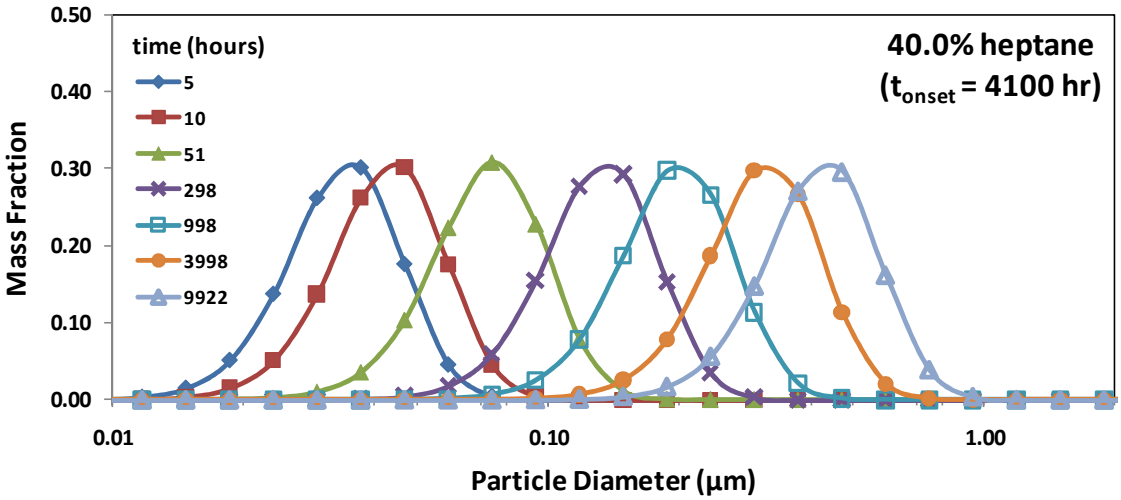

Figure 4.7: The predicted particle size distributions as a function of time for 40.0% heptane in K-1 crude oil. The experimental onset time for asphaltene precipitation in this system was around 4000 hours.

The final step in predicting the onset time is to determine the time at which particles larger than 0.5µm in diameter start to appear in the system because the smallest particles that can be observed by microscopy are approximately 0.5 µm. It must be noted that, even particles larger than 0.5µm will have a low probability of detection unless their concentration in the liquid mixture reached a certain threshold (i.e. minimum detectable value). For example, if the concentration of the 0.5 micron particle was 1 particle per mL of solution and the sample size for microscopy was 10 µL the probability of detection of this particle would be only 1%. In other words, out of every 100 samples seen under the microscope, one of them will show the onset of precipitation. Understandably, this is not a reliable definition of the onset time. Therefore, a minimum threshold concentration of the particles needs to be defined for positive identification of the onset of precipitation, as will be discussed below.

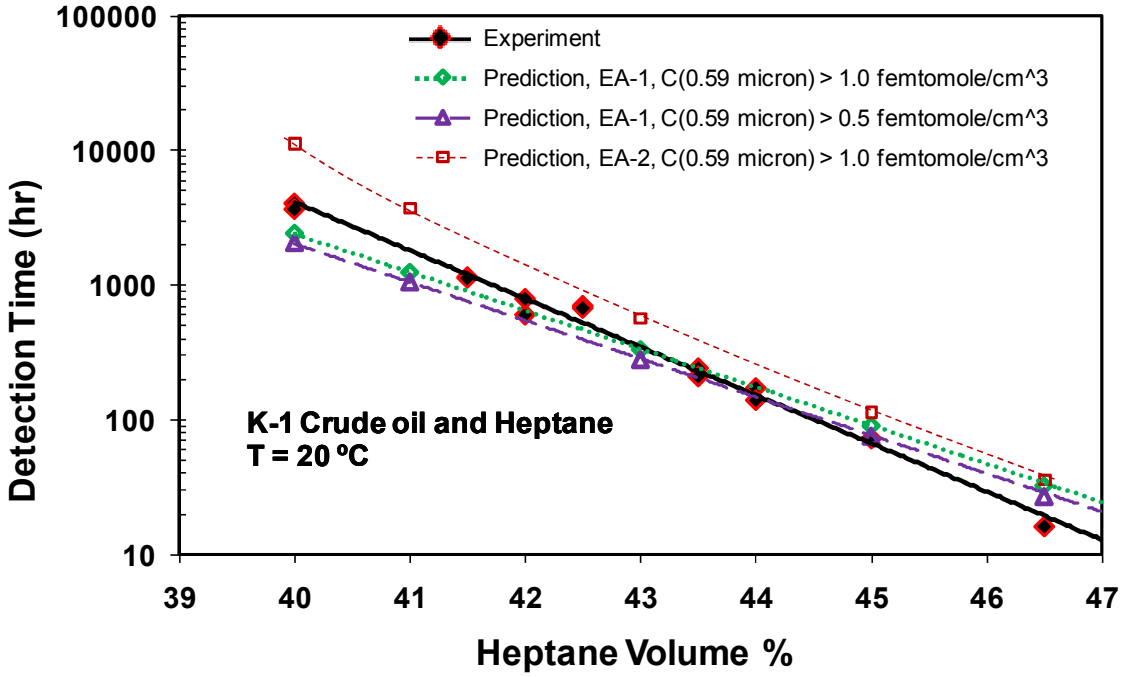

Figure 4.8: Comparison of the experimental and predicted precipitation onset times for various concentrations of heptane in K-1 oil using extrapolations EA-1 and EA-2. The dotted lines represent the predicted times at which the concentration of the 0.59 µm particle reaches the respective threshold values listed in the legend. For details about the extrapolation see Figure 4.6.

In order to define the threshold concentration, the simulation was carried out for 46.5, 47.8 and 50.0 vol.% experiments to fit the corresponding data from centrifugation experiments. Because only discretized particle sizes are allowed in the geometric population balance, the particle diameters can be obtained from Eq. 20, where R=2, d_1= 0.0025 µm, and *i* is the index for unique particle diameters allowed. Upon varying *i*, it is found that the a calculated diameter of 0.59 µm was the closest to the 0.5 µm limit for detection and it was chosen as the basis to define the onset of precipitation. The calculated concentration of the 0.59 µm particle for the various heptane concentrations at the corresponding onset times for these concentrations varied from 0.5-1.0 femtomole/cm^3.

Using this concentration range as the threshold value, we calculated the precipitation onset time for various heptane concentrations (Figure 4.8). Comparing predicted onset plot for EA-1 with the experimental data, one notices that there is excellent agreement between the experimental and simulated values, even though the slopes differ slightly. The model presented here is able to capture the trend of the exponential relationship between the precipitation onset time and the heptane concentration. Note that only microscopy experiments (and no centrifugation experiments) were conducted in the 40%-45% heptane range shown in Figure 4.8 and the predicted onset times are calculated by using the model.

Next, the second extrapolation approach (EA-2) was used to obtain the predictions for the onset time and the results are also compared with the experimental data in Figure 4.8. Extrapolation EA-2 which represents an upper bound for the onset time and assumes that the solubility of asphaltenes is higher than that given by extrapolation EA-1. Therefore, at a given heptane concentration there would be smaller amount of asphaltenes precipitated using approach EA-2 which will yield a lower starting concentration of the destabilized asphaltene nano-aggregates. Consequently, with EA-2 the rate of aggregation will be significantly slower and it will take the particles longer to reach the detectable size of 0.5 microns and the onset time of precipitation will be substantially longer. The predictions for EA-2 in Figure 4.8 demonstrate this trend. Because, the two approaches EA-1 and EA-2 provide good bounds for the experimental data, it can be concluded that these two approaches will also be reasonable upper and lower limits for the solubility plot shown in Figure 4.6.

Sensitivity Analysis

Geometric scaling factor (R)

The geometric scaling factor (R) in the model describes how the number of molecules in any particle scales from a given particle size to the next larger one in the system. Unless otherwise mentioned, the default value of R = 2 was used for all simulations shown in this paper. When R is reduced, the scaling for the number of molecules per particle between two consecutive particle species is reduced, effectively reducing the gaps in particle diameters for this discretized distribution. Therefore, at lower R, there will be more intermediate particles sizes between any two limits of particle size. Three different values of R were tested with the model for sensitivity analysis: R = 1.5, 2 and 3.

Figure 4.9 shows the simulated profiles with different values of R, establishing that this model can be generalized for different values of the geometric scaling factor, R.

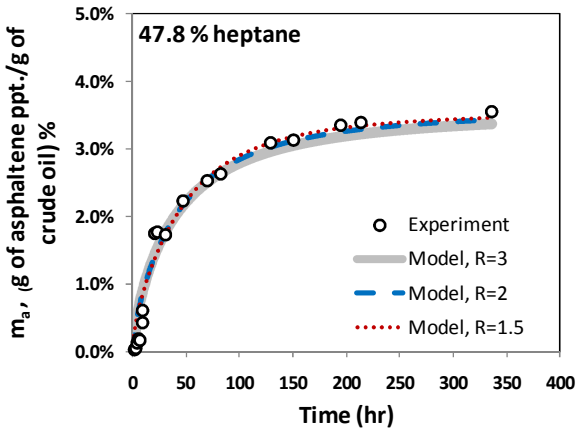

Figure 4.9: Experimental and simulated evolution of separated aggregates for different values of geometric scaling using Smoluchowski kernel for 47.8% heptane, using different values of R.

Initial diameter of asphaltene nano-aggregate

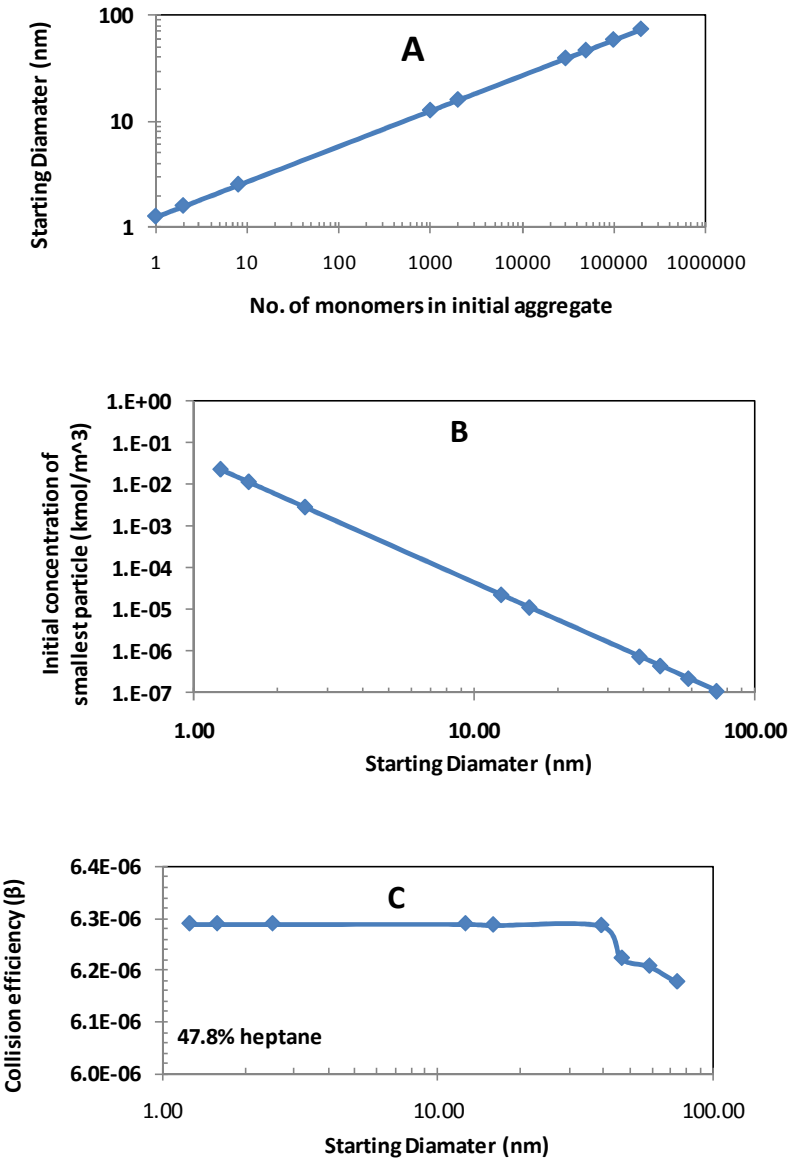

Figure 4.10: Plots to show the effect of the starting size of asphaltene nano-aggregates on the particle size distribution: (A) Diameter of the smallest particle, (B) Concentration of the starting particle, (C) Optimized collision efficiency as a function of the starting diameter. R = 2, Df = 3.

Simulations for the mass of asphaltenes precipitated with time assumed that the asphaltenes exist as nano-aggregates in the crude oil and each aggregate is comprised of 8 asphaltene molecules. In order to demonstrate the effect of the number of asphaltene

molecules per nano-aggregate on the aggregation kinetics, the initial particle diameter and number density were varied keeping the total mass of the precipitated asphaltenes constant. Figure 4.10 (A) shows the increase in the particle diameter of the nano-aggregate with the increase in the number of asphaltene molecules per particle. In the case of larger starting nano-aggregates, their concentration was reduced accordingly as shown in Figure 4.10 (B) in order to conserve the total mass of precipitated asphaltenes, which is an experimental measurement depending only on the volume of heptane in the system. Simulated results for the best-fit value of collision efficiency as a function of starting diameter are shown in Figure 4.10 (C). It can be seen that the collision efficiency is essentially independent of the particle diameter (and of the number of monomers in an aggregate), as long as starting particle size is below 40nm. This result can be explained by observing the mode diameter of the growing asphaltene particles as a function of time.

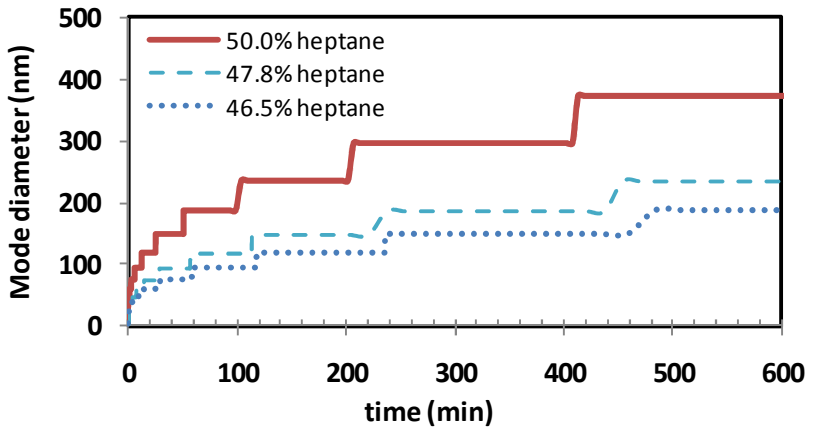

Figure 4.11: Mode diameter for three different heptane concentrations as a function of time. The step-like plots result from only discrete particle sizes being allowed in the geometric population balance. R = 2, Df = 3.

From Figure 4.11 it is observed that within the first 10 minutes of the experiments, the mode diameter reaches sizes of 40nm (or larger) for the three heptane

concentrations shown. Therefore, using an effective starting diameter of 40 nm in the model is equivalent to a 10-minute offset in the experimental results, when compared to a starting size of 2-3 nm. A 10-minute offset is within the error range of the experimental techniques described in Section 2. Figure 4.12 shows the calculated mode diameters for three different values of the number of asphaltene molecules in the initial nano-aggregate, which demonstrates that the growth of the particles is the same for these three values. Hence, it is can be concluded that the number of asphaltene molecules in the initial nano-aggregate has little or no effect on the aggregation kinetics of asphaltenes.

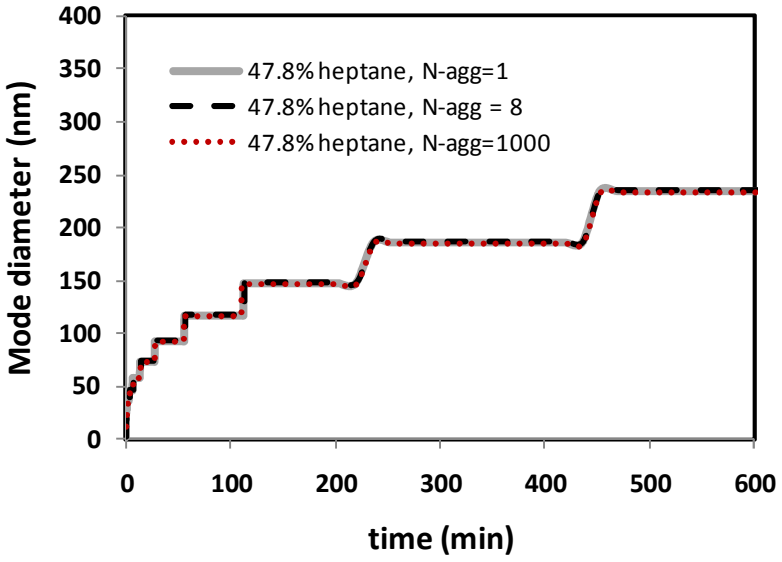

Figure 4.12: Mode of particle diameter vs. time for three different number of asphaltene molecules in the initial nano-aggregate: N-agg = 1, 8, 1000 for 47.8% heptane. R = 2, Df = 3.

This observation was confirmed by comparing our predictions for onset time for 40% heptane as shown in Figure 4.13. It is observed the predicted onset times for the

three cases superimpose each other on the plot. Similar observations are also observed for the predicted results of 40% heptane.

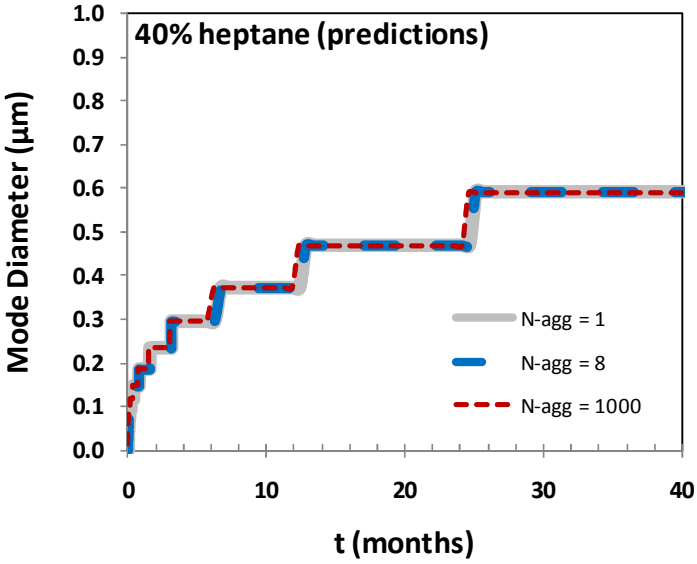

Figure 4.13: Mode of particle diameter vs. time for three different number of asphaltene molecules in the initial nano-aggregate: N-agg = 1, 8, 1000 for 40.0% heptane. R = 2, Df = 3.

Figure 4.14(A) shows the slope of the mode diameter vs. time data from Figure 4.11 for different heptane concentrations. The step-like plot from Figure 4.11 was fitted to a Michaelis–Menten type fit and which was then differentiated to obtain the rate of change of the mode diameter (i.e. the slope). It is observed that 50% heptane has the highest initial rate of change, demonstrating that the particles have the fastest growth for 50% heptane. Figure 4.14(B) shows the rate of change of the mode diameter plotted as a function of mode diameter for different heptane concentrations. It is observed that as the mode diameter reaches the 0.8 µm, the rate of change of the mode diameter reaches a zero value. It should be noted that the time required for the mode diameter to reach a

value of 0.8 μm depends on the driving force for aggregation i.e. the heptane concentration.

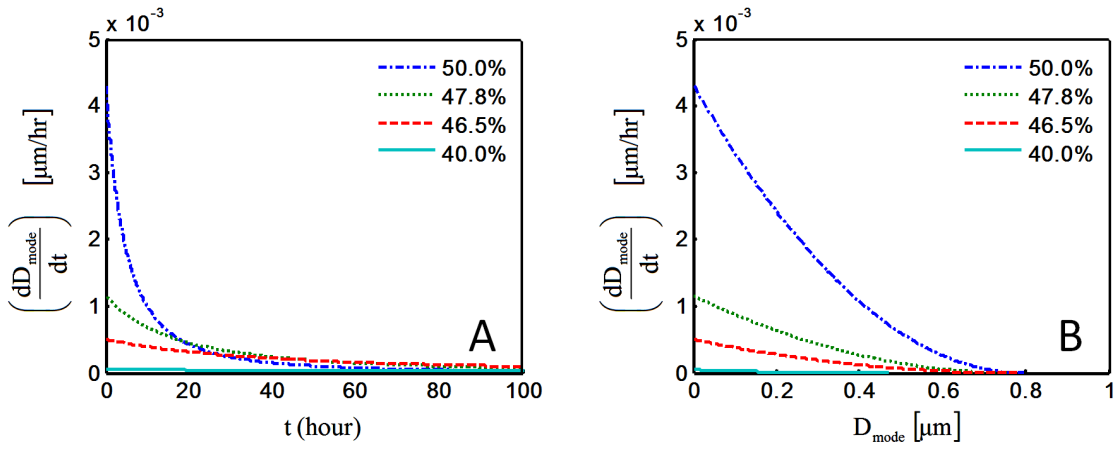

Figure 4.14: (A) Slope of the mode diameter plot from Figure 4.11 as a function of time for three experimental heptane concentrations (46.5%, 47.8% and 50.0% heptane). The calculated values of the slope for 40.0 % heptane based on model predictions are also included for comparison. (B) Slope of the mode diameter as a function of the mode diameter. R = 2, D_f = 3.

Conclusions

A generalized geometric population balance model has been successfully developed to simulate the growth of asphaltene aggregates from the nanometer scale to micron-size particles. The Smoluchowski kernel has been incorporated to describe the aggregation of the asphaltene nanoaggregates which is induced by the addition of a precipitant e.g. heptane. By incorporating a discretization scheme for the particle sizes which is based on the number of asphaltene molecules in the particles and not on the volume of the particles, the model is able to account for the conservation of the total mass of asphaltenes.

The model has been validated with experimental data for various heptane concentrations and a good fit has been observed in each case. The particle size

distribution (PSD) of the asphaltene aggregates as a function of time was also determined and it was observed that the shift of the PSD to larger diameters is faster in the case of higher heptane concentrations because of higher driving force for asphaltene aggregation. Calculations for the rate of change in mode diameters also demonstrated that the growth in the aggregate size increases with heptane concentration. In order to make predictions for the onset time at lower heptane concentrations, two limits were chosen for the solubility of asphaltenes and it was demonstrated that these limits provide a good lower and upper bound for the experimental values of the onset time for precipitation. This work is based on experimental data obtained at room temperature. However, the effect of temperature on the precipitation kinetics is covered in detail in our recent publication.[27]

A sensitivity analysis was performed to investigate the dependence of the model on the geometric scaling factor (R) and the size of the initial asphaltene aggregate. The model was able to match the experimental data for three different values of R and can be used when the particle sizes vary over several orders of magnitude. The simulation results were invariant to the size of the initial asphaltene aggregate up to a size of 40 nm for the initial aggregate size.

List of variables

β	Collision efficiency
μ_m	Viscosity of the medium (kg/m/s)
ρ_o	Oil density (kg/m^3)
ϕ_o	Volume fraction of oil in the oil-heptane mixture
C_k	Molar concentration of *k*-th aggregate (kmol m^{-3})
C_1	Molar concentration of asphaltene nanoaggregates (kmol/m^3)
d_i	Diameter of *i-th* aggregate (m)
d_p	Diameter of primary unit (m)
d_1	Diameter of an asphaltene nanoaggregate
D_f	Fractal dimension of the aggregate
k	Number of nanoaggregates units in an asphaltene particle
$K_{i,j}$	Collision kernel between aggregate sizes *i* and *j* (m^3 kmol^{-1} s^{-1})
m_A	Mass fraction of destabilized asphaltene per unit mass of oil resulting from the addition of a specified quantity of heptane is (kg/kg)
$M_{w,\,A}$	Molecular weight of the asphaltene molecules
n_a	Number of primary asphaltene units (molecules) in any aggregate
N_a	Avogadro constant
N_{agg}	Number of asphaltene molecules per nanoaggregate
R	Geometric scaling between two subsequent aggregates
R_g	Ideal gas constant (J/ K/kmol)
t	Time (seconds)
T	Temperature (K)
V_m	Volume of nanoaggregate (m^3)

References

1. Rassamdana, H., Sahimi, M., Asphalt flocculation and deposition: II. formation and frowth of fractal aggregates, AIChE J. , 1996, 42, 3318-3332.

2. Rastegari, K., Svrcek, W. Y., and Yarranton, H. W.., Kinetics of asphaltene flocculation, Ind. Eng. Chem. Res. 2004, 43, 6861-6870.

3. Rahmani, N. H. G., Dabros, T., Masliyah, J. H., Evolution of asphaltene floc size distribution in organic solvents under shear, Chemical Engineering Science, 2004, 59, 685–697.

4. Gawrys, K. L., Blankenship, G. A., Kilpatrick, P. K., Solvent entrainment in and flocculation of asphaltenic aggregates probed by small-angle neutron scattering, Langmuir, 2006, 22, 4487-4497.

5. Hirschberg, A., deJong, L. N. J., Schipper, B. A., Meijer, J. G., Influence of temperature and pressure on asphaltene flocculation, Soc. Pet. Eng., J. 1984, 24 (3), 283-293.

6. Wang, J. X., Buckley, J. S., A two-component solubility model of the onset of asphaltene flocculation in crude oils, Energy & Fuels 2001, 15, 1004-1012.

7. Wattana, P., Wojciechowski, D. J., Bolaños, G., Fogler, H., S., Study of asphaltene precipitation using refractive index measurement, Petroleum Science and Technology, 2003, 21, 3-4, 591 - 613.

8. Kraiwattanawong, K., Fogler, H. S., Gharfeh, S. G., Singh, P., Thomason, W., H., Chavadej, S., Thermodynamic solubility models to predict asphaltene instability in live crude oils, Energy & Fuels, 2007, 21, 1248-1255.

9. Pina, A., Mougin, P., and Béhar, E., Characterization of asphaltenes and modeling of flocculation-state of the art, Oil & Gas Science and Technology - Rev. IFP, 2006, 61, 3, 319-343.

10. Angle, C.W., Long, Y., Hamza, H., Lue, L., Precipitation of asphaltenes from solvent-diluted heavy oil and thermodynamic properties of solvent-diluted heavy oil solutions, Fuel, 2006, 85, 4, 492-506.

11. Murzakov, R. M., S. A. Sabanenkov, and Z. I. Syunyaev, Influence of petroleum resins on colloidal stability of asphaltene-containing disperse systems, Z. I. Khim. Tekhnol. Topl. Masel, 1981, 10, 40-41.

12. Maqbool, T.; Balgoa A.T.; Fogler H. S. Revisiting Asphaltene Precipitation from Crude Oils: A Case of Neglected Kinetic Effects. 2009, *Energy Fuels*, *23* (7), 3681–3686.

13. Elimelech, M., Gregory, J., Jia, X., Williams, R., Particle deposition and aggregation: measurements modeling and simulation, Butterworth-Heinemann Ltd., Oxford, 1995.

14. Hounslow M. J., Ryall R. L., Marshall, V. R., A discretized population balance for nucleation, growth, and aggregation, AIChE J., 1988, 34, 1821-1832.

15. Runkana, V., Somasundaran, P., Kapur, P. C., Reaction-limited aggregation in presence of short-range structural forces, AIChE J. , 2005, 51(4), 1233-1245.

16. Kranenburg, C., The fractal structure of cohesive sediment aggregates, Estuarine, Coastal and Shelf Science, 1994, 39, 451-460.

17. Batterham, R. J., J. S. Hall, and G. Barton, "Pelletizing Kinetics and Simulation of Full-Scale Balling Circuits," Proc. 3rd Int. Symp. on Agglomeration, Nurnberg, W. Germany, A136 (1981).

18. Wu, C. C., Huang, C., Lee, D.J., Effects of polymer dosage on alum sludge dewatering characteristics and physical properties, Colloids and Surfaces A: Physicochemical and Engineering Aspects, 1997, 122, 89-96.

19. Rahmani, N. H. G., Dabros, T., Masliyah, J. H., Evolution of asphaltene floc size distribution in organic solvents under shear, Chemical Engineering Science, 2004, 59, 685–697.

20. Betancourt, S. S.; Ventura, G. T.; Pomerantz, A. E.; Viloria, O.; Dubost, F. X.; Zuo, J.; Monson, G.; Bustamante, D.; Purcell, J. M.; Nelson, R. K.; Rodgers, R. P.; Reddy, C. M.; Marshall, A. G.; Mullins, O. C.Nanoaggregates of Asphaltenes in a Reservoir Crude Oil. Energy Fuels 2009, 23, 1178– 1188

21. Mostowfi, F.; Indo, K.; Mullins, O. C.; McFarlane, R. Asphaltene Nanoaggregates Studied by Centrifugation Energy Fuels 2009, 23, 1194– 1200

22. Mullins, O.C.; The Modified Yen Model. Energy & Fuels, 24, 2179-2207

23. Indo, K.; Ratulowski, J.; Dindoruk, B.; Gao, J.L.; Zuo, J.L.; Mullins, O.C.; Asphaltene Nanoaggregates Measured in a Live Crude Oil by Centrifugation. Energy & Fuels, 23, 4460-4469.

24. Friedlander, S. K., Smoke, dust and haze: fundamentals of aerosol dynamics, Oxford University Press, New York, 2000.

25. Scott, G. D., D. M. Kilgour, The density of random close packing of spheres, Brit. J. Appl. Phys., 1969, 2, 863-866

26. Khoshandam, A. and Alamdari, A.; Kinetics of Asphaltene Precipitation in a Heptane−Toluene Mixture, Energy Fuels, 2010, 24 (3), pp 1917–1924

27. Maqbool, T.; Srikiratiwong, P.; Fogler H. S. The Effect of Temperature on the Precipitation Kinetics of Asphaltenes. 2010, Energy Fuels, Accepted for publication

CHAPTER 5

CHARACTERIZING ASPHALTENES PRECIPITATED AS A FUNCTION OF TIME

Introduction

Asphaltenes are considered to be one of the most problematic and the least understood organic deposits because of their complex chemical structure and composition (Wattana 2004). Operationally defined on the basis of solubility, asphaltenes are the components of crude oils that are soluble in aromatics, but are insoluble in light alkanes (Bestougeff and Byramjee 1994; Speight 1999). They comprise of polycyclic aromatic hydrocarbons with a random distribution of heteroatoms (e.g. N, S, O) and trace metals (e.g. V, Ni, Fe) (Hammami 2007).

Asphaltenes are precipitated from crude oils by adding n-alkane solvents, in an volume ratio of at least l:40 (oil:precipitant). They are dark brown to black friable solids with no definite melting point. In addition to the classical definition, asphaltenes tend to be classified by the particular alkanes used to precipitate them. Thus, there are pentane asphaltenes, hexane asphaltenes and heptane asphaltenes.

Asphaltenes are a family of polydisperse molecules with varying properties. Kaminski et. al (2000) developed a technique to separate asphaltenes into various polarity based fractions by changing the ratio of the polar and non-polar components in the solvent mixture. It was later demonstrated that the more polar fractions of asphaltenes

have a higher dielectric constant (Wattana 2005) and higher amount of metals like Ni and V (Wattana 2004). It was also shown that the asphaltenes from the field deposits, which were more unstable and problematic asphaltenes, had a higher dielectric constant and greater wt.% of metals like Ni and V as compared to the asphaltenes from the matching crude oils, which were more stable and less prone to precipitation (Wattana 2005).

Literature from the past several decades indicates that there is a critical concentration of the precipitant required for the asphaltenes to precipitate. Below this critical concentration (also known as the precipitation onset point), the asphaltenes were believed to be stable in the crude oil and would not precipitate (Escobedo 1995; Buckley 1999; Wang 2003; Wattana 2003; Mousavi-Dehghania 2004). However recent work has shown that the precipitation of asphaltenes is a kinetic process and can span over several months in some cases (Maqbool 2009). It is proposed that the asphaltenes that precipitate earlier are likely to be more unstable than the other asphaltenes in the crude oil. In most of the operations in the petroleum industry the residence/processing time may vary from a few hours to a few days. Characterizing the properties of different fractions of asphaltenes precipitated as a function of time will help us in identifying the asphaltenes that are the most problematic and will aid in designing more effective chemical treatments for mitigating asphaltene problems.

Experimental Methods

A known volume of crude oil was taken in a flask and heptane was then added to the crude oil using a syringe pump. The crude oil was kept well-stirred using a magnetic stirrer and heptane was added until the desired heptane concentration was attained. The heptane flow was stopped and the flask was sealed with a stopcock to prevent heptane evaporation and to limit the exposure to air. Samples were withdrawn at different times from the oil-heptane mixture and centrifuged at 10000 rpm for 10 minutes to separate the asphaltenes precipitated up to that time. The precipitated asphaltene fraction was then washed with hot heptane in a Soxhlet apparatus for 24 hours to remove residual oil. The washed asphaltenes were dried in an oven until their mass was constant.

Dielectric Constant Measurements

Solutions of asphaltene samples in toluene were prepared at different concentrations and their dielectric constant was measured by low frequency dielectric spectroscopy using HP 4192 analyzer. The cell was first calibrated with toluene. All measurements were performed at a frequency of 100 kHz and a temperature of 25°C. The measurements were conducted by Vanton Research Laboratory, Inc. located in Concord, California.

Metal content analysis

The measurements for trace metals were conducted at Intertek QTI labs located in Whitehouse, New Jersey. Inductively Coupled Plasma - Optical Emission Spectroscopy (ICP-OES) was used for these measurements.

Polarity based fractionation of asphaltenes

Binary mixtures of polar (methylene chloride) and non-polar (n-pentane) solvents were used for the procedure. Initially 1 part of asphaltene was completely dissolved in 15 parts of methylene chloride (CH_2CL_2) by weight. Pentane was added in discrete increments of 10 vol. % until the first fraction of asphaltenes precipitated. For the asphaltenes used in this study the first fraction precipitated at a methylene chloride – pentane ratio of 70:30 and is referred to as the $F^{70/30}$ fraction. The precipitated asphaltenes were removed by centrifugation and additional pentane was added to the supernatant in 10 vol. % increments, yielding the $F^{60/40}$, $F^{50/50}$, $F^{40/60}$, $F^{30/70}$ and $F^{20/80}$ fractions, where the first index refers to the vol. % of methylene chloride and the second index refers to the vol. % of pentane. Because the $F^{70/30}$ fraction precipitates upon the addition of the smallest quantity of pentane (a non-polar solvent), it is the most polar fraction of all the asphaltenes being fractionated. For the same reasons the asphaltenes in the $F^{20/80}$ and the supernatant of $F^{20/80}$ are the least polar fractions.

Results and Discussion

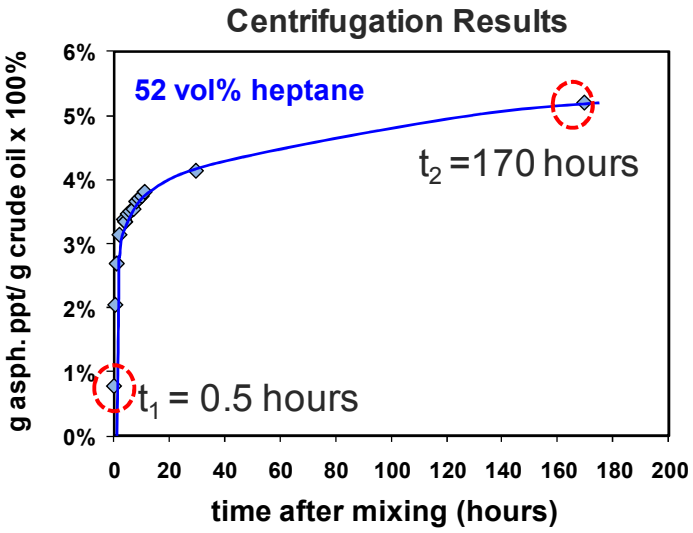

Figure 5.1: Centrifugation plot showing which asphaltene fractions are likely to exhibit the greatest difference in terms of stability. Asphaltene fractions precipitating at the earliest time (ca. 0.5 hours) and those precipitating at the end (ca. 170 hours) were collected for comparison of the dielectric constants. Results are for K1 oil.

Figure 5.1 shows the times when samples were collected for the dielectric constant measurements for the K1 oil. The asphaltene fractions precipitating at the earliest time (ca. 0.5 hours) and at the plateau value of the centrifugation plot were chosen because they would likely represent the biggest difference in properties related to asphaltene stability. However, it should be noted that the total asphaltene content of the K1 oil is 10.9 wt. %. Therefore, less than half of the total asphaltenes from the K1 crude oil have precipitated by 170 hours for 52 vol. % heptane (Figure 5.1). The asphaltenes remaining in solution at 170 hours will be even more stable than those precipitating by 170 hours. Therefore, it was decided to compare the characterization results of

asphaltenes precipitating at 0.5 hours and 170 hours to the total asphaltenes (comprising of a mixture of precipitated and soluble asphaltenes).

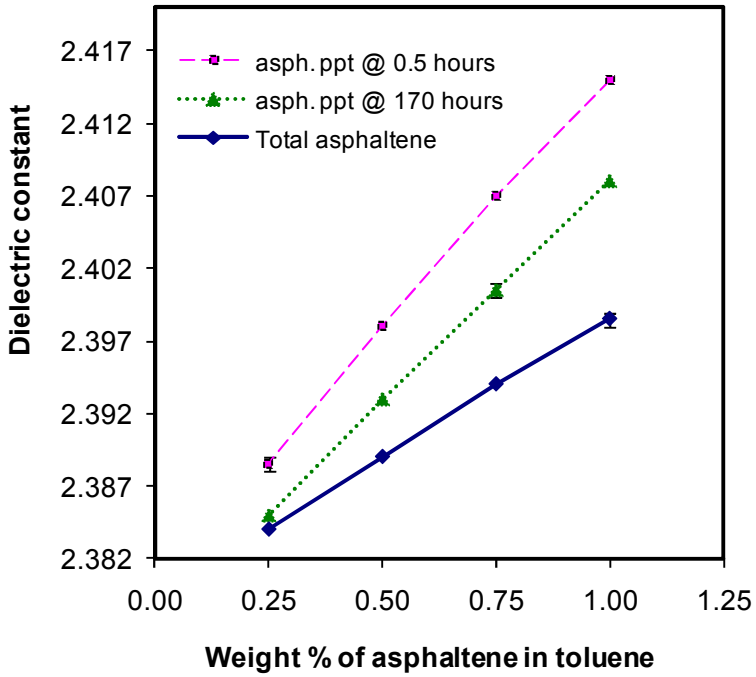

Figure 5.2: Comparison of the dielectric constant of solutions of asphaltenes in toluene precipitated at various concentrations. Data for asphaltenes fractions precipitating at 0.5 hours and 170 hours is compared to the total asphaltenes. Results are for K1 oil.

The results for the dielectric constant measurements for the three K1 crude oil asphaltene fractions dissolved in toluene are shown in Figure 5.2. One observes that the dielectric constant of the 0.5 hour asphaltenes is higher than the other two asphaltenes fractions and the total asphaltenes have the lowest dielectric constant.

Table 5.1: Comparison of the dielectric constant of pure asphaltene samples obtained by extrapolating the data from Figure 5.2 to 100% asphaltene.

Sample	Dielectric Constant
Asphaltene precipitate @ 0.5 hours	5.9
Asphaltene precipitate @ 170 hours	5.4
Total Asphaltene	4.3

Table 5.1shows the values of the dielectric constant of the asphaltene fractions by extrapolating the data in Figure 5.2 to 100%, in order to obtain the values for pure asphaltenes. The reason for the earliest precipitating asphaltenes (at 0.5 hours) to have the largest value of the dielectric constant is likely that these asphaltenes are the most unstable fraction of all the asphaltenes in this crude oil. Asphaltenes are a family of molecules with a distribution of properties that govern their stability. It has been shown earlier (Wattana 2004, Wattana 2005) that the unstable asphaltenes have more polar nature and higher values of dielectric constant than the other asphaltenes. The larger values of the dielectric constant for the 0.5 hour asphaltene sample is consistent with those results. The total asphaltenes exhibit the lowest dielectric constant among the three samples because they are a collection of all the asphaltenes present in a crude oil – those that may precipitate at 0.5 hours, 170 hours or that do not precipitate at all. Therefore, the dielectric constant of the total asphaltenes is averaged out and is lower than the other two fractions that precipitate out at certain times.

It also needs to be pointed out that in the asphaltene collection approach shown in Figure 5.1 the 0.5 hour asphaltenes comprise all asphaltenes precipitating between 0 and 0.5 hours. Similarly, the 170 hour sample has all asphaltenes precipitating between 0 and 170 hours. Therefore, the 170 hour sample also contains the asphaltenes from the 0.5

hour sample. Hence, it is expected that if the samples were collected in a manner that would eliminate any overlap in the precipitation time, a greater difference would be observed in the properties of the 0.5 hour and 170 hours asphaltene samples and the dielectric constant value for the latter would be closer to that of the total asphaltenes. Keeping this point in consideration, a new asphaltene collection procedure was developed. The experiments for the GM2 oil were started at 39 vol. % heptane and after about 1 hour the entire batch of the sample was centrifuged and all the asphaltenes precipitated until that time were removed and will be referred to as Fraction # 1 (Figure 5.3). The supernatant was transferred to a clean Erlenmeyer flask and was mixed with a magnetic stirrer until 49 hours when the entire sample was centrifuged again to collect the asphaltenes precipitated between 1 hour and 49 hours (i.e. Fraction # 2). Similarly the next fraction of the asphaltenes precipitated between 49 and 278 hours was collected (Fraction # 3). The supernatant from Fraction # 3 was again transferred to a clean Erlenmeyer flask and additional heptane was added to increase the heptane concentration from 39 to 50 vol. %. The asphaltenes precipitated for 50 vol. % heptane between 278 hours and 510 hours were collected as Fraction # 4. Finally, Fraction # 5 was collected by increasing the heptane concentration of the supernatant from Fraction #4 to 60 vol. % heptane. All these fractions were washed individually in a Sohxlet apparatus with hot heptane for 24 hours and dried in an oven until their weight was constant. These fractions were used for investigating the metal content and polarity-based separation of asphaltenes.

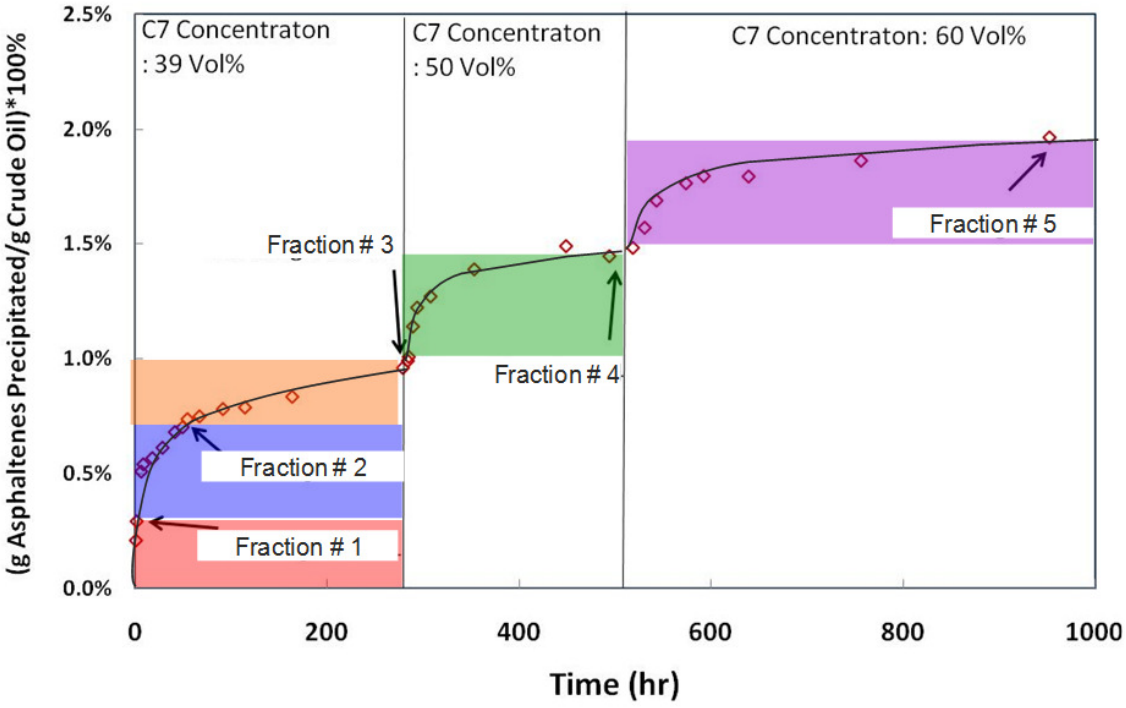

Figure 5.3: Plot showing the improved procedure for collection of asphaltene samples where the entire batch of oil-precipitant mixture was centrifuged at certain times to remove all the asphaltenes precipitated up to that time for a given heptane concentration. Results are for GM2 oil.

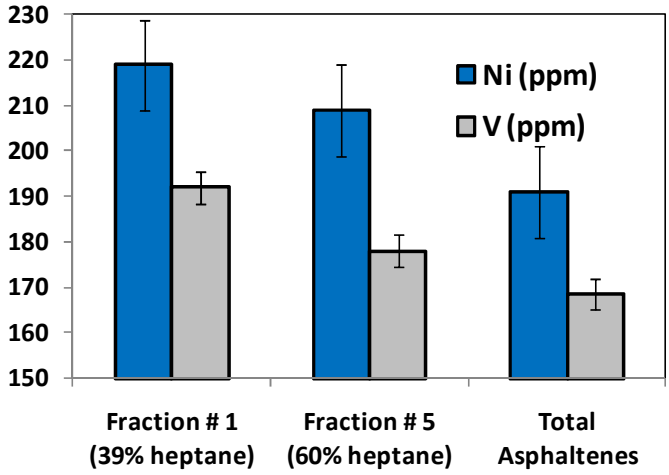

Figure 5.4: Comparison of the Ni and V concentrations in the three asphaltene fractions for GM2 oil.

The results of the metal content analysis of Fractions 1, 5, and total asphaltenes for GM2 oil are shown in Figure 5.4. It is observed that the Fraction 1 has the highest content of both Ni and V. This result is consistent with the findings of Wattana et al. (2005) who demonstrated that the more unstable asphaltene fractions usually have a higher content of Ni and V than the more stable asphaltenes from the same crude oil. It must be noted that even though Figure 5.4 demonstrates a trend in the trace metal content of the three samples, the differences in the values are not very large. Therefore, considering the uncertainties in the values for the metal content, the intermediate fractions – 2,3 and 4 from Figure 5.3 – were not analyzed because the values of Ni and V for these samples will be bounded by Fraction # 1 and the total asphaltenes.

The results for the polarity based fractionation for Fraction 1, 5 and the total asphaltenes for the GM-2 oil are shown in Figure 5.5. Going from left to right in Figure 5.5 increases the relative amount of pentane in comparison to the methylene chloride in the solvent mixture and reduces the overall polarity of the solvent mixture. The asphaltene samples which have a greater weight % on the left side of the plot are the more polar asphaltenes because they precipitate with small additions of pentane. On the other hand, the asphaltene samples which lie predominantly on the right side of this plot are less polar, because they require relatively greater amounts of pentane in order to precipitate out of solution. $F^{70/30}$ and the $F^{60/40}$ asphaltenes are essentially equal for all the three samples. The $F^{50/50}$ asphaltene is the highest for Fraction 1 and lowest for the total asphaltenes. Additionally, $F^{30/70}$ is lower for Fraction 1 as compared to Fractions #5 and total asphaltenes. Therefore, it can be concluded that Fraction 1 which consists of the asphaltenes that precipitate out at the earliest time is the most unstable and most polar of

all the asphaltene fractions described in Figure 5.3. It is also noted that in spite of a reasonable trend in the polarity based fractionation, there are only small differences in the measured values for these three samples (Figure 5.5). This finding is similar to measurements for the trace metal content discussed earlier, which suggests that while there are some differences in the asphaltenes precipitated at different times, the magnitude of the differences is small. Hence, more precise techniques like NMR or high resolution mass spectrometry may be needed to resolve the differences in properties of these asphaltene fractions.

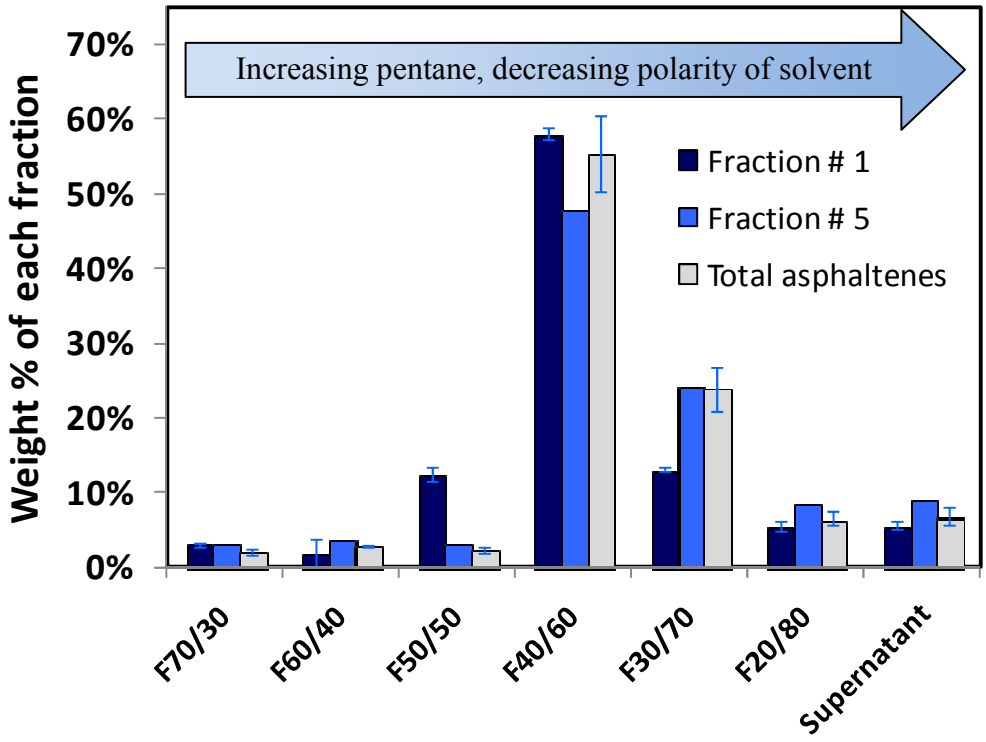

Figure 5.5: Results for polarity-based fractionation for three different asphaltene fractions for GM2 oil.

Conclusions

Asphaltenes that precipitated after the addition of heptane to crude oil were collected at different times after heptane addition. It was shown that the asphaltenes that precipitate earliest in the process are the most unstable fraction. They have a higher dielectric constant and contain greater quantities of metals like Ni and V than other asphaltenes. Additionally, they also contain relatively larger quantities of the high polarity fractions as compared to the asphaltenes that precipitate later.

References

1. Bestougeff, M.A. and Byramjee, R.J. (1994) Chemical Constitution of Asphaltenes. Asphaltenes and Asphalts 1. T. F. Yen and G.V. Chilingarian. Amsterdam, The Netherlands: Elsevier, 40A: 67.

2. Buckley J.S. Predicting the Onset of Asphaltene Precipitation from Refractive Index Measurements. Energy & Fuels 1999,13, 328-332.

3. Escobedo, J.; Mansoori, G.A. Viscosimetric Determination of the onset of asphaltene flocculation: a novel method. SPE Production and Facilities 1995, 10, 115-118

4. Hammami, A.; Ratulowski, J. in Asphaltenes, Heavy Oils, and Petroleomics, O.C. Mullins; E.Y. Sheu; A. Hammami; A.G. Marshall, Eds.; Springer: New York, 2007; pp 617-660

5. Kaminski, T. J.; Fogler, H. S.; Wolf, N.; Wattana, P.; Mairal, A. Classification of Asphaltenes via Fractionation and the Effect of Heteroatom Content on Dissolution Kinetics. Energy & Fuels 2000, 14, 25-30

6. Maqbool, T.; Balgoa A.T.; Fogler H. S. Revisiting Asphaltene Precipitation from Crude Oils: A Case of Neglected Kinetic Effects. 2009, Energy Fuels, 23 (7), 3681–3686

7. Mousavi-Dehghania, S. A.; Riazi, M. R.; Vafaie-Seftic, M. and Mansoori, G. A. An analysis of methods for determination of onsets of asphaltene phase separations. Journal of Petroleum Science and Engineering 2004, 42, 145-156

8. Speight, J.G. (1999) The Chemistry and Technology of Petroleum. New York: Marcel Dekker, Inc.

9. Wang, J.X.; Buckley, J.S. Asphaltene Stability in Crude Oil and Aromatic Solvents - The influence of oil composition. Energy & Fuels 2003, 17, 1445-1451

10. Wattana, P., Wojciechowski, D.J., Bolaños, G. and Fogler, H.S. (2003) Study of asphaltene precipitation using refractive index measurement. Petroleum Science and Technology, 21 (3-4), 591 – 613.

11. Wattana, P. (2004) Precipitation and characterization of asphaltenes. Ph.D. Thesis in Chemical Engineering, College of Engineering, University of Michigan – Ann Arbor

12. Wattana, P. (2004) Precipitation and characterization of asphaltenes. Ph.D. Thesis in Chemical Engineering, College of Engineering, University of Michigan – Ann Arbor.

13. Wattana, P. and Fogler, H.S. Characterization of Polarity-Based Asphaltene Subfractions Energy & Fuels 2005, 19, 101-110

CHAPTER 6

CONCLUSIONS

Revisiting Asphaltene Precipitation from Crude Oils: A Case of Neglected Kinetic Effects

Most studies on thermodynamics of asphaltene stability have neglected the kinetic effects associated with the precipitation and aggregation of asphaltenes. The experimental duration of these studies generally varies between near-instantaneous to one day, implicitly assuming that the system will reach equilibrium in this short time-span. These short time span experiments can provide misleading results because systems that appear to be stable are actually unstable at longer times, as shown in this study using two different crude oils. This research shows that in order to understand the destabilization of asphaltenes from crude oils, the associated kinetic effects must be considered. Data from microscopy and centrifugation experiments demonstrates that depending upon the precipitant concentration, the onset time for asphaltene precipitation can vary from a few minutes to several months. We have also shown that the commonly referred criteria of a critical precipitant concentration required for asphaltene precipitation is not a fundamental parameter, but an experimental artifact originating from the relatively short waiting times used in the earlier studies. Therefore, the application of thermodynamic models using short term experimental data may need to be reexamined. In order to get the correct thermodynamic values, the experiments need to be conducted over long periods and by using this approach we have been able to obtain the solubility of asphaltenes as a

function of the precipitant concentration. The research presented here opens up a new paradigm for the understanding of asphaltene stability in crude oils and for the related thermodynamic approaches.

The Effect of Temperature on the Precipitation Kinetics of Asphaltenes

An experimental and theoretical approach to identify the effect of temperature on the kinetics of asphaltene precipitation from crude oil – precipitant mixtures has been discussed. We have demonstrated that at higher temperatures the precipitation onset time for asphaltenes is shorter and their solubility is higher. We have established that the change in temperature leads to a change in viscosity which in turn affects the collision kernel for the Brownian flocculation of asphaltenes and controls the onset time for precipitation. Other possible factors affecting the onset time due to changes in temperature have also been discussed and analyzed for their individual contributions for asphaltene precipitation kinetics. It has been shown here other factors like the expansion of hydrocarbons, the possibility of oxidation (or other chemical changes) upon heating the crude oil to 50°C and loss of light hydrocarbons due to evaporation have little or no effect on asphaltene precipitation kinetics for the experimental conditions discussed here. This study provides a unified approach to understand the variety of factors that change as a result of temperature variation and evaluates their individual contributions to changes in asphaltene precipitation kinetics and their solubility.

Modeling the Aggregation of Asphaltene Nanoaggregates in Crude Oil-Precipitant Systems

A generalized geometric population balance model has been successfully developed to simulate the growth of asphaltene aggregates from the nanometer scale to micron-size particles. The Smoluchowski kernel has been incorporated to describe the aggregation of the asphaltene nanoaggregates that induced by the addition of a precipitant e.g. heptane. By incorporating a discretization scheme for the particle sizes which is based on the number of asphaltene molecules in the particles and not on the volume of the particles, the model is able to account for the conservation of the total mass of asphaltenes.

The model has been validated with experimental data for various heptane concentrations and a good fit has been observed in each case. The particle size distribution (PSD) of the asphaltene aggregates as a function of time was also determined and it was observed that the shift of the PSD to larger diameters is faster in the case of higher heptane concentrations because of higher driving force for asphaltene aggregation. Calculations for the rate of change in mode diameters also demonstrated that the growth in the aggregate size increases with heptane concentration. In order to make predictions for the onset time at lower heptane concentrations, two limits were chosen for the solubility of asphaltenes and it was demonstrated that these limits provide a good lower and upper bound for the experimental values of the onset time for precipitation.

A sensitivity analysis was performed to investigate the dependence of the model on the geometric scaling factor (R) and the size of the initial asphaltene aggregate. The model was able to match the experimental data for three different values of R and can be

used when the particle sizes vary over several orders of magnitude. The simulation results were invariant to the size of the initial asphaltene aggregate up to a size of 40 nm for the initial aggregate size.

Characterizing Asphaltenes Precipitated as a Function of Time

Asphaltenes that precipitated after the addition of heptane to crude oil were collected at different times after heptane addition. It was shown that the asphaltenes that precipitate earliest in the process are the most unstable fraction. They have a higher dielectric constant and contain greater quantities of metals like Ni and V than other asphaltenes. Additionally, they also contain relatively larger quantities of the high polarity fractions as compared to the asphaltenes that precipitate later.

CHAPTER 7

FUTURE WORK

Characterization of asphaltenes precipitated as a function of time

As discussed in Chapter VI, asphaltene samples precipitated from a crude oil precipitant mixture exhibit differences in their dielectric constant, polar nature and metal content. In order to develop a deeper understanding of the difference in these asphaltene fractions the following studies are recommended.

Molecular weight distribution of different asphaltene fractions:

It has been reported in literature that the more unstable asphaltenes have a greater molecular weight.[1] However, the VPO measurements reported in this study reflect the molecular weights of asphaltene aggregates rather than individual asphaltene molecules.[1] Recent studies have been able to identify the molecular weight of asphaltene molecules. Two-step laser mass spectrometry (L^2MS) technique has been shown to effectively measure the molecular weight distribution of asphaltenes and is free from artifacts resulting from aggregation and insufficient laser power.[2] For asphaltenes from different sources, the molecular weight distribution ranged from 200 units to 1000-1500 units with a peak in the range of 500-600 units. This technique can be applied to the asphaltene fractions precipitated at different times to potentially establish the differences

in their molecular weight distributions – the heavier asphaltene molecules would likely be less stable in the oil-precipitant mixture.

Aromaticity of different asphaltene fractions:

In a recent study on the characterization of asphaltenes which were exposed to hydrotreatment process it was demonstrated that the asphaltenes became more aromatic and yielded highly polycondensed dealkylated aromatic structures with increasing severity of the process.[3] The same characterization approach can also be used to study the aromatic nature of the asphaltenes precipitated as a function of time. It is expected that the more aromatic asphaltenes will be the first ones to precipitate out because the driving force for the precipitation of asphaltenes in the experiments discussed in Chapter VI is the addition of heptane – a non-aromatic hydrocarbon. Therefore, addition of heptane will lead to the decrease in the overall aromaticity of the crude oil-precipitant mixture and the most aromatic asphaltenes will likely be the first ones to precipitate out. NMR and FTIR studies on the asphaltene fractions will also be helpful in obtaining information about the aromaticity and the functional groups present in different asphaltene fractions which may affect their stability as well.[4,5]

References

1. Wattana, P. (2004) *Precipitation and characterization of asphaltenes. Ph.D. Thesis in Chemical Engineering*, College of Engineering, University of Michigan – Ann Arbor.

2. Pomerantz, A. E.; Hammond, M. R.; Morrow, A. L.; Mullins, O. C. and Zare, R. N. *Asphaltene Molecular-Mass Distribution Determined by Two-Step Laser Mass Spectrometry*. Energy & Fuels 2009, 23, 1162–1168

3. Purcell, J. M.; Merdrignac, I.; Rodgers, R. P.; Marshall, A. G.; Gauthier T. and Guibard, I. *Stepwise Structural Characterization of Asphaltenes during Deep Hydroconversion Processes Determined by Atmospheric Pressure Photoionization (APPI) Fourier Transform Ion Cyclotron Resonance (FT-ICR) Mass Spectrometry.* Energy Fuels 2010, 24, 2257–2265

4. M. Daaou, D. Bendedouch, Y. Bouhadda, L. Vernex-Loset, A. Modaressi, and M. Rogalski. *Explaining the Flocculation of Hassi Messaoud Asphaltenes in Terms of Structural Characteristics of Monomers and Aggregates.* Energy Fuels 2009, 23, 5556–5563

5. Y. Bouhadda, P. Florian, D. Bendedouch, T. Fergoug, D. Bormann. *Determination of Algerian Hassi-Messaoud asphaltene aromaticity with different solid-state NMR sequences.* Fuel 89 (2010) 522–526

APPENDIX - A

SUPPLEMENTAL INFORMATION FOR GEOMETRIC POPULATION BALANCE MODEL

A.1 Separation of asphaltene aggregates in centrifuge

The centrifuge is used as a separator to separate the micron-size aggregates from the fluid medium leaving behind the ultrafine aggregates. Centrifuge operation and design variables coupled with the physical properties of solid and fluid are used to get an estimation of the separation efficiency of aggregates of varying size. The separation capability of the centrifuge depends on the radius of centrifuge, the rpm, centrifugation time, fluid viscosity, aggregate size and densities of fluid and solid. The separation efficiency is estimated based on Stokes law of settling. Effect of Brownian dispersion is neglected in this calculation of separation efficiency for centrifugation. Considering the fact that the volume fraction of asphaltene aggregates in the oil-precipitant mixture is dilute, we can neglect the effect of particle collisions that retard particle settling.

Consider the *i*-th aggregate immersed in a liquid at distance *x* from the centre of centrifuge. The velocity of the aggregate inside the centrifuge is not constant, but increases as it moves outward in radial direction because of the influence of centrifugal force. The force balance on the *i*-th aggregate is written as,

$$(w_i - w_i^{'})\omega^2 x = F_d = 3\pi d_i \mu_m u \qquad \text{(A.1)}$$

Left hand side of the expression represents the centrifugal force which is equated to the drag force on the aggregate. The drag force on the aggregate is also expressed in terms of Stoke's law. In Equation (A.1), $w_i - w_i^{'}$ represents the apparent mass (corrected for buoyancy) of the aggregate and ω is the angular velocity. The radial distance of the aggregate from the centrifugal axis at time t is represented by x. In Equation 34, d_i represents the diameter of the i-th aggregate, u represents the aggregate velocity, μ_m represents the viscosity of the oil-heptane medium. The medium viscosity and density are estimated by applying log-average and volume average mixing rules respectively.

Mass of i-th aggregate is written as,

$$w_i = \frac{\pi d_i^3 \varepsilon}{6}\rho_A + \frac{\pi d_i^3}{6}(1-\varepsilon)\rho_m \tag{A.2}$$

Where ρ_m represents medium density and ε represents the solid fraction in the aggregate

Mass of displaced medium is written as,

$$w^{'} = \frac{\pi d_i^3}{6}\rho_m \tag{A.3}$$

Velocity of particle is given by,

$$u = \frac{dx}{dt} \tag{A.4}$$

Combining Equations (A.1)- (A.4) gives,

$$\frac{dx}{dt} = \frac{\varepsilon d_i^{\,2} \Delta\rho\omega^2}{18\mu_m} x$$

(A.5)

For an aggregate to get separated, it needs to reach the bottom of the centrifuge tube during centrifugation. If an aggregate reaches the bottom of the tube while centrifuging for a duration of time t, then the initial location of the aggregate (x_o) can be estimated using Equation 38. Considering that the aggregate travels from its initial location (x_o) to its final location (x_f) in time t, Equation 38 can be integrated to obtain

$$\ln \frac{x_f}{x_0} = \frac{\varepsilon d_i^{\,2} \Delta\rho\omega^2 t}{18\mu_m} \tag{A.6}$$

The distance traveled by the i-th aggregate in time t is given by

$$\Delta x_i = x_f - x_0 = x_f \left[1 - \exp\left(- \frac{\varepsilon d_i^{\,2} \Delta\rho\omega^2 t}{18\mu_m} \right) \right] \tag{A.7}$$

Considering the fact that the i-th aggregate travels a distance Δx_i to reach the bottom in centrifugation time t, all i-th aggregates having initial location within a distance of Δx_i from bottom get separated during the centrifugation process. The i-th aggregates initially located outside this range do not get separated under the centrifugation condition. As can be seen from Equation (A.7), Δx_i is a function of aggregate size, density difference, rotational speed, medium viscosity and the radius of centrifuge tube. Different aggregates get separated to different fraction based on the size of aggregate. Separation efficiency of i-th aggregate, s_i represents the fraction of the i-th aggregate that get separated in the centrifuge. Assuming that the aggregates are homogeneously distributed

along the axis of the centrifuge, we define the separation efficiency of *i*-th aggregate in a centrifuge tube with liquid height *L* as,

$$s_i = \frac{\Delta x_i}{L} \quad \text{for } \Delta x_i < \mathrm{L}$$
$$= 1 \qquad \text{for } \Delta x_i > \mathrm{L} \tag{A.8}$$

If the aggregate displacement in the centrifugation condition is such that $\Delta x_i > L$ (this may happen for large aggregates) then all aggregates of this size get separated. For these large aggregates $s_i = 1$ and for the smaller aggregates $s_i < 1$.

The evolution of asphaltene aggregates by centrifugation, m_A (t) is written as,

$$m_A(t) = \frac{\sum_{i=1}^{N} R^{i-1} M_{w,A} N_{agg} s_i C_i(t)}{\mathrm{w_o}} \tag{A.9}$$

Where $\mathrm{w_o}$ represents mass of oil per unit volume of mixture.

It needs to be noted that C_i(t) in Equation (A.9) is obtained from simulating the population balance equations.

A typical centrifugal separation of aggregates is done for 10 minutes at 14000 r.p.m. Radius of centrifuge is $7.3\text{x}10^{-2}$ m and the oil-heptane mixture that is filled in the tube is about $3.0\text{x}10^{-2}$ m. Separation efficiency curve for centrifugal operation of 2 min, 10 min, 10 hour and 10 days are shown in Figure A1. The right most curve for 2 minutes of centrifugation shows that the particles larger than 700 nm have a separation efficiency of 1 (i.e. complete separation by centrifugation). With increasing centrifugation time, more and more of the smaller aggregates are separated. As observed in Figure A1, the separation efficiency for 10 minutes of centrifugation is 1 for particles of sizes larger than

200 nm. The calculated separation efficiency corresponding to a centrifugation time of 10 minutes for different particle sizes is used in the model to calculate what fraction of the particles of a given size will be centrifuged out.

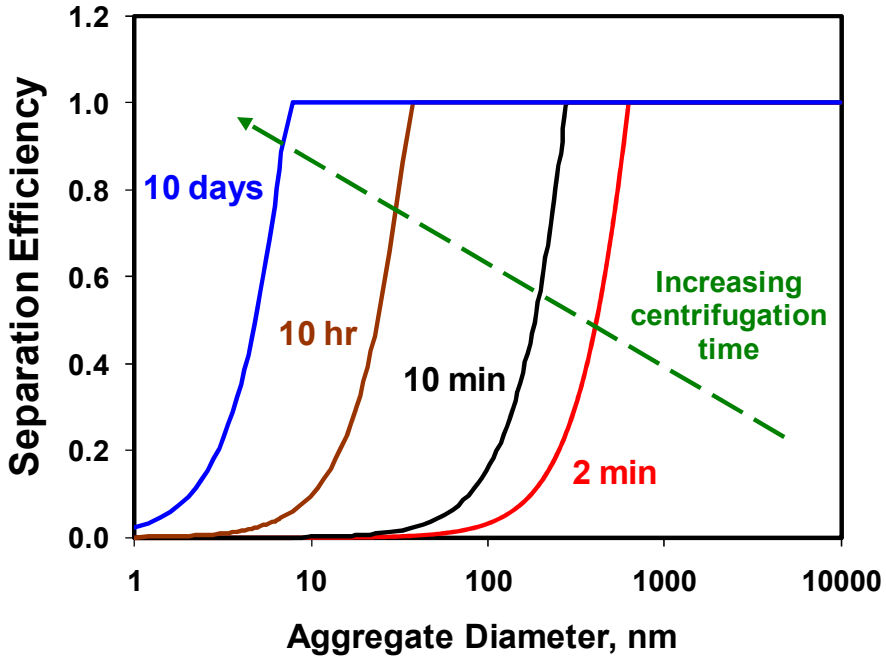

Figure A.1: Separation efficiency of asphaltene particles during the centrifugation process

A.2 Sensitivity analysis for the geometric scaling factor, R

The geometric scaling factor (R) in the model describes how the number of molecules in any particle scales from a given particle to the next larger one in the system. The number of molecules in the i^{th} particle is given by R^{i-1}. For example, for R =2, there will be 1, 2, 4 and 8 monomers in the 1st, 2nd, 3rd and 4th species of particles respectively.

The resulting mass fraction distributions for R = 2 and 1.5 are shown as a function of time in Figure A.2. It is seen that the height of the peaks is higher for R = 2 as compared to R = 1.5 for all the times shown in the plots. This observation can be explained by the fact that when R is reduced, the scaling for the number of molecules per particle between two consecutive particle species is reduced, effectively reducing the gaps in particle diameters for this discretized distribution. Therefore, at lower R, there will be more intermediate particles sizes between any two limits of particle size. This fact can be confirmed by comparing the particle size distribution (PSD) at any time-point. It is observed that Figure A.2 (B) has more number of particles sizes than Figure A.2 (A) along any PSD at a given time. It should be noted that data markers in Figure A.2 are the only particles sizes allowed by the geometric population balance and the connecting lines are only a visual guide – there are no intermediate particles sizes between any two consecutive data markers shown. Because more intermediate particle sizes are allowed for lower R, the mass is distributed more evenly over the distribution and hence the peaks heights are lower for R = 1.5. A summation of the mass fractions at each point represented by a data-marker for any given PSD yields a total mass fraction of 1.0.

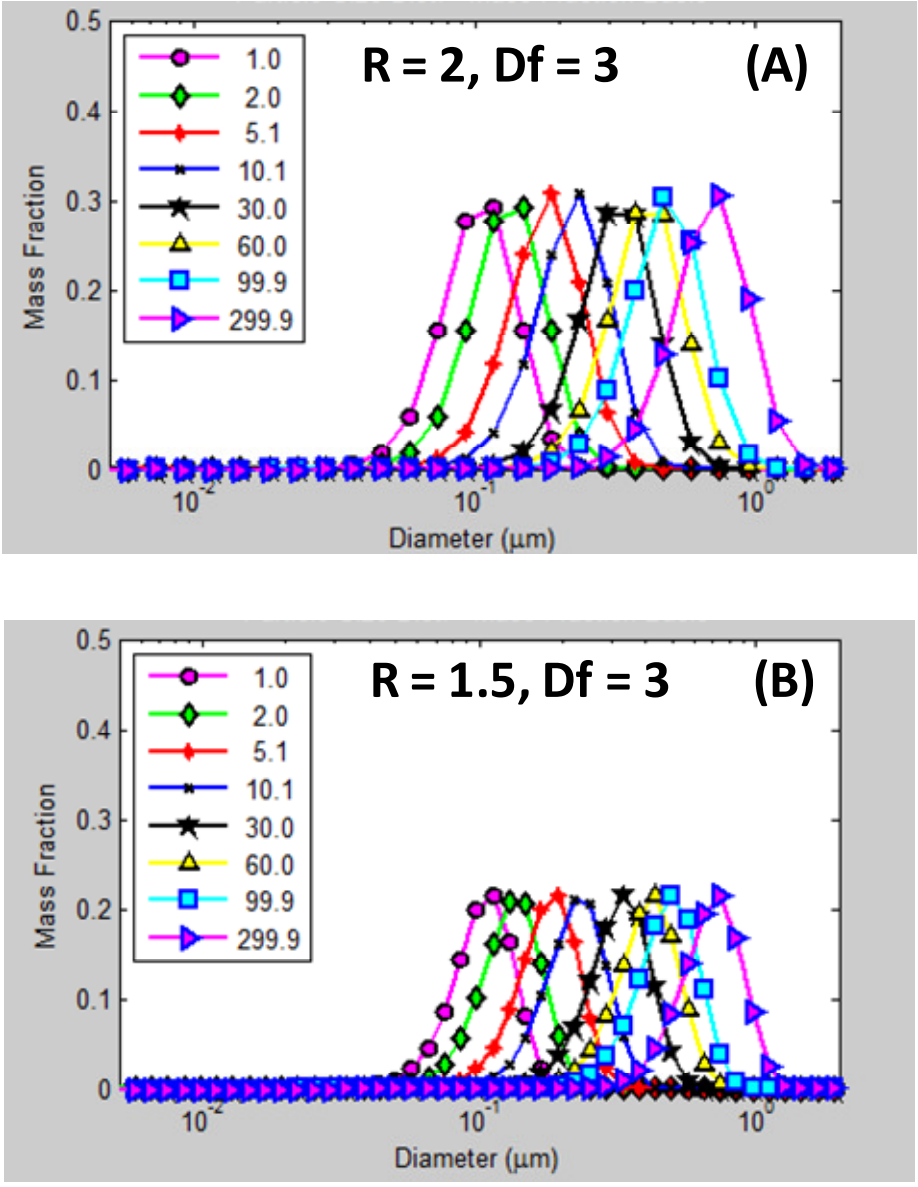

Figure A.2: Calculated particle size distribution as a function time for (A) R = 2 and (B) R=3. The system is K-1 oil with 47.8% heptane.

Another aspect of comparison is dependence of the collision efficiency (β) on the geometric scaling factor (R). In this model, β is the only fitting parameter and is calculated by finding the best fit for the centrifugation plot shown earlier. Figure A.3 shows the variation of β with R for three different heptane concentrations. The decrease in β with an increase in R can be explained by the fact that at smaller values of R the

spacing between the particle sizes is smaller than that at a larger R. Therefore with each successful collision, the magnitude of increase in the particle sizes is smaller when R is small. Therefore, in order to reach the larger particle sizes, the collisions need to have a higher efficiency at smaller values of R. At larger values of R there is a smaller number of discrete particle sizes allowed by the geometric population balance. Consequently, the particles grow to larger sizes faster and hence a smaller collision efficiency is needed to fit the data.

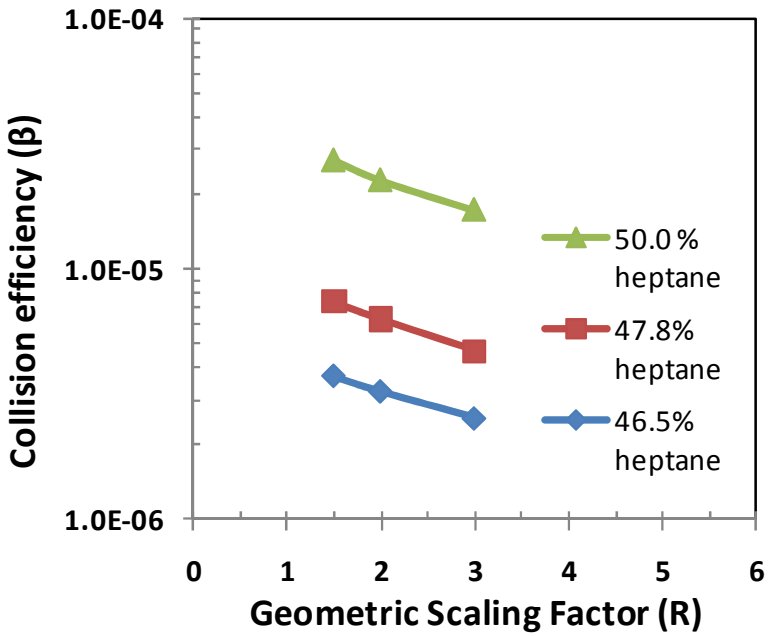

Figure A.3: Variation of the collision efficiency (β) with different values of R. The data for three different heptane concentrations in K-1 oil are shown.

A.3 Sensitivity Analysis for the Fractal Dimension (D_f)

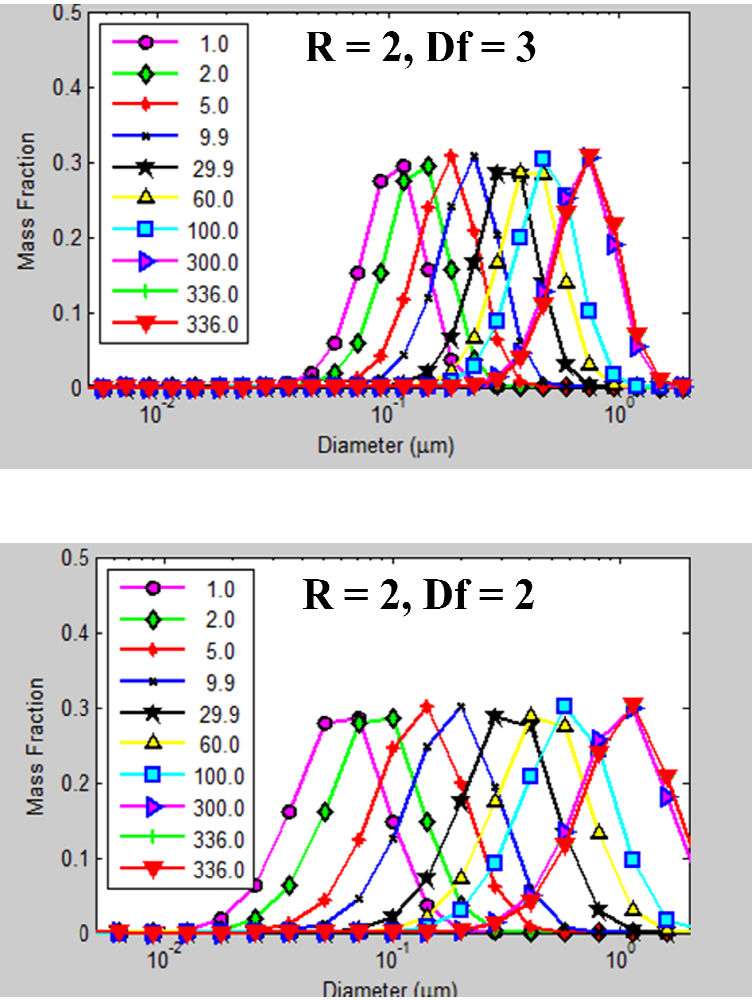

Figure A.4: Calculated particle size distribution as a function time for (A) $D_f = 2$ and (B) $D_f = 3$. The system is K-1 oil with 47.8% heptane.

Figure A.4 shows the results for the calculated particle size distribution using two different values of fractal dimension, D_f. At smaller values of the fractal dimension the particles are less spherical. Therefore, one of their dimensions is relatively longer than the other and they span a greater range of diameters. Hence, the spacing between the particle sizes in the discretized range of particle sizes is larger at smaller D_f which leads to a broader peak for the particle size distributions as is seen from the comparison of the distributions for $D_f = 3$ and $D_f = 2$ (Figure A.4).

A.4 Rate of change of mode diameter as a function of different variables

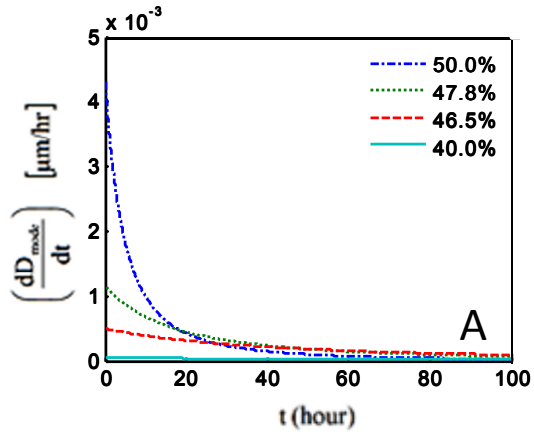

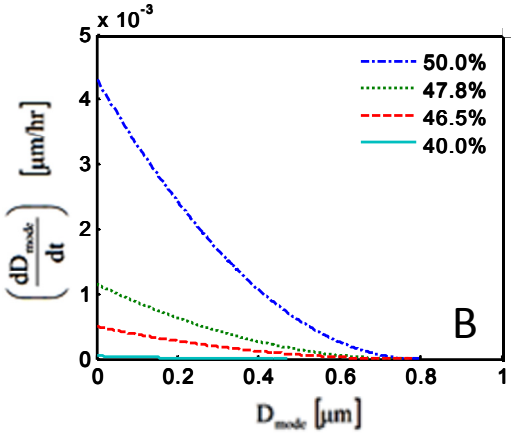

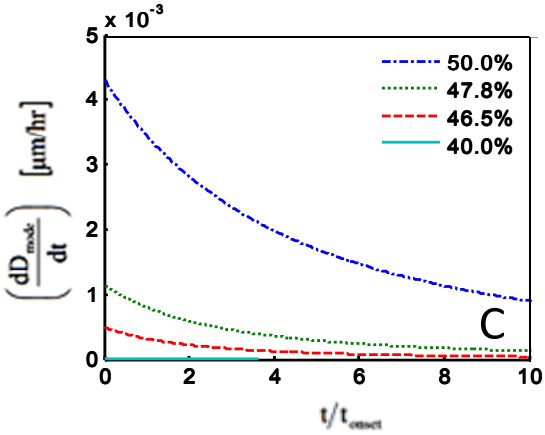

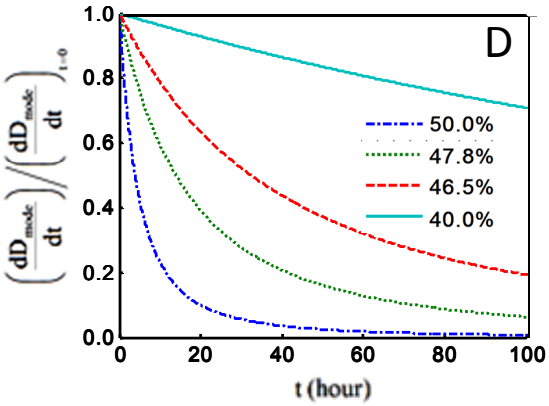

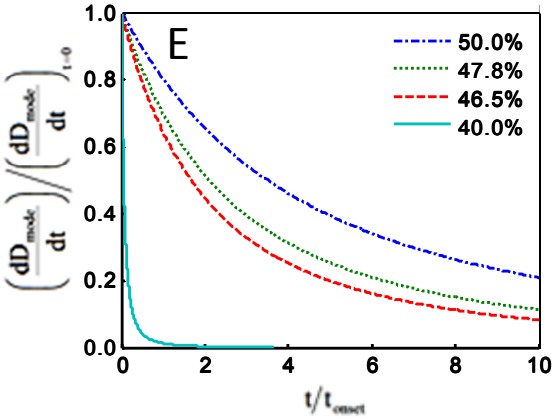

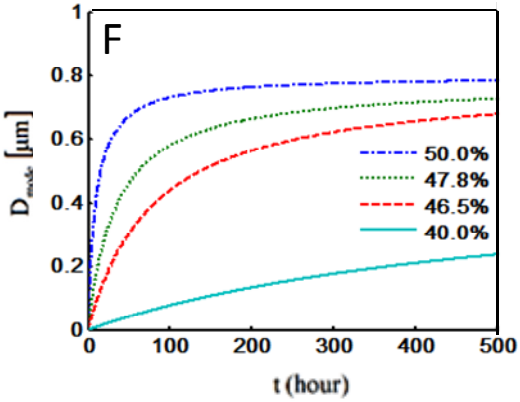

APPENDIX - B

SAMPLE CALCULATIONS FOR HEPTANE LOSS IN A CONTROL SYSTEM

System: Pure heptane was taken in a flask fitted with Mininert sampling valves and was maintained at 50°C. The flask was opened for sampling from time to time but no samples were withdrawn.

Initial mass of heptane, m_1 = 81.4695 g

Final mass of heptane after six samplings at 50□C over a span of 40 hours, m_2 = 80.7354 g

Loss of heptane, wt % = $(m_1 - m_2)/ m_1$ x 100% = 0.90 wt%

Adding a 50% factor of safety in these calculations, the heptane loss would be: 1.5 x 0.90% = 1.35 wt%

These calculations are performed on a mass basis and the conversion to a volume basis would depend on the vol % of heptane in the oil-precipitant mixture.